Digital Comprehensive Summaries of Uppsala Dissertations
from the Faculty of Science and Technology 2298

Musculoskeletal Development in Jawed Vertebrates

Gene function, cis-regulation, and 3D phenotypes in zebrafish

JAKE LEYHR

ACTA UNIVERSITATIS
UPSALIENSIS
2023

ISSN 1651-6214
ISBN 978-91-513-1879-0
urn:nbn:se:uu:diva-509354

UPPSALA
UNIVERSITET

Dissertation presented at Uppsala University to be publicly examined in Ekmansalen, Evolutionsbiologiskt centrum, Norbyvägen 14, Uppsala, Friday, 6 October 2023 at 13:15 for the degree of Doctor of Philosophy. The examination will be conducted in English. Faculty examiner: Professor Chrissy Hammond (University of Bristol).

Abstract
Leyhr, J. 2023. Musculoskeletal Development in Jawed Vertebrates. Gene function, cis-regulation, and 3D phenotypes in zebrafish. *Digital Comprehensive Summaries of Uppsala Dissertations from the Faculty of Science and Technology* 2298. 107 pp. Uppsala: Acta Universitatis Upsaliensis. ISBN 978-91-513-1879-0.

Vertebrate skeletons are an intricate framework of bony and cartilaginous structures that form through carefully orchestrated developmental processes, guided by interacting genetic pathways that regulate cellular differentiation, migration, and tissue morphogenesis. The specific timing and localisation of gene expression shapes the diverse array of skeletal elements, from the flexible cartilages of the embryonic stage to the hardened bones that provide structural support in adulthood, and the joints and connective tissues that articulate the musculoskeletal system. This thesis aims to use the zebrafish (*Danio rerio*) as a model organism to study the role and regulation of three genes in controlling musculoskeletal development from larvae to adulthood: *nkx3.2*, *gdf5*, and *mkx*. In the first study, we used CRISPR/Cas9 genome editing to knock out *nkx3.2* and characterise the resulting mutant phenotypes, including a jaw joint fusion and occipital and vertebral defects. In the second study, we extended the phenotypic characterisation of *nkx3.2* mutants into the skeleton-associated soft tissues using a novel synchrotron-based tomographic imaging technique and revealed a series of defects in the jaw musculature, Weberian ligaments, and fluid-filled sacs of the ear. In the third study, we identified and functionally characterised a novel cis-regulatory element responsible for driving *nkx3.2* expression in the early developing jaw joint, with its presence and activity being highly conserved in jawed vertebrates but absent in jawless vertebrates. In the fourth study, we examined the role of *gdf5* in skeletal development by generating a knockout mutant line, finding striking defects in fin radial development including a clear endoskeletal disc segmentation phenotype resulting in a complete absence of posterior radials in the pectoral fin. Finally, in the fifth study, we studied the regulation of *Mkx*, an important factor in tendon and ligament development, and identified a novel enhancer with different species-dependent activity patterns. In summary, this thesis contributes to our understanding of the derived and conserved functions of *Nkx3.2*, *Gdf5*, and *Mkx* in the development of the vertebrate skeleton and associated connective tissues, and provides a novel high-resolution 3D imaging method for future studies.

Keywords: Nkx3.2, Gdf5, Mkx, zebrafish, jaw joint, skeleton, fin development, cartilage, tendon, ligament, enhancer, CRISPR/Cas9, mutant, microCT, synchrotron

Jake Leyhr, Department of Organismal Biology, Evolution and Developmental Biology, Norbyv 18 A, Uppsala University, SE-75236 Uppsala, Sweden.

ISSN 1651-6214
ISBN 978-91-513-1879-0
URN urn:nbn:se:uu:diva-509354 (http://urn.kb.se/resolve?urn=urn:nbn:se:uu:diva-509354)

"The fish and I were both stunned and disbelieving to find ourselves connected by a line." - William Humphrey

List of papers

This thesis is based on the following papers, which are referred to in the text by their Roman numerals.

I Waldmann L*, **Leyhr J***, Zhang H, Öhman-Mägi C, Allalou A, Haitina T. (2021). The Broad Role of Nkx3.2 in the Development of the Zebrafish Axial Skeleton. *PLoS One* 16(8), e0255953. DOI:10.1371/journal.pone.0255953

II **Leyhr J**, Sanchez S, Dollman K, Tafforeau P, Haitina T. (2023). Enhanced contrast synchrotron X-ray microtomography for describing skeleton-associated soft tissue defects in zebrafish mutant. *Frontiers in Endocrinology* 14, 1108916. DOI:10.3389/fendo.2023.1108916

III **Leyhr J***, Waldmann L*, Filipek-Górniok B, Zhang H, Allalou A, Haitina T. (2022). A novel cis-regulatory element drives early expression of Nkx3.2 in the gnathostome primary jaw joint. *eLife* 11, e75749. DOI:10.7554/eLife.75749

IV Waldmann L*, **Leyhr J***, Zhang H, Allalou A, Öhman-Mägi C, Haitina T. (2022). The role of Gdf5 in the development of the zebrafish fin endoskeleton. *Developmental Dynamics* 251(9), 1535-1549. DOI:10.1002/dvdy.399

V **Leyhr J**, Haitina T. A novel *Mohawk* enhancer drives species-dependent reporter expression in musculoskeletal system-associated tissues in zebrafish. *(Manuscript)*

* These authors contributed equally to this study.
Reprints were made with permission from the respective publishers.

The following manuscripts were also prepared during the PhD but are beyond the scope and not included in this thesis:

- **Leyhr J**, Haitina T, Bird NC. Hidden in plain sight: does the first intercostal ligament contribute to the Weberian apparatus? *(Manuscript)*

- Mayeur H, **Leyhr J**, Leurs N, Michel L, Sharma K, Lagadec R, Klopp C, Martin K, Blaxter M, Howe K, McCarthy S, Mead D, Baril T, Hayward A, Martinand-Mari C, Tafforeau P, Dollman KN, Haitina T, Sanchez S, Korsching S, Mazan S, Debiais-Thibaud M. The sensory shark: high-quality phenotypic, genomic and transcriptomic data for the small-spotted catshark *Scyliorhinus canicula* reveals insights into the evolution of sensory organs in jawed vertebrates. *(Manuscript)*

- Johanson Z, **Leyhr J**, Challands T, Violaris A, Sanchez S, Dollman KN, Smith MM. Bone repair in the Devonian lungfish *Dipterus valenciennesi* after injury. *(Manuscript)*

- Ford C, de Sena-Tomás C, Aleman AG, Rangaswamy U, **Leyhr J**, Gao CZ, Nim HT, See M, Coppola U, Waxman JS, Ramialison M, Haitina T, Smeeton J, Sanges R, Targoff KL. Nkx2.7 is a Novel Regulator of Pharyngeal Arch Development. *(Manuscript)*

Contents

Abbreviations

2D	Two-dimensional
3D	Three-dimensional
bp	base pair
Cas	CRISPR associated
cDNA	Complementary DNA
CE	Contrast enhancement
CRISPR	Clustered regularly interspaced short palindromic repeats
crRNA	CRISPR RNA
Ct	Cycle threshold
DICE	Diffusible iodine-based contrast enhancement
dpf	Days post fertilisation
DNA	Deoxyribonucleic acid
DSB	Double-strand break
ECM	Extracellular matrix
FDR	False discovery rate
gDNA	Genomic DNA
GFP	Green fluorescent protein
I_2E	Iodine in ethanol
microCT/μCT	Micro-computed tomography
mRNA	Messenger RNA
NHEJ	Non-homologous end joining
OA	Osteoarthritis
OPT	Optical projection tomography
PAM	Protospacer adjacent motif
PCA	Principal components analysis
PCR	Polymerase chain reaction
PPC-SRμCT	Propagation phase contrast synchrotron radiation micro-computed tomography
qPCR	Quantitative PCR
RNA	Ribonucleic acid
RNP	Ribonuleoprotein
sgRNA	Single guide RNA
SMMD	Spondylo-megaepiphyseal-metaphyseal dysplasia
tracrRNA	Trans-activating crRNA
WT	Wild-type

Introduction

Jawed vertebrates (gnathostomes) are a group of animals distinguished by their hard internal skeletons comprised of bone and/or cartilage. This skeleton is principally responsible for supporting and protecting the body and internal organs. Associated with the skeleton are related connective tissues such as tendons and ligaments, with distinct but to some extent overlapping cellular identities. A complex and interacting array of factors, primarily regulatory proteins, that are expressed in specific embryonic locations at particular times controls the development of the skeleton and associated structures. Gnathostomes have evolved a diverse array of skeletal structures for different purposes, as well as differing modes of skeletal development that necessitate altered expression of developmental factors. By studying the regulatory genomics and development of living vertebrates in a phylogenetic context we can shed light on the evolutionary history of vertebrate skeletons both in terms of morphology and genetics.

This thesis uses the zebrafish (*Danio rerio*) as a model organism to study the role and regulation of three evolutionarily conserved genes known to be involved in the skeletal development of gnathostomes: NK-3 Homeobox 2 (*Nkx3.2*), Growth Differentiation Factor 5 (*Gdf5*), and Mohawk Homeobox (*Mkx*). Zebrafish development from the embryo to adult was studied to gain insights into different stages of skeletal development, from the condensation of mesenchymal cells into cartilage and early tendon differentiation through to the mineralisation of bones. Our generated zebrafish knockouts for *nkx3.2* and *gdf5* were associated with significant craniofacial, axial, and appendicular skeletal defects, respectively, that are comparable to phenotypes observed in mouse, frog, and chick models, suggesting a broadly conserved role for these genes in skeletal development, although with differences associated with specific skeletal structures.

For these studies, well-established traditional techniques including histological thin sections were used to examine mutant phenotypes. However, to describe *nkx3.2* mutant skeleton-associated soft-tissue phenotypes, we used a cutting-edge phase-contrast synchrotron microtomography method and demonstrated its promise for providing near-histological resolution in three dimensions. Beyond studying gene function using knockouts, the cis-regulation of tissue-specific *Nkx3.2* and *Mkx* gene expression by two proximal enhancers was investigated and suggests a highly conserved regulation of *Nkx3.2* contrasted with a more variable regulation of *Mkx* in different groups of jawed vertebrates.

Background

Vertebrate phylogeny and diversity

The subphylum Vertebrata can be divided into two groups, Gnathostomata (jawed vertebrates) and Agnatha (jawless vertebrates). The earliest-branching stem gnathostomes with jaws were the placoderms, a now-extinct group of armoured fish whose taxonomy has been long debated. Recent studies generally resolve placoderms as a paraphyletic grade (Brazeau, 2009; Giles et al., 2015; Long et al., 2015b; Qiao et al., 2016) although King et al. (2017) support placoderm monophyly. Placoderms record the appearance of jaws comprised of gnathal plates originally considered distinct from, but now considered homologous to, the dentary, maxilla, and premaxilla found in living bony fish (Zhu et al., 2013; Zhu et al., 2016; Vaškaninová et al., 2020). Crown gnathostomes are divided into Osteichthyes (bony fish) and Chondrichthyes (cartilaginous fish) (Figure 1).

The two main groups of osteichthyans are the Actinopterygii (ray-finned fish) and Sarcopterygii (lobe-finned fish including tetrapods). Actinopterygii includes almost every species conventionally thought of as "living fish", and the vast majority are in the Teleostei clade, including zebrafish. Teleost species number almost 30,000, comprising 96% of all living fish (Nelson et al., 2016). The non-teleost actinopterygians include the bichirs, sturgeon and paddlefishes, and gars and bowfins - members of the Cladistia, Chondrostei, and Holostei respectively, totalling less than 50 species (Nelson et al., 2016). Teleosts are relatively derived in their morphology, physiology, and genomes (Arratia, 2015; Glasauer and Neuhauss, 2014; Davesne et al., 2020) so the few basal species of Actinopterygii can be valuable representatives of more primitive actinopterygian states (Braasch et al., 2016; Bi et al., 2021).

Sarcopterygii includes two groups of extant "fish" - one includes coelacanths and lungfish, represented by just eight extant species, but the second and by far the largest group of sarcopterygians are the tetrapods, the four-limbed vertebrates that dominate the land (Clack, 2012). Tetrapoda encompasses Amphibia (including frogs, salamanders, and caecilians) and Amniota (including turtles, "lizards", snakes, crocodiles, and birds in Sauropsida (Benton, 2005; Hedges, 2012) and mammals in Synapsida). Mammalia is divided into monotremes, marsupials, and placental mammals, with the latter being the most speciose and including humans and model species such as the mouse (Wilson and Reeder, 2005).

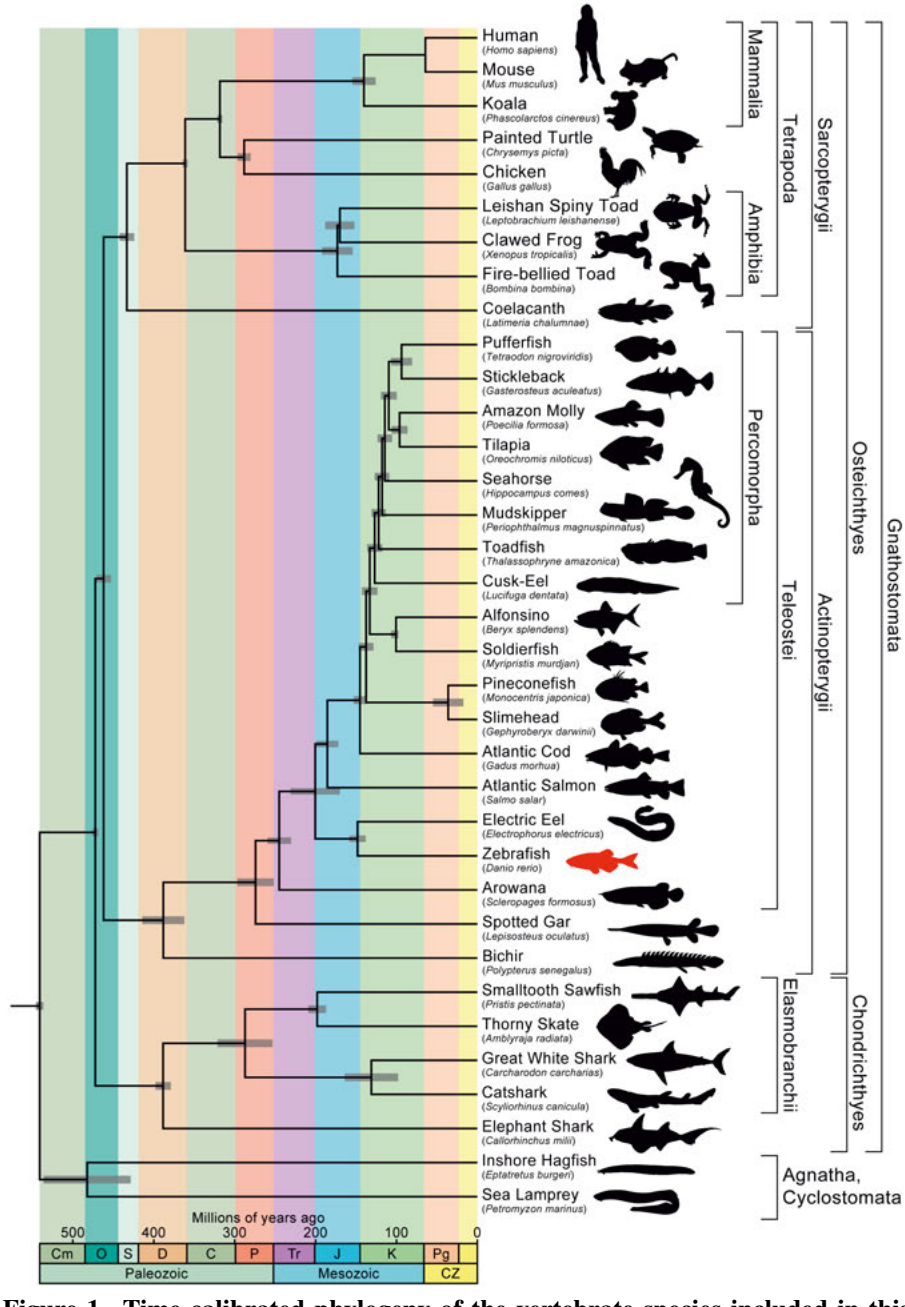

Figure 1. Time-calibrated phylogeny of the vertebrate species included in this thesis. Grey bars indicate 95% confidence intervals of divergence times from Marjanović (2021), Ghezelayagh et al. (2022), Hughes et al. (2018), and Miyashita et al. (2019). Cm - Cambrian, O - Ordovician, S - Silurian, D - Devonian, C - Carboniferous, P - Permian, Tr - Triassic, J - Jurassic, K - Cretaceous, Pg - Palaeogene, CZ - Cenozoic.

Extant Chondrichthyes are divided into the Holocephali and Elasmobranchii. Holocephali includes the elephant shark and other chimaeras, while the larger group of elasmobranchs are further divided into the Selachimorpha ("true sharks") and Batoidea (skates and rays) (Nelson et al., 2016). The evolutionary origin of chondrichthyans from the common ancestor with osteichthyans is illustrated by a rich grade of transitional fossils classified as Acanthodii. For a long time, acanthodians were ambiguously classified, with members scattered throughout Osteichthyes and/or Chondrichthyes as monophyletic or paraphyletic groups (Brazeau, 2009; Davis et al., 2012; Friedman and Brazeau, 2010), but recent work has concluded that most acanthodian species are a paraphyletic grouping along the chondrichthyan stem (Brazeau and Winter, 2015; Brazeau and Friedman, 2015; Giles et al., 2015; Long et al., 2015a; Maisey et al., 2017; Zhu et al., 2013).

There are only two groups of agnathans alive today, the hagfishes and lampreys, both classified in the Cyclostomata. When studying crown gnathostomes, agnathans are necessarily the closest outgroup to make comparisons to in order to understand the ancestral state that these gnathostomes evolved from. However, cyclostomes are also highly morphologically derived relative to ancestral vertebrates, making direct comparisons of homologous structures difficult (Janvier, 2008; Donoghue, 2017).

In this thesis, I used the zebrafish model organism for all physical experiments, and much of the literature guiding these efforts was based on experiments in zebrafish, clawed frogs, mice, and human tissues. For computational analyses of the evolutionary conservation of genomic regulatory elements in Papers **III** and **V**, a wide range of species representing most of the aforementioned major groups of vertebrates were included, shown in Figure 1.

The vertebrate skeleton

The vertebrate skeleton functions to structure the body into distinct regions, provide support against gravity and muscular forces, and protect vital organs. Anatomically, the term endoskeleton refers to the internal skeleton such as the limb bones and spine, while more superficial skeletal elements that develop in the dermis (skin) such as scales and osteoderms, are termed the exoskeleton or dermal skeleton (Francillon-Vieillot et al., 1990; Laurin et al., 2021). The dermal skeleton also includes the majority of the skull and facial bones, some of which, such as the mammalian dentary (lower jaw), were more superficial in ancestral forms but have since evolved to develop under layers of muscles and connective tissues, leading Hirasawa and Kuratani (2015) to describe them as "sunken exoskeleton".

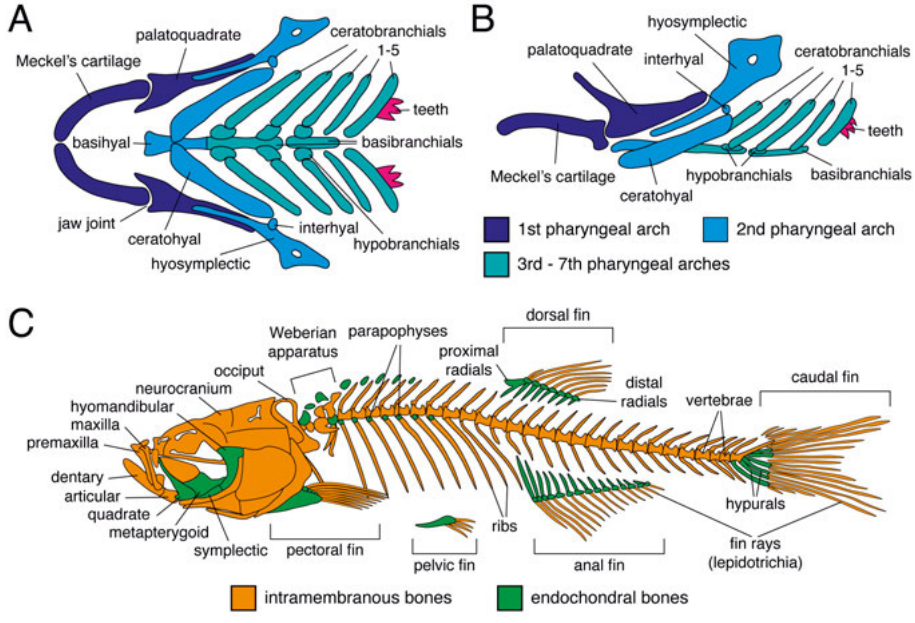

Figure 2. Zebrafish skeletal anatomy. (A) Ventral view of the larval pharyngeal arch cartilages. (B) Lateral view of the larval pharyngeal arch cartilages. (C) The juvenile/adult zebrafish skeleton is comprised of bones of intramembranous and endochondral origins. Diagrams modified from Kimmel et al. (2001) and Le Pabic et al. (2022).

Within the skeleton, it is common to topographically distinguish the cranial, axial, and appendicular skeletal elements. The cephalic bones are found in the head, ending at the base of the skull, where the axial skeleton begins, comprising the vertebral column and ribs, and the appendicular skeleton includes the limbs, fins, and the girdles that connect them to the axial skeleton. Within the cranial skeleton, the lower (ventral) part includes the pharyngeal skeleton that comprises fish jaws, gills, and supporting elements (Figure 2A, B).

In larval zebrafish, the first pharyngeal arch includes Meckel's cartilage and the palatoquadrate, articulated by the jaw joint to form the lower and upper jaws, respectively, of the mouth. The second arch is comprised of a midline basihyal cartilage, flanked by paired ceratohyals and hyosymplectic that are articulated at the so-called hyoid joint by a small cartilage called the interhyal. The more posterior arch elements are known as the ceratobranchials, which articulate with midline basibranchials via small hypobranchial cartilages. The ceratobranchials bear the gills and small tooth-like denticles called gill-rakers, but only the most posterior, ceratobranchial 5 (pharyngeal arch 7) bears true teeth (Figure 2A, B).

A rich collection of Mesozoic synapsid fossils in addition to ontogenetic observations has established that the primary jaw joint, first established in placoderms and retained in all crown gnathostomes, moved up into the middle ear of therian (placental and marsupial) mammals, forming the incudomalleolar joint (Anthwal et al., 2013; Luo, 2011; Tucker, 2017). This is the joint between the malleus and incus bones, homologous to the articular and quadrate bones of non-mammals which ossify around Meckel's cartilage and the palatoquadrate, respectively. Simultaneously, a new secondary jaw joint between the dentary and squamosal bones evolved to maintain mammalian lower jaw function.

Bones are comprised primarily of elastic proteinaceous collagen I fibres and the inorganic mineral hydroxyapatite (Hall, 2005). The flexible protein fibres and inflexible mineral crystals provide bones with rigidity while also being fracture-resistant. Although often thought of as dry, inert structures, bones are in fact dynamic living tissues that additionally function as mineral reservoirs that can be metabolised to support ion homeostasis (Kerschnitzki et al., 2014; Peacock, 2010). Bones develop by two major modes: intramembranous ossification and endochondral ossification (Francillon-Vieillot et al., 1990; Laurin et al., 2021). Dermal bones all develop by intramembranous ossification compared to only a minority of endoskeletal bones, as the latter primarily form by endochondral ossification in mammals. The mode of development of homologous endoskeletal bones can also differ between species. For example, while the vertebrae and ribs develop by endochondral ossification in mammals, in the zebrafish and other actinopterygians, they form by intramembranous ossification (Le Pabic et al., 2022) (Figure 2C).

Both modes of ossification begin with mesenchymal cells, loosely-packed unspecialised cells embedded in a fluid-like matrix. In intramembranous ossification, membranous mesenchymal cell populations condense and differentiate into bone precursor cells called osteoblasts. These osteoblasts secrete collagens and proteoglycans, forming a matrix that is able to bind calcium salts into hydroxyapatite. These calcified regions expand out as spicules from the first ossification centre(s) until an entire bony element is formed (Percival and Richtsmeier, 2013). Endochondral ossification, on the other hand,

relies on a cartilage intermediary between the mesenchyme and ossification. The mesenchyme condenses and differentiates into cartilage cells called chondrocytes, which proliferate and produce their own cartilaginous extracellular matrix (ECM) of proteoglycans and collagen II fibres (Hall, 2005). The three-dimensional spatial orientation of the clonal division of these proliferating chondrocytes shapes each cartilage structure into its final morphology (Kaucka et al., 2017).

Eventually, these chondrocytes, beginning with the oldest and therefore more centrally located, stop dividing and become hypertrophic, increasing in volume and secreting a modified ECM capable of binding calcium (Amizuka et al., 2012; Chen et al., 2023). Some of the hypertrophic chondrocytes die by apoptosis (Gibson, 1998), leaving space for nearby osteoblasts to invade via blood vessels and begin to deposit bone matrix (Hall, 2005). Other hypertrophic chondrocytes transdifferentiate into progenitors of osteoblasts and other important cell types such as adipocytes (Yang et al., 2014a; Yang et al., 2014b; Zhou et al., 2014; Aghajanian and Mohan, 2018; Long et al., 2022). Eventually, the entire cartilage template is replaced by bone, although this process often remains incomplete until adulthood in long bones like the tetrapod femur, as the cartilaginous ends grow with the organism between embryonic development and adulthood, with the mineralising bone front following behind (Anderson and Shapiro, 2010).

While these two modes of ossification are distinct and the bones they form are often classified distinctly as "endochondral bone" or "intramembranous bone", mixed bones - fused ossifications of both types - also exist. This is the case in tetrapod long bones, where much of the thin cortical bone around the endochondral diaphysis ossifies directly from the membranous periosteum (Dwek, 2010). Another interesting case is the mammalian mandible, where in different species endochondral ossification of secondary cartilages are variably involved in forming the symphysis and condylar, coronoid, and angular processes of the otherwise intramembranous dentary (Anthwal and Tucker, 2012; Fabik et al., 2021).

In addition to serving as a template for endochondral bones during development, cartilage is also maintained in adult skeletons in flexible synovial joints, capping the bones. This articular cartilage provides a smooth, cushioned surface for bones to contact at, protecting them and maintaining the articulation with minimal friction (Sophia Fox et al., 2009). Degradation of articular cartilage is a pathology of osteoarthritis (OA), causing the bones at a joint to rub against each other directly with increased friction, resulting in bone lesions and inflammation (Glyn-Jones et al., 2015). The joint is enclosed in a synovial capsule filled with lubricating molecules including lubricin and hyaluronic acid in the cavity between the articulating elements, further decreasing friction (Rhee et al., 2005; Tanaka et al., 2008). Interestingly, the same superficial

joint cells that produce the lubricating molecules also act as the stem cell population that produces new articular chondrocytes (Li et al., 2017). All of this is in contrast to the other types of bony joints; the inflexible sutures and intervertebral discs, which have a completely different composition and set of properties (Smeeton et al., 2016), beyond the scope of this thesis. The type of cartilage found in both templates for endochondral ossification and articular cartilage is hyaline cartilage, where the ECM is predominantly made up of glycosaminoglycans, in contrast to the elastic cartilage found in intervertebral discs and fibrous cartilage in the attachment sites of tendons and ligaments to bones, which have larger fractions of elastic and collagen fibres in the ECM respectively (Hall, 2005).

The above description of skeletal tissues is largely only applicable to osteichthyans, as chondrichthyans possess a quite different, and derived, skeletal system. The chondrichthyan skeleton is comprised of cartilage both in embryonic stages and in adults. The hyaline cartilage that dominates the shark skeleton is comparable to the hyaline cartilage of endochondral template cartilages in osteichthyans (Hall, 2005), but it doesn't undergo endochondral ossification and instead remains as cartilage, the matrix expanding as the fish grows. Chondrichthyans altogether lack bone, although they have mineralised hard tissues called tesserae superficially surrounding and reinforcing cartilage elements in addition to possessing mineralised vertebral centra produced by areolar calcification (Dean and Summers, 2006). Tesserae are produced as cartilage just beneath the perichondrium undergoes prismatic and globular calcification to form small, approximately hexagonal plates that grow and fuse together as the fish develops (Dean et al., 2009; Debiais-Thibaud, 2019).

Accessory to the hard endoskeletal elements themselves are the connective tissues that articulate them and transmit muscular force to control them. Ligaments directly connect bones to other bones (or cartilage to other cartilage in chondrichthyans) in joints, while tendons connect skeletal elements to muscles. These two tissues are distinct but quite related, both being made up of dense, fibrous connective tissue with a large collagen component in the ECM for transmitting mechanical forces (Asahara et al., 2017). Proteoglycans such as decorin and fibromodulin are also present to organise the collagen fibrils (Jepsen et al., 2002). Tenocytes and ligamentocytes are fibroblast cells that reside in tendons and ligaments between the collagen fibrils, producing the collagens and proteoglycans for the ECM in response to mechanical stress (Kjær, 2004). There is a gradient of different collagen types present at the tendon interface with a bone (enthesis), transitioning from tendinous collagen I bundles to mineralised fibrocartilage comprised of collagen II and X (Schweitzer et al., 2010). At the other end of the tendon, at the interface between tendon and muscle (myotendinous junction), a similar gradient is present as the two tissue types interweave their extracellular matrices to become connected (Nassari et al., 2017).

The genetic basis of skeletal development

Cartilage and bone

Different skeletal elements arise from different lineages of cells in the early vertebrate embryo. Most of the axial skeleton derives from the paraxial mesoderm (specifically the sclerotome) that lies either side of the neural tube, while the appendicular skeleton, part of the axial skeleton, and part of the craniofacial skeleton derives from the lateral plate mesoderm (Berendsen and Olsen, 2015). The remaining majority of the craniofacial skeleton derives from the neural crest, a specialised population of cells that arises from the ectoderm of the neural plate through a process of epithelial to mesenchymal transition and is sometimes considered the "fourth germ layer" of vertebrates (Hall, 2000), distinct from the endoderm, ectoderm, and mesoderm. Mesenchymal cells from the aforementioned mesoderm and neural crest are able to differentiate into a wide variety of cell types, including skeletogenic cartilage and bone (Chen et al., 2016b; Ullah et al., 2015).

The first stage of differentiation towards both endochondral and intramembranous ossified elements is the condensation of the mesenchyme, which is mediated by SMAD-mediated TGFβ/BMP signalling (Bénazet et al., 2012; Lim et al., 2015) to activate downstream genes promoting cell migration and cell-cell adhesion such as N-adherins, N-CAM, and syndecan (Hall and Miyake, 2000). In intramembranous elements, this condensed mesenchyme is committed to an osteogenic cell fate and differentiates into osteoblasts as a result of canonical Wnt signalling (Day et al., 2005) inducing the expression of *Runx2* (Ducy et al., 1997; Komori et al., 1997), while in endochondral elements the upregulation of *Sox9* and other *Sox* genes causes the mesenchyme condensations to differentiate into early chondrocytes and start producing cartilaginous ECM (Bi et al., 1999; Han and Lefebvre, 2008).

These early chondrocytes proliferate under the control of Indian Hedgehog (Ihh) and PTHrP (St-Jacques et al., 1999) at the same time as they produce extracellular matrix, until genes including *Runx2*, *Runx3*, and *Mef2c* are upregulated and cause the chondrocytes to stop proliferating and mature into much larger hypertrophic chondrocytes (Arnold et al., 2007; Yoshida et al., 2004). These hypertrophic chondrocytes shift collagen production from predominantly type II to type X (Kielty et al., 1985; Chen et al., 2023), and produce secreted factors that induce nearby perichondral cells to differentiate towards osteoblasts (Chung, 2004). An essential osteoblast-specific gene downstream from Runx2 is osterix (*Osx*; also called *Sp7*), as it has been demonstrated that the absence of this gene completely blocks the differentiation of osteoblasts and therefore results in a boneless skeleton (Nakashima et al., 2002). At the same time, the hypertrophic chondrocytes also express *VegF*, inducing the invasion of blood vessels and the precursors of osteoblasts from the perichondrium (Bluteau et al., 2007; Mayr-Wohlfart et al., 2002).

The osteoblasts, osteoclasts, and hypertrophic chondrocytes all secrete matrix metalloprotease (MMP) enzymes that degrade the cartilage ECM (Holmbeck et al., 2005; Inada et al., 2004; Stickens et al., 2004; Chen et al., 2023). The degraded matrix serves as the template for bone formation by the osteoblasts, depositing a new organic protein matrix of collagen I, osteocalcin, and osteopontin, which facilitates the deposition of hydroxyapatite (Sroga et al., 2011), mineralising the structure into mature bone and trapping some osteoblasts inside as osteocytes (Franz-Odendaal et al., 2006).

Many skeletal joints, including the zebrafish jaw joint, form as two cartilaginous elements go through their early stages of development. Beginning as a single mesenchymal condensation, the prospective joint domain (interzone) is specified in the middle as the two cartilage elements develop and mature on either side of this domain (Smeeton et al., 2016). Within the interzone, cells produce signals that repress chondrocyte maturation to prevent the development of a single continuous cartilage element, instead producing a gap of relatively undifferentiated mesenchyme or immature chondrocytes. These cells go on to form the articular cartilage and joint-associated tissues such as ligaments and the synovial membrane, while the two cartilage elements mature and eventually ossify. In mouse appendicular joints, it has been demonstrated that there is an additional influx of cells into the joint-forming tissues from outside the interzone (Shwartz et al., 2016), although it is not clear if this is also true of zebrafish joints.

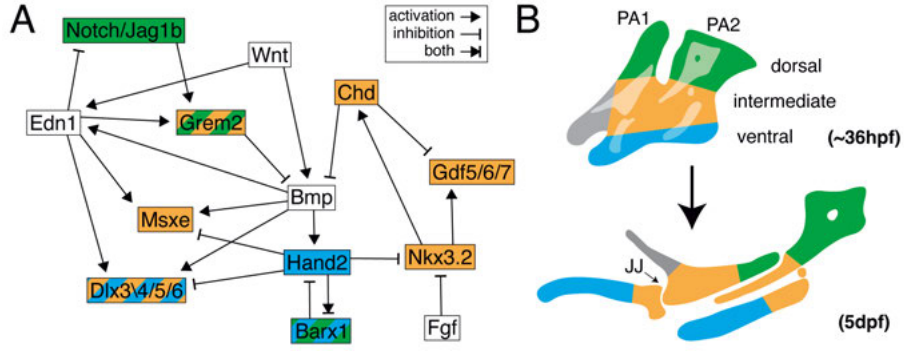

Figure 3. Gene regulatory network patterning the pharyngeal arches including the jaw joint. (A) Circuit diagram of known genes that interact to pattern the dorsal, intermediate, and ventral domains of the condensed mesenchyme in the pharyngeal arches. White boxes represent signals from overlying epithelia. (B) Schematic of embryonic pharyngeal arches 1 and 2 (PA1, PA2) colour coded into dorsal, intermediate, and ventral domains, and the same colours apply to the larval arches, describing their positional origin. JJ: jaw joint. Schematic modified from Barske et al. (2016).

In the development of the zebrafish jaw joint, the embryonic interzone arises from the intermediate domain of early condensing mesenchyme, which is specified by a complex network of interacting genes (Alexander et al., 2011;

Alexander et al., 2014; Barske et al., 2016; Nichols et al., 2013; Smeeton et al., 2016; Zuniga et al., 2010; Zuniga et al., 2011)(Figure 3). Several of these genes, including *nkx3.2* and *gdf5*, are specifically expressed in a subset of the intermediate domain that will form the jaw joint and induce downstream factors to promote joint cell fates in this region. However, after this initial specification of the interzone, joints aren't shaped entirely by genetic factors alone. Cyclic mechanical forces applied to the developing joint induce local cell growth patterns that are required to properly sculpt interlocking Meckel's cartilage and palatoquadrate surfaces in the larval zebrafish jaw (Brunt et al., 2015; Godivier et al., 2023), and this is mediated by Wnt signalling (Brunt et al., 2017).

Nkx3.2

NK3 homeobox 2 (Nkx3.2), also called Bapx1 or bagpipe, is a transcription factor first described as playing a role in the formation of the midgut musculature in the fruit fly *Drosophila* (Azpiazu and Frasch, 1993), but has since been studied extensively in the context of gnathostome skeletal development (Rainbow et al., 2014). *In vitro* and *in vivo* studies suggest Nkx3.2 functions as an inhibitor of chondrocyte maturation, maintaining chondrocytes in an immature state by directly repressing the expression of Runx2, a transcription factor that promotes the differentiation of osteoblasts and the maturation of chondrocytes (Provot et al., 2006; Yamashita et al., 2009). This transcriptional repressor activity is mediated by the binding of Nkx3.2 to SMAD proteins and the histone deacetylase protein HDAC1 (Kim and Lassar, 2003). Conversely, as chondrocytes are induced to mature and hypertrophy, *Nkx3.2* is negatively regulated (Choi et al., 2012). Nkx3.2 can also activate chondrogenesis in a context-dependant manner by repressing the expression of inhibitors of chondrogenesis, including *Runx2*, promoting the expression of *Sox9* (Lengner et al., 2005; Murtaugh et al., 2001). This induction and maintenance of chondrogenesis is implicated in the role of Nkx3.2 in the development of the axial skeleton from the sclerotome, where *Nkx3.2* is upregulated by Shh, Pax1, Pax9, and Meox1 (Murtaugh et al., 2001; Rodrigo et al., 2004; Rodrigo et al., 2003; Zeng et al., 2002).

A major role of Nkx3.2 has been established in the formation of the primary jaw joint of gnathostomes. Studies in the zebrafish, frog, and chick reveal a consistent focal expression domain of *Nkx3.2* between Meckel's cartilage and the palatoquadrate of the first pharyngeal arch skeleton (Miller et al., 2003; Wilson and Tucker, 2004), while in the jawless lamprey, *Nkx3.2* is expressed throughout the pharyngeal ectoderm and endoderm (Cerny et al., 2010; Kuraku et al., 2010). The jaw joint expression of *Nkx3.2* in gnathostomes is driven by Edn1 signalling (Miller et al., 2003; Nair et al., 2007) and restricted from expanding by Fibroblast Growth Factor (FGF) and Bone Morphogenetic

Protein (BMP) signalling (Wilson and Tucker, 2004) as well as the presence of Hand2 (Miller et al., 2003; Nichols et al., 2013)(Figure 3).

The absence of *Nkx3.2* expression leads to the loss of the jaw joint resulting from the fusion of Meckel's cartilage and the palatoquadrate in the zebrafish, frog, and chick (Lukas and Olsson, 2018a; Miller et al., 2003; Wilson and Tucker, 2004). On the other hand, when *nkx3.2* is overexpressed, additional (ectopic) joints can appear near the primary jaw joint (Lukas and Olsson, 2018b). Homologous to this joint is the incudomalleolar joint in the mammalian middle ear, and as *Nkx3.2* expression is present in this joint (Tucker et al., 2004), it might be expected that loss of Nkx3.2 in mouse embryos would result in a fusion between the incus and malleus. However, while there are defects in middle-ear associated structures such as the tympanic ring and gonium, where *Nkx3.2* is also expressed, the incudomalleolar joint itself appears unaffected (Tucker et al., 2004).

In addition to inducing the formation of some synovial joints by preventing chondrocyte maturation during development, Nkx3.2 also functions in maintaining the adult articular cartilage in an immature state required for its role in cushioning the bone surfaces. Osteoarthritis is associated with a downregulation of *Nkx3.2* in the articular cartilage, leading to a shift towards chondrocyte hypertrophy (Caron et al., 2015). Experimental overexpression of *Nkx3.2* has been shown to buffer against OA phenotypes in mice, reducing the severity and progression of the disease by preventing the maturation of articular chondrocytes (Oh et al., 2021).

Beyond joints, knockout of *Nkx3.2* expression in mice has been reported to result in defects in the axial skeleton, specifically the loss of vertebral ossification centres, and the loss of the supraoccipital bone and size reduction of the basioccipital and basisphenoid bones in the occipital region of the cranium (Lettice et al., 1999; Tribioli and Lufkin, 1999). Similarly, the rare human skeletal disease spondylo-megaepiphyseal-metaphyseal dysplasia (SMMD) is caused by homozygotic mutations in *NKX3.2*, resulting in defects in vertebral ossification and a short stature (Hellemans et al., 2009; Simsek-Kiper et al., 2019).

Gdf5

The GDF family of proteins are members of bone morphogenetic protein (BMP) class of the transforming growth factor beta (TGFβ) superfamily of ligands that play a major role during skeletogenesis (Salazar et al., 2016). Growth and Differentiation Factor 5 (Gdf5), also known as BMP14, CDMP1, and Contact, is translated into a large precursor protein with two key domains: a prodomain containing an N-terminal signal peptide, and a C-terminal mature domain (Fujimura et al., 2008). The precursor proteins pair up to form

homodimers at their mature domains before the prodomain is cleaved away, leaving the dimer of mature domains that constitute the active ligand (Gipson et al., 2020). This ligand is then transported outside of the cell where it interacts with two pairs of Type I and Type II transmembranal serine-threonine kinase receptors on other cells and triggers intracellular signalling that alters target gene expression (Baur et al., 2000; Klammert et al., 2015; Nishitoh et al., 1996). In addition to forming homodimers (e.g. Gdf5/Gdf5), BMPs including Gdf5 can form heterodimers with each other (e.g. Gdf5/Bmp2) which have altered diffusion properties and receptor binding affinities, and therefore potentially different functional activities that are just beginning to be explored (Kim et al., 2019; Gipson et al., 2023).

Experiments in chick and mouse limbs have revealed a role for Gdf5 in chondrogenesis, as overexpression of *Gdf5* during mesenchyme condensation leads to enhanced recruitment of mesenchymal cells, increasing the number of chondroprogenitor cells (Buxton et al., 2001; Tsumaki et al., 1999). Gdf5 also functions to promote chondrocyte proliferation, maturation, and hypertrophy, increasing the size of skeletal elements (Buxton et al., 2001; Coleman and Tuan, 2003; Storm and Kingsley, 1999). In the interdigital joints, a Turing mechanism of Gdf5 in concert with pSMAD and Nog functions to specify the initial joint domains during digit patterning (Grall et al., 2023).

Consistent with these functions in the appendicular skeleton, *Gdf5* expression in amniotes is detected in the condensing mesenchyme of the digits as well as the early knee, elbow, and interdigital joints (Merino et al., 1999; Shwartz et al., 2016; Storm and Kingsley, 1996). It functions in restricting joint markers to the joint-forming site (Storm and Kingsley, 1999) and promoting the differentiation of synovial joint tissues including the capsule and associated ligaments (Decker et al., 2015; Shwartz et al., 2016). In the frog and zebrafish, *gdf5* is expressed in the early limb/pectoral fin bud mesenchyme (Bruneau et al., 1997; Satoh et al., 2005) before being restricted to the joints later in development in frog (Satoh et al., 2005), while little is known about later pectoral fin expression in zebrafish. In addition to the pectoral fins, *gdf5* expression is also detected in the condensed mesenchyme of zebrafish median fins (Crotwell et al., 2001). *gdf5* is also expressed in the intramandibular joints in frogs and zebrafish, including the primary jaw joint, where it appears to be regulated by Nkx3.2 (Miller et al., 2003; Schwend and Ahlgren, 2009; Square et al., 2015).

There is an apparent paradox in that Gdf5 can simultaneously promote chondrogenesis in one context, but repress it in a joint interzone context. One proposed model to explain this dual role suggests that Gdf5 functions in the joint interzone to antagonise chondrogenic BMP signalling via competitive binding to the Bmpr1a receptor while promoting this same signalling when it binds to the Bmpr1b receptor found outside of the interzone (Lyons and Rosen, 2019).

Similar to Nkx3.2, Gdf5 plays a role in the maintenance of adult articular cartilage. During the development of OA, it appears that *Gdf5* is first upregulated in an attempt to repair the early phenotypes (Reynard et al., 2014), but as the disease progresses expression decreases (Kania et al., 2020). Indeed, human single nucleotide polymorphisms (SNPs) linked to the downregulation of *GDF5* tend to be associated with OA (Miyamoto et al., 2007; Evangelou et al., 2009), and attempts to increase *Gdf5* expression in articular cartilage are associated with lesion repair leading to a reduced severity of OA pathologies (Katayama et al., 2004; Parrish et al., 2017; Sun et al., 2021).

The mouse phenotype brachypodism is associated with knockout mutations in *Gdf5*, and characterised by a reduced limb bone length, reduced phalanges (brachydactyly), and deformations to the interdigital joints (Gruneberg and Lee, 1973; Storm et al., 1994; Storm and Kingsley, 1996; Settle et al., 2003). Similar phenotypes are seen in Grebe- and Hunter-Thompson-type chondrodysplasia, rare human genetic diseases also associated with homozygous mutations in *GDF5* (Martinez-Garcia et al., 2016; Thomas et al., 1996). Milder brachydactylies are also associated with rare prodomain or heterozygous mutations to *GDF5* in humans (Stricker and Mundlos, 2011).

Tendons and ligaments

Tendons develop in different parts of the body, and while many of the major regulators of tendon development are common to all these various tendons, the induction of tendon development can be driven by unique tissue interactions in different locations (Schweitzer et al., 2010). Axial tendons derive from the somites of the early embryo, which are divided into the sclerotome and dermomyotome (Nassari et al., 2017). Cells in the sclerotome later differentiate into skeletal tissues, while cells in the dermomyotome develop into the skin (dermis) and muscles. A subsection of the sclerotome that lies adjacent to the dermomyotome is termed the syndetome, and this is the progenitor of axial tendons, marked by the characteristic expression of the Scleraxis transcription factor (Scx) (Brent et al., 2003). Signals from the dermomyotome such as FGFs induce the formation of the syndetome from the sclerotome (Brent et al., 2005; Brent and Tabin, 2004), hence the syndetome is found adjacent to the dermomyotome. Additional signals from these three tissue populations keep them distinct from each other, such as Pax1 expression in the sclerotome repressing Scx (Brent et al., 2003).

Limb tendon progenitor cells arise from the lateral plate mesoderm rather than the sclerotome (Pryce et al., 2009), but are also marked by *Scx* expression, originally in dorsal and ventral sub-ectodermal patches of the proximal limb bud and moving distally as the limb bud grows (Murchison et al., 2007; Schweitzer et al., 2001). Signals from muscles are not required for progenitor induction in the distal limb, unlike axial progenitors (Kardon, 1998;

Schweitzer et al., 2001). These progenitor cells reorganise themselves in the limb until they are condensed and positioned between differentiating muscles and cartilage (Schweitzer et al., 2001), with the exception of progenitors in the autopod as they are first induced between muscles and cartilage, at least partially as a result of signals from the cartilage tissue (Huang et al., 2015). Cranial tendon progenitors are less well-characterised but are known to derive from the cranial neural crest, express *Scx*, and don't require signals from adjacent muscles for induction (Grenier et al., 2009). Throughout the body, TGFβ ligands are major signalling factors from the cartilage and muscles that induce the differentiation of tendon progenitors from adjacent mesenchyme (Pryce et al., 2009).

While the signals inducing the different tendon progenitors are varied in type and origin, more consistent signals for differentiation take over once these cells are aligned between muscles and cartilage. Both the adjacent muscle and cartilage tissues contribute signals to begin the differentiation and maintenance of tendons, including the expression of Scx (Chen and Galloway, 2014; Grenier et al., 2009; Edom-Vovard et al., 2002). Scx functions to upregulate the expression of many key structural tendon proteins involved in progenitor aggregation as well as in the mature tendon matrix. These include a range of collagens (Espira et al., 2009; Léjard et al., 2007), tenomodulin, which functions in the maturation of the collagen matrix (Docheva et al., 2005; Shukunami et al., 2006; Shukunami et al., 2018), and proteoglycans (Alberton et al., 2012). Scx-null mouse lines display normal early tendon progenitor cells, but then later have severe defects in the long force-transmitting tendons and intermuscular tendons as a result of the loss of many of these proteins (Murchison et al., 2007). However, ligaments and muscle-anchoring tendons are unaffected, indicating that Scleraxis is not required for the differentiation of all types of tendons or ligaments, but rather for tendon cell recruitment during elongation (Huang et al., 2019). Similar tendon defects are observed in zebrafish *scx* mutants, in addition to secondary skeletal deformations that indicate the influence of muscle attachments in cranial cartilage morphogenesis and rib mineralisation (Kague et al., 2019). Finally, Scx also functions in the progenitors of the enthesis eminence where tendons attach (Blitz et al., 2013; Killian and Thomopoulos, 2016). Later in development, tendons are matured and maintained by mechanical stimulation that promotes TGFβ signalling (Subramanian et al., 2018), leading to the upregulation of Scx (Maeda et al., 2011; Mendias et al., 2012) and downstream ECM component proteins including thrombospondin 4, tenomodulin, and collagen I (Jelinsky et al., 2010; Subramanian and Schilling, 2014; Subramanian et al., 2023).

Scleraxis was the first identified regulator of tendon cell fate and has since been intensively studied, but is clearly not the sole master regulator of tendon or ligament differentiation, necessary or sufficient for each stage of development. Other transcription factors with overlapping key roles in tendons and

ligaments that overlap with Scx include Early Growth Response 1 (Egr1) and Mohawk Homeobox (Mkx) (Subramanian and Schilling, 2015; Bobzin et al., 2021).

Mkx

Mohawk Homeobox is a TALE-family Iroquois-like homeodomain transcription factor that was also previously named Irxl1, and first identified as being expressed in a range of embryonic mouse tissues including overlapping with Scx in the syndetome and digit tendon progenitors (Anderson et al., 2006; Takeuchi and Bruneau, 2007). Like Scx, Mkx expression is responsive to mechanical stimulation, such that expression is positively correlated with the degree of mechanical stress (Maeda et al., 2011; Kayama et al., 2016). Although the onset of expression occurs later than Scx (Anderson et al., 2006), Mkx is involved in regulating many of the same genes, upregulating collagens, tenomodulin, fibromodulin, and decorin (Ito et al., 2010; Liu et al., 2010; Otabe et al., 2015), partially by upregulating TGFβ2 and therefore TGFβ signalling (Liu et al., 2015). This regulation of TGFβ2 is likely mediated by the interaction of Mkx (and Scx) with Smad3 (Berthet et al., 2013), a transcription factor with additional separate functions in suppressing muscle and cartilage cell fates (Kang et al., 2005; Liu et al., 2001).

Mkx can also function in a repressor complex to downregulate myogenic factors such as MyoD and cartilage factors such as Sox9 (Anderson et al., 2009; Chuang et al., 2014; Nakahara et al., 2013; Suzuki et al., 2016). By repressing the cartilage and muscle factors from adjacent tissues while upregulating tendon-specific genes, Mkx contributes to tendon differentiation and also the maintenance of mature tendons. As may be expected then, *Mkx*-knockout mice display defects in tendons and ligaments associated with reductions in tendon-specific gene expression and upregulation of chondrogenic/osteogenic genes leading to ossified tendons (Ito et al., 2010; Liu et al., 2019; Suzuki et al., 2016). Reduced *MKX* expression is associated with degenerated ligaments in osteoarthritis-affected joints (Nakahara et al., 2013), suggesting that MKX may play a role in future medical applications for tendon and ligament maintenance and repair (Nourissat et al., 2015).

Compared to the aforementioned studies on the role of Mkx in mouse and human tendons and ligaments, very little is known about the role of Mkx in zebrafish or other non-mammals. Zebrafish *mkx* morphants display craniofacial defects in the muscles and pharyngeal arches that may be associated with tendon defects, although an earlier role for Mkx in neural crest cell differentiation and migration has also been suggested on the basis of broader expression patterns and morphant phenotypes (Chuang et al., 2010).

Gene regulation

Despite their diverse morphologies and functions, almost all the cells in all the tissues of an adult organism possess the same genome, having descended from the same progenitor - the original fertilised egg cell. It is only through the process of development that this cell replicates and the different daughter cell populations differentiate into different tissues, or rather, it is this process of division and differentiation that constitutes embryonic development. The differentiation of embryonic cells into distinct cell types and tissues is caused by effector proteins and RNAs, but above this are multiple levels of regulatory control that form complex hierarchies and feedback loops whereby the expression or suppression of one set of genes results in the expression or suppression of a downstream set of genes. This spatiotemporal regulation of gene expression combined with feedback from the immediate cellular environment is what drives differentiation during development (Peter and Davidson, 2015). The primary mechanism of this regulatory control, and the one relevant to this thesis, is the cis-regulation of gene expression by transcription factor proteins.

Eukaryotic protein-coding genes are comprised of a non-coding promoter region and coding sequences (exons) separated by non-coding sequences (introns). The promoter region is comprised of DNA sequences with binding affinities for transcription factors and other mediator and cofactor proteins. When these proteins are present in the cell nucleus, they bind to the DNA of the promoter and recruit RNA polymerase II which begins to transcribe the gene into RNA. This RNA undergoes a process of maturation whereby the intronic sequences are spliced out, and finally the mature RNA is then exported from the nucleus and translated into a protein by ribosomes. As most gene promoters require binding by specific transcription factors to begin transcription, only cells in which those transcription factors are present will express the gene. For example, if a promoter requires a transcription factor that is only present in red blood cells to be activated, then this gene will only be expressed in red blood cells (Reddy et al., 1994).

Enhancers are short non-coding DNA sequences, with a wide range of possible sizes but averaging $\sim$400bp in length (Mills et al., 2020), that are very similar in principle and function to promoters (Andersson and Sandelin, 2020) but reside thousands to millions of base pairs away from the start of a transcriptional start site on the same chromosome (Lettice et al., 2003; Lee et al., 2020). They also possess specific transcription factor binding motifs for the purpose of regulating gene expression. The proteins bound to an enhancer and the proteins bound to a gene's promoter interact and bind to each other, forming a DNA loop that bring the enhancer and promoter DNA sequences into close proximity (Furlong and Levine, 2018; Chen et al., 2022). This looping is also driven by the cohesin ring and mediator complexes (Kagey et al., 2010). The resulting protein complex that forms at the transcriptional start

site enhances transcription of the gene, often making the difference between negligible expression and high expression (Figure 4).

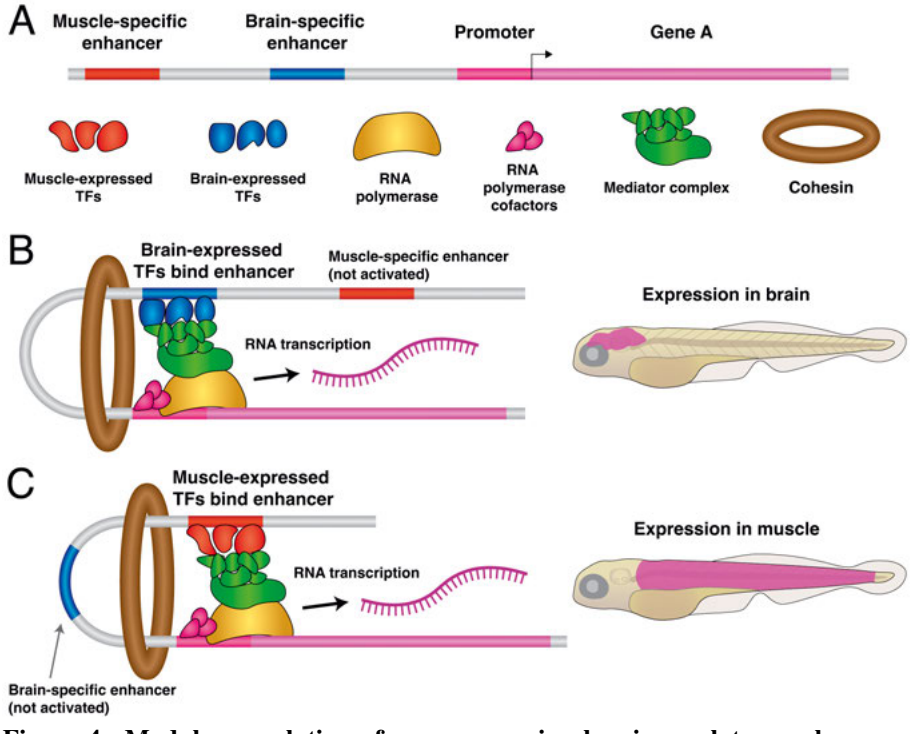

Figure 4. Modular regulation of gene expression by cis-regulatory enhancers. (A) Key components of cis-regulation by enhancers. Top: DNA sequence of Gene A, its upstream promoter element, and two upstream tissue-specific enhancers. Bottom: protein components involved in enhancer regulation, including transcription factors (TFs). (B) In the brain tissue, where the brain-expressed TFs are present, they bind to the brain-specific enhancer and lead to looping of the DNA via recruitment of cohesin and the mediator complex, and other cofactors help recruit RNA polymerase to the gene promoter to induce transcription, expressing Gene A in the brain. (C) In the muscle tissue, the same process takes place when the muscle-specific enhancer is bound by muscle-expressed TFs, leading to the expression of Gene A in the muscle.

Multiple enhancers can target the same gene, providing a modular gene regulatory mechanism (Chen et al., 2016a). This is particularly relevant for genes that are expressed in multiple distinct tissues, as their expression can be driven by different upstream factors. For example, Pax6 is expressed in multiple tissues in the developing mouse embryo, and multiple enhancers each contribute to a subset of the total gene expression: one enhancer promotes expression in the pancreas, another in the brain, and another in the retina and iris (Kammandel et al., 1999). These different tissues are characterised by the presence of different specific transcription factors, such that a pancreas-specific enhancer will contain pancreas-specific transcription factor binding motifs, and a brain-

specific enhancer will contain brain-specific transcription factor binding motifs. Enhancers contain multiple different binding motifs and therefore bind multiple transcription factors, some of which can be more general, including pioneer factors that make the condensed DNA (chromatin) accessible, and some of which can be more tissue-specific and actually activate the enhancers (Xu et al., 2021; Brennan et al., 2023). It is the unique combination of motifs that prescribe the specific regulatory function of each enhancer, not necessarily any single particular binding motif alone (Rowan et al., 2010).

Transcription factor binding is not an all-or-nothing event. The closer a DNA sequence motif is to the optimal sequence the transcription factor binds, the more the enhancer will be activated resulting in a greater degree of target gene expression. However, there is a trade-off between activity and cell/tissue-specificity, such that many enhancers have evolved to possess sub-optimal binding motifs in order to avoid ectopic expression of their target genes (Farley et al., 2015). This combinatorial specificity, dependent on the arrangement, spacing, and affinity of different binding sites in a given regulatory element (Farley et al., 2015; Grossman et al., 2018), permits extremely precise spatiotemporal control of gene expression.

Moving beyond the simple, idealised model of one enhancer per gene per tissue, in fact, multiple enhancers can exist with near-identical or overlapping activities to provide a degree of functional redundancy (Hobert, 2010; Kvon et al., 2021). In these cases, one enhancer may be sufficient to drive tissue-specific expression in most circumstances, with the other(s) only being strictly necessary in rare conditions, contributing to the robustness of gene expression in the face of genetic and environmental perturbations (Osterwalder et al., 2018; Perry et al., 2010; Wang and Goldstein, 2020). A single enhancer is also capable of contributing to the gene expression of multiple target genes, although this seems to be relatively rare and the target genes tend to be neighbours in a cluster of paralogous genes, all proximal to the shared enhancer (Guo et al., 2012; Tsai et al., 2016; Miller and Posakony, 2020).

The modularity of motifs and enhancer elements, along with their mutual redundancy also makes them extremely evolvable, as mutations can tinker with gene expression without severely disrupting the core expression domains and producing fatal developmental defects (Indjeian et al., 2016; Koshikawa et al., 2015; Prescott et al., 2015). Despite this, it is common to detect enhancers as conserved non-coding elements in multi-species genome alignments (Gehrke et al., 2015; Portnoy et al., 2005; Visel et al., 2008), indicative of a substantial degree of functional constraint, although this functional constraint is also possible without significant sequence constraint (Yang et al., 2015).

Zebrafish as a model organism

The zebrafish (*Danio rerio*) is a small (∼4cm long) freshwater teleost fish, first described in the early 19th Century (Hamilton, 1822). It's native habitats are the tropical streams, ponds, and rice paddies of South Asia, in and around India (Engeszer et al., 2007). Zebrafish were used by a small number of research groups as early as the 1930s to study behaviour and development (Laale, 1977), but it wasn't until the 1970s that it began to be established as a model vertebrate species. George Streisinger, a molecular biologist at the University of Oregon and fish hobbyist, wanted to study the vertebrate nervous system and development, but found the mouse (*Mus musculus*) quite intractable. After exploring the many fish species available in pet shops, he settled on zebrafish, known as an easy-to-raise and -maintain pet, and pioneered many of the fundamental lab and genetic techniques during the 1970s and 80s (Streisinger et al., 1981). Following his death in 1984, Streisinger's lab and work was taken up by Charles Kimmel, who continued to champion the widespread adoption of zebrafish as a vertebrate model species.

The key advantages of zebrafish as a model vertebrate species that originally struck Streisinger were numerous and still highly relevant today. Their small size and shoaling nature make them a space-efficient species, requiring approximately 200cm^3 of tank space per individual where a mouse or chicken, for example, require 10-100x larger cages each. Sexually mature females can produce several hundred viable eggs each week, which the males externally fertilise by releasing sperm into the water at the same time as the females release the eggs, so the timing of fertilisation can be controlled. The embryos develop externally and in a transparent chorion (soft shell), permitting close *in vivo* observation from the moment of fertilisation through to hatching, unlike many other organisms that either grow the embryos *in utero* (e.g. mouse) or have opaque eggs (e.g. frog). Finally, zebrafish develop extremely rapidly and have a short generation time - it takes just 24 hours to progress from a fertilised egg to a fish-shaped embryo with the basic body plan and tissues established (a mouse embryo takes almost 2 weeks to reach an equivalent stage), and just 10-12 weeks to a sexually mature adult (Westerfield, 2000).

During the late 1980s and early 90s zebrafish grew in popularity, marked by the publication of the standard embryological staging table (Kimmel et al., 1995), and "The Big Screen" in 1996. This screen was a massive effort driven by Christiane Nüsslein-Volhard, Wolfgang Driever, and Mark Fishman to chemically induce and genetically map thousands of individual mutations in zebrafish causing specific developmental defects, identifying 372 genes involved in various developmental processes (Haffter et al., 1996). This data set the stage for many future studies into the specific functions of hundreds of developmental genes.

In the last 3 decades, the number of publications featuring zebrafish has exploded, from <100 in 1990 to over 5,000 in 2016 (Meyers, 2018). In the 2000s, transgenic techniques using the Tol2 and Sleeping Beauty transposons were developed (Davidson, 2003; Kawakami, 2007; Kwan et al., 2007), and the genome was sequenced at the Sanger institute, finished and published in 2013 (Howe et al., 2013). Precise mutagenesis of the zebrafish genome with Zinc-Finger Nucleases (ZFNs) and Transcription Activator-Like Effector Nucleases (TALENs) were developed (Foley et al., 2009; Hwang et al., 2014) around the same time, although now for the most part superseded by CRISPR/Cas9 genome editing technology (Hwang et al., 2013; Varshney et al., 2015). Today, zebrafish are used as a model organism in many fields, from development (Bakkers, 2011; Schmidt et al., 2013; Tonelli et al., 2020) to regeneration (Gemberling et al., 2013), and from infectious diseases (Sullivan and Kim, 2008) to cancer biology (Liu and Leach, 2011) and toxicology (Hill et al., 2005).

Methods

Zebrafish husbandry

All animal experimental procedures were approved by the local ethics committee for animal research, Uppsala djurförsöksetiska nämnd (permit numbers C161/4 and 5.8.18-18096/2019). All procedures for the experiments were performed in accordance with the Swedish Board of Agriculture's Regulations and General Advice about Laboratory Animals. Embryos and larvae were sedated with 0.16% MS-222 (tricaine) and euthanised with an overdose of MS-222 (300mg/L).

Zebrafish embryos were grown in petri dishes containing egg water in 28.5°C incubators. Larvae were introduced to the embryo zone system tanks at 5 days post fertilisation (dpf) in 400mL system water and fed with rotifers until 10dpf when dry food was introduced. Water drops were also introduced at 10dpf followed by a low flow at 15dpf and high flow at 30dpf, raising the water volume to 3L or 10L. At 3 months post fertilisation (mpf), these zebrafish are classified as adults and moved to the main system. Adult zebrafish were kept in 3L or 10L system tanks with a water temperature of 28°C and a photoperiod of 14:10 light:dark hours in the SciLifeLab Genome Engineering Zebrafish Facility at Uppsala University. Adults were fed three times daily with dry pellets (2x) and rotifers (1x).

Conserved non-coding element identification and sequence analysis

Enhancers with a conserved function in regulating target gene expression are likely to possess a conserved sequence as the transcription factor-binding motifs are constrained by selection for binding the correct transcription factors. Therefore, to identify putative enhancer elements, I searched for Conserved Non-coding Elements (CNEs) located in the immediate vicinity of genes of interest as candidates for eventual *in vivo* analysis by generating transgenic reporter lines.

To ensure that this immediate vicinity of the genes of interest was homologous and thus capable of containing homologous CNEs, the synteny of the region immediately flanking the genes of interest was assessed with a manual review of the upstream and downstream genes in a range of Gnathostome species in

the Ensembl or NCBI genome databases. These Gnathostome species were selected based on two primary criteria.

First, the species must have a high-quality genome sequence publicly available, and second, in order to be able to make Gnathostome-wide conclusions, the selected species should include a good representation of all the major groups in the infraphylum. Therefore, the two broadest divisions of Gnathostomata: Osteichthyes and Chondrichthyes, had to be represented. Within Osteichthyes, both actinopterygians and sarcopterygians were included, and within these groups a phylogenetically diverse range of species was chosen. These included both non-tetrapod and a range of tetrapod sarcopterygians, and basal actinopterygians as well as several members of the more derived and highly diverse teleosts, including the zebrafish. It would have been desirable to include a similarly broad range of chondrichthyans, or at least represent the 3 primary clades Holocephahali, Selachimorpha, Batoidea, but at the time of part of the work in this thesis there was only one readily available high-quality whole-genome assembly available, that of the holocephalan elephant shark *Callorhinchus milii* (also known as the Australian ghostshark or plough-nose chimaera), so this became the sole representative of Chondrichthyes in most analyses of the *nkx3.2* enhancer JRS1. A greater diversity of chondrichthyan genomes representing the major clades was however included in the later analysis of the *mkx* locus. Representatives of both orders within the Cyclostomata, the inshore hagfish *Eptatretus burgeri* and sea lamprey (*Petromyzon marinus*, were used as a non-gnathostome vertebrate outgroup to ensure that any detected CNEs were Gnathostome-specific.

Sequences representing the gene of interest as well as the flanking 5' and 3' intergenic sequences from the chosen Gnathostome species were primarily extracted from the Ensembl database in FASTA format along with annotation data in VISTA format. Some other genome sequences were obtained from the NCBI Genomes database in FASTA format only, without annotation data. These sequences were aligned using the web-based mVISTA tool for the sensitive comparative alignment of long sequences (Frazer et al., 2004), which displays conservation as peaks along the aligned sequences. Aligned non-coding sequences of 100-1000bp marked by peaks of conservation were identified as CNEs and extracted for further analysis using the web-based MEME suite tools (Bailey et al., 2009). CNE sequences were searched for conserved motifs using MEME, and these motifs were matched to putative transcription factor-binding sites using Tomtom (Gupta et al., 2007) against the JASPAR Core (2018) Vertebrates database. The function of predicted transcription factor-binding motifs were inferred from a manual literature review of the transcription factors predicted to bind to these motifs.

Generation of transgenic constructs and zebrafish transgenesis

Transgenesis is a broad term for any introduction of foreign DNA into the genome of a particular organism. This DNA could be synthetic, from another species, or a complex construct combining multiple sequences of different origins. Applications for transgenic techniques are wide ranging, but in this thesis the purpose of transgenic experiments was to validate identified CNEs as active enhancer elements using fluorescent reporter constructs (Kvon, 2015).

Enhancer elements upregulate transcription when they are active, so the goal was to test whether or not identified CNEs were capable of this, using the production of a transcript encoding a fluorescent protein as a simple reporter for this activity. Therefore, we designed DNA constructs with a candidate CNE cloned upstream of the coding sequence for a fluorescent reporter protein such as mCherry. Even if the candidate CNE possesses enhancer activity, it will likely not be sufficient to drive substantial transcription of the reporter gene on its own, so a minimal promoter is added to the 3' end of the CNE sequence in the construct. This minimal promoter sequence is also unable to drive transcription by itself, so the reporter protein will only be produced if and when the candidate CNE acts as an enhancer. A poly-A tail is also added to the 3' sequence of the reporter coding sequence to aid in transcription termination and translation.

These constructs were produced using Multisite Gateway cloning (Invitrogen), a technology that involves recombining multiple DNA fragments from several plasmids into a single large plasmid construct combining all the desired elements: the candidate CNE with its minimal promoter, the reporter coding sequence, and the poly-A tail (Figure 5). First, specific primers were designed to amplify the CNE sequence from genomic DNA, with attB sites added to the 5' ends of both primers, along with the minimal promoter sequence in the reverse primer. The entry clone plasmid was produced by recombining the resulting PCR product into a pDONR plasmid vector via the BP reaction. The other two entry clones, containing the reporter coding sequence and the poly-A tail were obtained from the Tol2Kit (Kwan et al., 2007). All three entry clones were recombined into the pDEST vector containing tol2 sites via the LR reaction producing the final expression clone plasmid. At each recombination stage, att sites recombined between the fragment and vector to produce new att sequences in the process e.g. in the BP reaction, attB4 and attP4 sites recombine to produce an attL4 and attR4 site (Figure 5), catalyzed by the BP Clonase enzyme mix that includes integration host factor (IHF) and integrase. The LR Clonase Enzyme mix also includes both these enzymes, but with the addition of excisionase (Hartley et al., 2000; Walhout et al., 2000).

Following each recombination reaction, the resulting plasmids were transformed into chemically competent *E. coli* bacteria and cultured in the presence

of an antibiotic to produce a large number of copies of the plasmid, before undergoing plasmid extraction to isolate a concentrated plasmid solution for use in the next step. The plasmids contained antibiotic resistance genes against kanamycin or ampicillin to ensure only successfully transformed bacteria are cultured. The presence of a toxic ccdB gene between the att sites on the stock pDONR vector plasmid and pDEST plasmid ensured that only plasmids that successfully recombined, excising this gene and having it replaced by the desired inserts, would survive in the culture (Bernard et al., 1994).

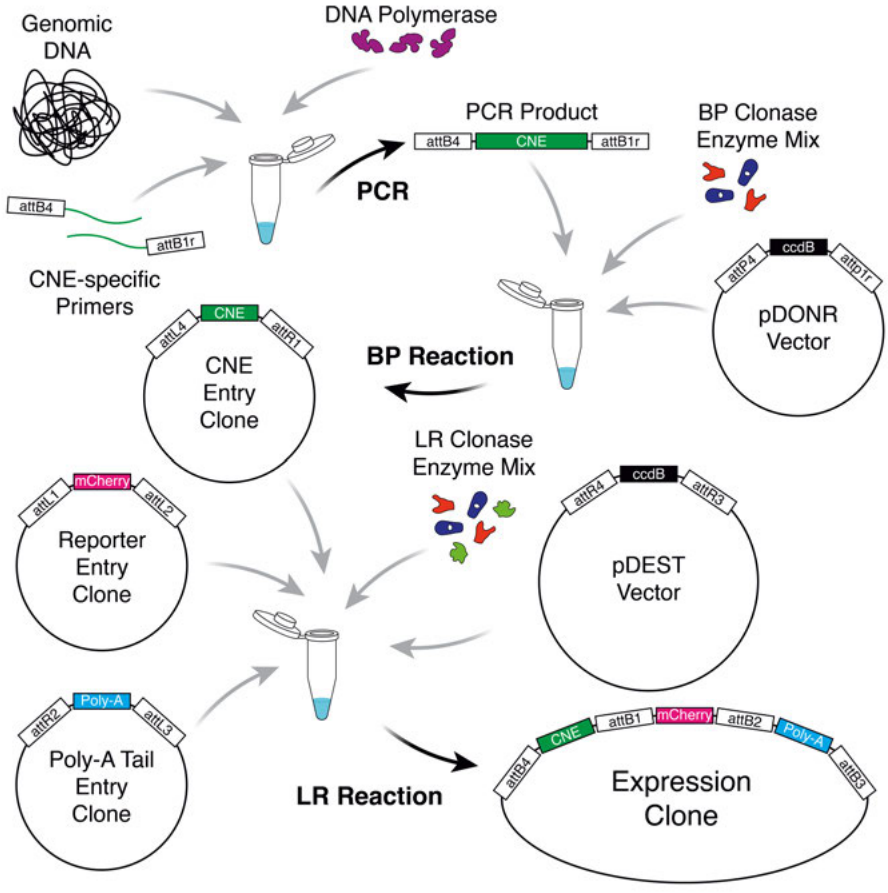

Figure 5. Gateway Cloning procedure. A PCR reaction with CNE-specific primers with flanking attB sites amplifies the CNE fragment. The BP reaction recombines attB and attP sites to produce the CNE in an entry clone plasmid. The LR reaction recombines multiple attL and attR sites from entry clones and the pDEST vector to produce an expression clone containing a reporter gene (mCherry) under the regulatory control of the upstream CNE.

The end goal was to incorporate the construct into the zebrafish genome such that the reporter construct is present in all the cells in the body. This allows the study of potential expression patterns of the reporter as the construct reports

the cells in which the enhancer is activated by the binding of tissue-specific transcription factors (Figure 6). These cells are the same in which the native enhancer is also active, informing us about how this enhancer contributes to the expression of its target gene, both spatially and temporally. If the CNE is an enhancer that is active in, for example, the jaw chondrocytes in a given time window, then a fluorescent signal would be observed in those chondrocytes during that time window. If the CNE lacked enhancer activity, no fluorescent signal would be observed.

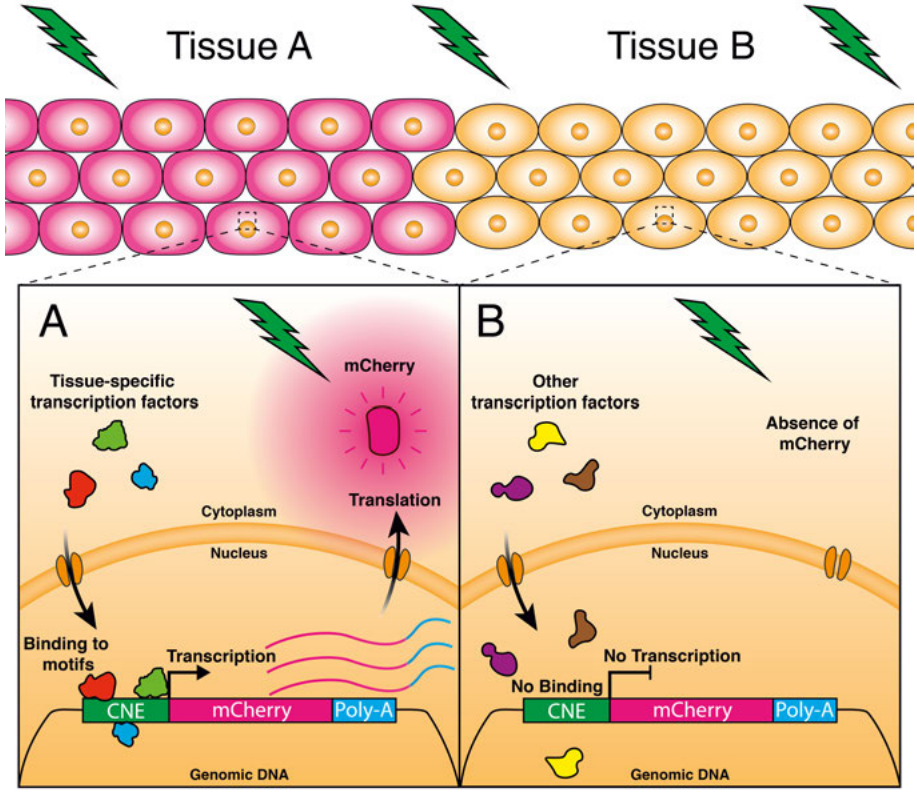

Figure 6. The reporter construct marks cells activating the candidate enhancer with mCherry fluorescence. (A) Tissue-specific transcription factors bind to the enhancer sequence of the transgenic construct in the genome, activating transcription of the reporter mCherry gene in this tissue and labelling it with the fluorescent protein upon excitation with green light (lightning bolts). (B) Other transcription factors present in the cells of a different tissue are unable to bind to the enhancer sequence, so mCherry is not transcribed and the tissue is not fluorescently labelled.

In order to integrate this reporter construct into the zebrafish genome, a solution containing the construct is injected into many zebrafish embryos as early as the one-cell stage of early embryonic development. mRNA coding for the Tol2 transposase was also added to the injected solution, as this gets translated

in the embryo to produce the Tol2 transposase enzyme which recognises Tol2 sites flanking the reporter construct, excising the construct between them and integrating it semi-randomly into the genome (Kawakami, 2007). The final component of the injection mix was phenol red, a dye that makes it easier to identify the location and volume of the injection.

The mix was injected into or close to the blastomere of the one-cell stage embryo. Ideally, the reporter construct should be integrated into the genome of this first cell, and as this cell repeatedly divides to produce all the cells of the body of the larval, juvenile, and ultimately adult fish, the reporter construct would be replicated into all these cells. However, it takes some time for the transposase to be translated and to act, so it is more common for zebrafish injected at the one-cell stage to only integrate the construct in one of the cells at the 2-cell or 4-cell stage, resulting in mosaic adults with variable presence of the construct.

For this reason, injected larvae (the F0 generation) were screened for mosaic reporter expression from 1-5dpf, and positive larvae were grown to adulthood before being outcrossed with wild-type zebrafish. The offspring of this cross (the F1 generation) were screened again as larvae. F0 fish with the reporter construct present in the germline, i.e in the genomes of its egg or sperm cells, produced stable transgenic F1 offspring containing the reporter construct in 100% of their cells. These F1 fish were then raised to adulthood and regularly bred to produce F2 fish stably expressing the transgenic construct, which themselves were raised and outcrossed to produce F3 fish, and so on, when the line required renewing as the F1 parents aged.

These enhancer reporter transgenic lines were regularly crossed with background reporter lines to produce double-transgenic offspring. The background reporter expression is extremely useful for determining precisely which tissues the enhancer is active in, serving as anatomical references. For example, background transgenic lines used in this thesis include *col2a1a:EGFP* (Dale and Topczewski, 2011) and *mylz2:GFP* (Ju et al., 2003), both expressing green fluorescent protein (GFP) under the control of full promoters rather than enhancers with minimal promoters. *col2a1a:EGFP* is expressed in chondrocytes, while *mylz2:GFP* is expressed in fast-twitch muscles, labelling these tissues with a bright green fluorescence. Transgenic background reporter lines were also used to study mutant phenotypes by fluorescence live-imaging cartilage structures affected by gene mutations.

Genome editing using CRISPR/Cas9

To study the function of a protein-coding gene, a commonly used technique is to prevent its translation into a functional protein in an organism and then observe the phenotypic effects caused by its absence. This type of functional evidence is called "loss-of-function" evidence and is often produced by introducing mutations to the gene. As all vertebrates are diploid, possessing two copies (alleles) of each gene in chromosome pairs, to completely knock out a target protein-coding gene, homozygous mutants with both alleles knocked out must be produced, while organisms with one functional gene copy and one knocked out copy are termed heterozygous mutants. Typically, homozygous mutants are produced by simply breeding two heterozygous parents to produce 25% homozygous offspring.

CRISPR/Cas9 is a genome editing technology derived from the natural phage defence systems of prokaryotes (Cong et al., 2013). Prokaryotic CRISPR/Cas systems can be categorised into two classes each with 3 subtypes, where Class II represents the primary collection of systems adapted for genome editing, within which Type II utilises Cas9 (Barrangou and Doudna, 2016; Tang and Fu, 2018) as I will outline below. CRISPR refers to the Clustered Regularly Interspaced Short Palindromic Repeats found in many prokaryotic genomes that derive from previous unsuccessful phage infections and have been co-opted by these prokaryotes to recognise and negate future infections (Marraffini, 2015). When a phage's DNA enters a prokaryotic cell, all four Cas (CRISPR-associated) proteins, Cas1, Cas2, Csn2, and Cas9, assemble into a complex that captures fragments of this genetic material adjacent to short DNA sequences called Protospacer Adjacent Motifs (PAMs) and then Cas1 and Cas2 inserts them into the CRISPR locus in the form of a so-called "spacer" DNA sequence (Heler et al., 2015; Wilkinson et al., 2019). Interestingly, in the Type I CRISPR/Cas system of *E. coli*, this integration into the genome by Cas1 and Cas2 is aided by IHF, the same Integration Host Factor enzyme that featured in the BP and LR reactions in the above transgenesis section (Nuñez et al., 2016; Wright and Doudna, 2016).

In the CRISPR array, spacers are separated by short palindromic repeats that are generated as the spacer is integrated. As the entire CRISPR locus is transcribed, the spacers and repeats are transcribed into one long RNA called pre-crRNA. tracrRNAs transcribed from elsewhere in the CRISPR locus bind to the repeats in the pre-crRNA, forming duplexes, and recruit the Cas9 enzyme and RNAse III (Deltcheva et al., 2011; Charpentier et al., 2015). The latter cleaves the pre-crRNA into short crRNAs to release isolated complexes of crRNA, tracrRNA, and Cas9 enzyme, called ribonucleoprotein (RNP) complexes. Each crRNA contains the repeat sequence that forms the duplex with the tracrRNA, in addition to an individual spacer sequence. As the CRISPR locus is comprised of many spacers, this process produces a variety of unique

crRNAs and subsequent RNPs, with all the spacers represented (Marraffini, 2015).

An RNP complex binds to the DNA of infecting phage by recognising the sequence that is complementary to the spacer sequence in the crRNA and then the Cas9 enzyme cleaves the DNA at this locus, preventing the virus from propagating and killing the cell. However, the complementary DNA sequence is also found in the CRISPR locus, the source of the crRNAs, and it would be problematic if this complex also bound and cleaved the prokaryote's own DNA. This doesn't happen because of the lack of the aforementioned PAM site, as Cas9 can only cleave dsDNA if the complementary sequence of the spacer is found immediately adjacent to a specific PAM sequence. This isn't the case in the CRISPR locus in the prokaryote's own genome, but it is the case in the genome of the infecting phage, as it was also required for the specific binding the Cas9 enzyme that, in concert with the Cas1, Cas2, and Csn2 proteins, produced the specific spacer sequence in the first place (during the previous infection) (Heler et al., 2015; Wilkinson et al., 2019).

If the cell (or its ancestors) never previously survived infection by a virus with a genetic sequence represented by a spacer sequence in the cell's CRISPR locus, it will lack a complementary spacer and therefore fail to cleave the viral DNA. A prior infection is required to prevent a future one. For this reason, CRISPR/Cas systems are sometimes referred to as prokaryotic "adaptive immune systems" (Barrangou et al., 2007).

This principle of guiding the Cas9 enzyme to a specific DNA sequence using a complementary RNA oligonucleotide clearly had potential for precise genetic engineering (Jinek et al., 2012). It was rapidly developed into a tractable and customisable system that has now been widely adopted, largely superseding slightly older methods such as TALENs (Joung and Sander, 2013; Varshney et al., 2016). Synthetic single guide RNAs (sgRNAs) that combine the sequences of the crRNA and tracrRNA of natural CRISPR systems into a single oligonucleotide are designed to be complementary to target sites in the genomes of the organism of interest. These target sites represent desirable locations to introduce mutations and must be adjacent to a PAM site (e.g. 5'-NGG-3', where "N" represents any base). When the genome is cleaved at this target site, the cell automatically attempts to repair the double-strand break through the process of Non-Homologous End-Joining (NHEJ).

The repair process is often successful, but typically imperfect, as a small number of nucleotides are either inserted in between the blunt ends or deleted from both ends, resulting in insertions or deletions (INDELs) to the target sequence (Figure 7). This is the most common use of CRISPR/Cas9 technology - introducing INDELs into a protein-coding sequence (exon) with the intention of disrupting the codon reading frame. When the number of inserted or deleted bases is not a multiple of 3 (e.g. +1bp, +4bp, -7bp, etc) the codon reading

frame is said to be "frameshifted" such that after the INDEL site, the amino acid chain will be translated from the sequence is completely different from the functional wild-type sequence. This alone would likely be sufficient to knock-out the function of the protein, provided the INDEL was targeted early in the sequence, but the frame shift also results in the introduction of premature stop codons that completely terminate translation and result in a highly truncated protein that we can be sure has its function nullified. It is these mutants, with premature stop codons that effectively eliminate key functional parts of the protein, that are analysed for phenotypic effects in order to infer the function of the gene.

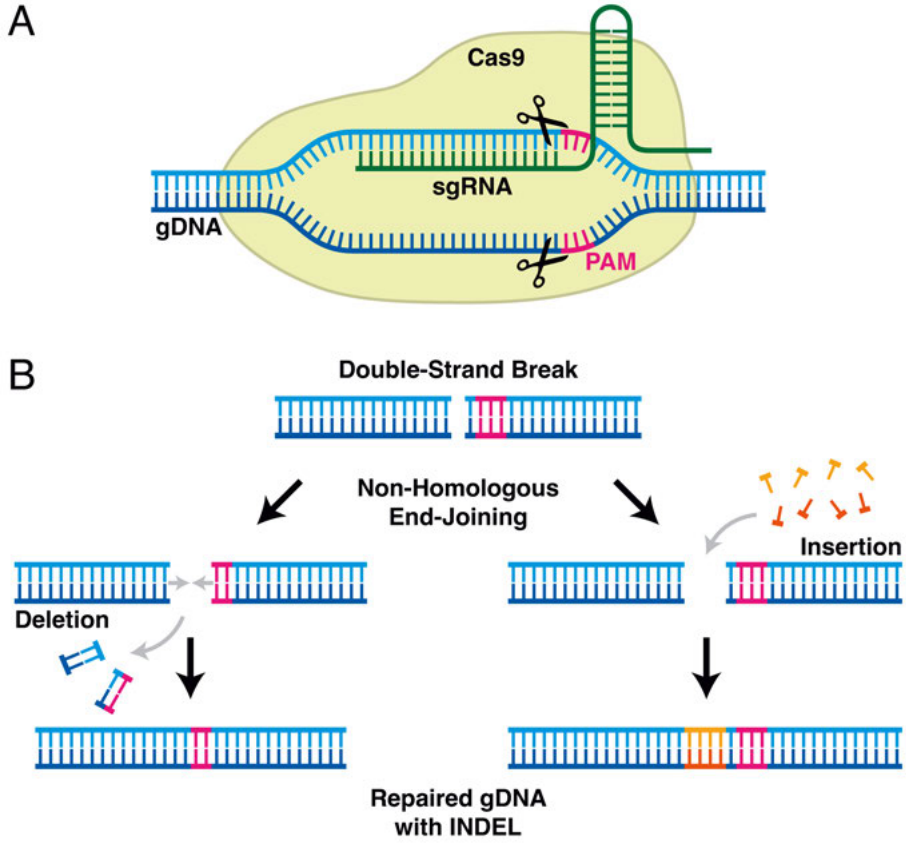

Figure 7. CRISPR/Cas9 genome editing. (A) The RNP opens up the double stranded DNA and the sgRNA sequence binds to the complementary DNA sequence. If the PAM sequence is present downstream of this sequence, the Cas9 induces a double-strand break at the target site. (B) The cell autonomously repairs double-strand breaks by non-homologous end-joining, typically resulting in insertion or deletion mutations at the target site.

We designed sgRNAs to target the exons of *nkx3.2* and *gdf5*, upstream of the sequences coding for the DNA-binding domain and ligand-forming mature domain that are essential for their respective functions. These sgRNA sequences were designed using the web tool CHOPCHOP (Labun et al., 2016) to avoid any off-target sequences and be adjacent to a Cas9 PAM site, sometimes modifying the first 2 nucleotides to GG to allow T7 transcription. DNA sequences of the sgRNAs were synthesised according to Varshney et al., 2016 and transcribed using the T7 promoter sequence via the HiScribe T7 High Yield RNA Synthesis Kit. Cas9 mRNA was transcribed using the mMessage mMachine T3 Transcription Kit. The sgRNA and Cas9 mRNA were purified and injected into zebrafish embryos at the one-cell stage, following the same principle as the injections for transgenesis described earlier.

F0 injected fish were raised to adulthood and incrossed to produce the F1 generation. These F1 fish were genotyped using Fragment Length Analysis (FLA). This involved using PCR to amplify the target sequence from gDNA of a tissue sample (caudal fin clip) and running the product through a capillary on a 3130XL ABI Genetic Analyzer (Applied Biosystems) to precisely determine its length. This length was then compared against the expected length from the non-mutated target site product to infer how many bases have been inserted or deleted at the target site. This was further confirmed by Sanger sequencing to examine the sequence. An individual heterozygous mutant was chosen based on the presence of an INDEL that caused a frame-shift and premature stop codon, and outcrossed with wild-type fish to produce heterozygous F2 offspring. These F2 fish were then incrossed to produce a number of homozygous mutants that could be studied for potential phenotypic effects.

Introducing a small INDEL into an exon can be sufficient to completely disrupt a protein-coding gene because of the nature of a codon-based translation system, but to knock out a non-coding regulatory element like an enhancer that instead functions through a series of transcription factor-binding sites, a different approach was needed (Ho et al., 2015; Osterwalder et al., 2018; Cunningham et al., 2018). Rather than introducing mutations to the *nkx3.2* enhancer sequence JRS1, we chose to delete the sequence from the genome entirely by co-injecting a pair of sgRNAs targeted to sites flanking the enhancer. As double-strand breaks were simultaneously introduced on either side of the enhancer sequence, this fragment was excised prior to the repair of the flanking sequences by NHEJ, deleting the sequence from the genome. As the deleted sequence is quite large - several hundred base pairs - genotyping was possible using conventional gel electrophoresis rather than FLA, following PCR with primers flanking the deletion region. A stable heterozygous zebrafish line was produced and incrossed to produce homozygous mutants as previously described.

Quantification of gene expression

Real-Time Quantitative Polymerase Chain Reaction (qPCR) was used to quantify the gene transcript levels between wild-type, heterozygous, and homozygous JRS1 enhancer mutant zebrafish. My samples comprised 6dpf larvae of these different genotypes, with the goal being to quantify the effects of the enhancer deletion on the expression levels of genes of interest.

A small piece of the tail of each euthanised larva was removed for genotyping, and larvae were then stored in RNAlater at -20°C until the genotyping was completed and larvae could be pooled into small groups according to their genotype. This is because single larvae are too small to yield a useable amount of RNA for this method. RNA was isolated from groups of genotyped larvae using TRIzol homogenisation followed by ethanol precipitation and genomic DNA digestion using DNase I, and stored at -80°C. This RNA was then copied into complementary DNA (cDNA) using reverse transcriptase enzymes and random hexamer primers, then stored at -20°C.

Pairs of primer oligonucleotides were designed to target specific genes of interest. These amplify cDNA strands that were produced from RNA transcripts of these genes. When possible, these primers were designed such that one of each pair crossed an exon-exon boundary in the processed transcript. This ensured that the primers would not amplify PCR products from any genomic DNA that might contaminate the reaction, as the exon sequences in the genome are separated by introns which are spliced out in transcripts and cDNA.

Each qPCR reaction contained sample cDNA, primers, and SYBR Mix (ThermoFisher Scientific) in water. The SYBR mix contains free nucleotides, DNA polymerase, various buffers, and the SYBR Green fluorescent dye. A standard 40 cycle PCR program was used with 15s at 95°C, 15s at 58°C and 60s at 72°C. As the temperature is cycled, the cDNA denatures and separates into single-stranded DNA (at 95°C), the primers anneal to their complementary sequences (at 58°C), and DNA polymerase synthesises complementary DNA between the primers to produce a new copy of the sequence of interest (at 72°C). This continues for 40 cycles, where the number of target sequences is approximately doubled every cycle, resulting in a gradual increase in the prevalence of the target sequence in the reaction from a minority to a vast majority.

Quantification of transcript abundance is made possible by the presence of the SYBR Green dye in the reaction that binds to double-stranded DNA to form a fluorescent complex. By reading the level of fluorescence, it is possible to quantify the double-stranded DNA concentration in the reaction volume as the cycles progress. As the sequence of interest targeted by the primers is amplified and increases in prevalence, there is a point where the fluorescence crosses a readable threshold. As the doubling of target sequences after each

qPCR cycle is quite consistent, even small differences in the initial concentration of the target sequence can result in significant differences in the timing of when that threshold is crossed. A sample with more transcripts of the gene of interest will require fewer cycles to reach the threshold, and a sample with fewer transcripts will require more. In this way, the number of cycles it takes for a reaction to cross this threshold (the Cycle threshold - Ct) is a measure of the number of transcripts of the targeted gene of interest that were initially present in the sample, i.e. the gene expression level. Standard dilution curves (R^2>0.99) were used to validate primer efficiencies, and specificity was validated using melt curves as well running PCR products on 2% agarose gels to identify a single band of the expected product size.

As there can be differences in the number of cells present in each initial sample, it's possible that Ct values could be skewed by these differences. To correct for this, gene expression levels of the gene of interest calculated by the Ct values are normalised against a constitutively expressed "reference" gene, in my experiments *rpl13a*. This gene produces 60S ribosomal protein L13a, an essential protein expressed in all cells. Following normalisation, expression of the gene of interest was compared between genotypes to obtain relative expression levels using the Pfaffl method (Pfaffl, 2001).

Skeletal staining

Skeletal phenotypes in larvae and juvenile zebrafish were assessed using skeletal staining. In this procedure, two chemical dyes, Alcian blue and alizarin red are used to stain cartilage blue and mineralised tissues (bones, teeth, and scales) red, respectively (Walker and Kimmel, 2007). Alcian blue binds to the mucopolysaccharides and glycosaminoglycans that are concentrated in the extracellular matrix of cartilage, while alizarin red binds to the calcium in the hydroxyapatite (calcium phosphate) of mineralised tissues. Following staining, the specimens can be bleached to remove any pigmentation and their tissues cleared to make the entire body transparent but still intact, permitting imaging of the stained internal skeletal structures (Figure 8).

Larvae and juveniles were euthanised with an overdose of MS-222 (300mg/L) and fixed overnight in a solution of 4% Paraformaldehyde (PFA) in 1x Phosphate Buffered Saline (PBS) to prevent decomposition and ensure longevity of the specimens, followed by a gradual dehydration into 50-70% ethanol solutions and stored at -20°C. Alcian blue solution was made with 0.02% Alcian Blue 8 GX and 50mM $MgCl_2$ in 70% ethanol, and alizarin red solution was made with 0.5% Alizarin Red S in water. Young larvae (<5dpf) were typically stained only with Alcian blue as they don't yet have any mineralised tissue, while older specimens were typically stained with both Alcian blue

and alizarin red solutions in a 100:1 ratio. Staining was performed at room temperature overnight.

Following staining, larger specimens were washed several times in 50% ethanol and water to remove unbound staining solution. Next, specimens were transferred to a bleaching solution of 1.5% H_2O_2 and 1% KOH in water and incubated at room temperature for approximately 30 minutes or until all visible pigmentation had been removed. Clearing was performed at room temperature first in a solution of 20% glycerol and 0.25% KOH in water, followed by 50% glycerol and 0.25% KOH in water and long-term storage in 50% glycerol and 0.1% KOH in water at 4°C. The lengths of each clearing time varied with specimen size and ranged from 30 minutes to several hours. Prior to clearing, large juveniles underwent a ∼20-minute digestion step in a solution of 1% trypsin in 35% Sodium Tetraborate Decahydrate (borax) to digest some of the translucent external tissue, improving the clarity of the specimen and in many cases enabling the easy removal of the skin and scales. This digestion also made it easier to dissociate the specimen for imaging of isolated structures such as the pectoral fins.

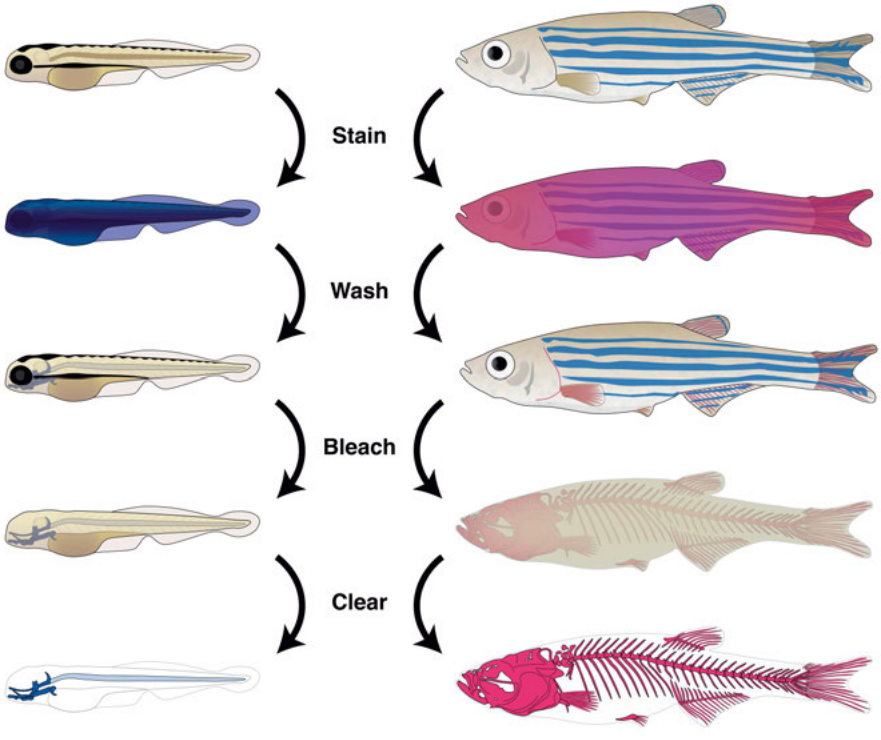

Figure 8. Skeletal Staining Procedure. Fixed zebrafish larvae (left) and juveniles (right) go through successive stages of staining, washing, bleaching, and clearing for visualisation of cartilage and bone in the skeleton. The procedure is described in detail in the main text.

Microscopy

Standard bright-field imaging of stained specimens was performed using a Leica M205 FCA fluorescence stereomicroscope and the attached Leica DFA 7000T camera without fluorescent light or filters. Stained specimens were mounted in glycerol on a watch glass, 35mm glass-bottomed dish, or microscope slide, depending on the desired orientation. The same microscope was used for screening and initial fluorescent imaging of live transgenic lines using the GFP and mCherry filters.

A Leica TCS SP5 inverted confocal microscope was used for higher-resolution live fluorescent imaging and time-lapses. Zebrafish embryos/larvae were anaesthetised using 0.16% MS-222 and embedded in 0.5% or 0.8% low-melting agarose containing 0.1% MS-222 on a 35mm glass-bottomed dish, covered in system water containing 0.16% MS-222. The excitation/emission wavelengths for EGFP were 488/507 and mCherry 587/610nm. Image stacks were combined into maximum projection images using the Leica Microsystem LAS-AF software or ImageJ (Schindelin et al., 2012).

Optical projection tomography

Conventional 2D imaging is suitable for many applications, but when analysing 3D skeletons, it can be difficult to image some anatomical structures from the optimal angle for reliable comparisons between specimens. Errors in imaging angle could lead to inaccurate measurements, and often the time required to manually position specimens as accurately as possible makes it inconvenient or infeasible to image a large number of specimens, limiting sample sizes.

Therefore, it is important to image fish skeletons in 3D to comprehensively characterise phenotypes. Optical Projection Tomography (OPT) (Sharpe et al., 2002; Sharpe, 2003) involves taking images of specimens from multiple angles; usually hundreds of images through 360 degrees of rotation, and using computer software to reconstruct a high-resolution 3D volume comprised of 3D pixels called voxels. Software can be used to align multiple specimens to produce average morphologies of a large number of specimens, and to compare different groups of specimens (e.g. different genotypes), highlighting even subtle phenotypic differences and permitting quantification and statistical analysis of these differences based on voxel intensity data.

The custom bright-field zOPT system used in this thesis was capable of imaging skeletal stained zebrafish larvae up to 9dpf (Allalou et al., 2017; Zhang et al., 2020). These specimens were manually pipetted into a capillary between a light source and camera, and images were captured at a 1.15μm pixel resolution as the capillary was rotated around 360 degrees by a stepper mo-

tor. A Filtered Back Projection algorithm and the ASTRA Toolbox (Palenstijn et al., 2013) were used for tomographic reconstruction in MATLAB (Release R2015b; MathWorks, Natick, MA), and volumes were aligned using the registration toolbox elastix (Klein et al., 2010; Shamonin et al., 2014). When quantification of between-group differences was necessary, individual fish were aligned to an average wild-type, and a voxel-wise method was used to detect voxels that differed significantly between groups. These differences represent the presence, absence, or differential density of a stained skeletal structure in a particular location in 3D space, i.e. morphological phenotypes. Manual segmentation of skeletal elements from individual fish or group averages also made it possible to examine these phenotypes more closely.

Geometric morphometrics

To analyse shape changes in mutant phenotypes, specifically the shape of the posterior Meckel's cartilage in JRS1 enhancer deletion mutants, 2D geometric morphometrics was performed on lateral maximum projection images obtained via OPT of 9dpf skeletal-stained larvae. This method mathematically describes the shape of the posterior Meckel's cartilage in order to align and compare them, displaying and quantifying how they differ between genotypes.

Sliding landmarks were digitized along the curved surface of the posterior Meckel's cartilage of groups of wild-type, heterozygous mutants, and homozygous mutants. These landmarks were then aligned using Generalised Procrustes Analysis to minimise the variability due to size and rotation and instead optimise the landmarks using minimised bending energies (Bookstein, 1991) to represent specific shape changes. The morphospace was examined using Principal Components Analysis (PCA) in the geomorph R package (Adams et al., 2021) and plotted using the borealis package (Angelini, 2021). Shifts in the morphospace were tested for significance with pairwise tests of linear model fit between a model based on allometric differences alone and a model based on allometric differences and differences in genotype.

All additional statistical analyses and visualisation (ggplot2; Wickham 2016) of quantitative data was also performed in R (R Development Core Team, 2021), and all P-values were adjusted for false discovery rate (FDR; Benjamini and Hochberg 1995).

X-ray micro-computed tomography

X-ray micro-Computed Tomography (μCT) is another method for 3D imaging with a micron-scale resolution, which uses X-rays in order to visualise structures based on material density with applications in metrological, geological, and biological imaging (Withers et al., 2021). There is a negative relationship between the wavelength (λ) of light and its energy (given by the equation $E = \frac{hc}{\lambda}$, where h is Planck's constant and c is the speed of light in a vacuum, another constant), such that smaller/shorter wavelengths possess higher energies. The wavelength of visible light ranges from approximately 400-700nm with energies on the order of 2eV (electron volts) while X-rays typically inhabit the 0.01-10nm wavelength range and can possess energies up to 200keV (kiloelectron volts)(Bearden, 1967; Tschentscher and Suortti, 1998). These properties allow X-ray light to pass through low-density structures such as skin and flesh with little refraction, while more dense tissues such as mineralised bone are able to partially block the penetration of photons. The principle behind traditional X-ray imaging, then, is to position a specimen between an X-ray source and a detector to collect an image of the photons that passed through the sample - the X-ray "shadow". The greater the electron density of the sample (either due to a large volume or by the presence of elements of high atomic number), the fewer photons project onto the screen of the detector (Germain and Ladevèze, 2021).

The X-rays are produced by an X-ray lamp which contains a cathode and anode, where the cathode is connected to the negative pole of a high voltage source and the anode to the positive pole. The cathode filament is heated to cause it to emit negatively-charged electrons, and the electric potential between the cathode and anode causes the electrons to accelerate towards the positive anode. On the surface of the anode is a dense metal (e.g. tungsten) target (Zhou et al., 2016). As the electrons enter this target material, they interact with the positively-charged nuclei and their motion is deflected and slowed. When electrons are slowed down they release energy in the form of photons, and the more they are slowed, the more energy they release in the form of shorter wavelength radiation such as X-rays. This relationship is described by rearranging the earlier equation to $\lambda = \frac{hc}{\Delta E}$, where ΔE is the difference in the energy of the electron before and after being slowed. This type of radiation is called *Bremsstrahlung*, German for "braking radiation". Depending on how closely an electron in the beam interacts with the nuclei of the target material, it will be slowed by different amounts and therefore generate X-rays with a range of different energy levels (with the upper limit being set by the acceleration voltage applied to the circuit). As a result, X-rays with a wide range of energies are produced. This X-ray spectrum is typically filtered through thin sheets of metal such as aluminium, copper, or tungsten to narrow the spectrum of energies in the beam, producing a "pink beam" from an original "white beam". By removing the lowest-energy X-rays that are more prone to scatter

and absorb in the specimen being scanned, noise and beam-hardening artefacts can be reduced (Du Plessis et al., 2017), and sometimes the highest-energy X-rays are filtered out to reduce saturation when scanning small or less dense specimens (Sanchez et al., 2012).

The detector is a regular camera sensor, but this alone would be unable to detect any X-rays - they would penetrate through the detector without interacting with the sensor array. Instead, in front of the detector is a scintillator: a sheet of crystal with specific properties that converts X-rays to visible light through a process called scintillation, which is similar to phosphorescence. The X-ray photons are absorbed by the scintillator material, giving its atoms a higher (excited) energy state, and to return to their original state, they immediately release the energy in the form of photons in the visible spectrum. These higher wavelength photons can then be detected by the camera sensor and form the image. The thickness of the scintillator influences the imaging resolution, because thicker scintillators can laterally spread or scatter the light, increasing the signal but at the expense of blurring the image. For the highest resolutions, extremely thin or structured scintillators are used (Martin and Koch, 2006; Douissard et al., 2012; Wollesen et al., 2022).

Naturally, the resolution of the detector also limits the resolution of the obtained images, but how this relates to the actual resolution in terms the pixel size is determined by the relative distances between the X-ray source, the sample, and the detector (Vásárhelyi et al., 2020). This is because, in lab-based μCT scanners the X-rays are emitted as a cone-shaped beam, so moving the sample closer to the source casts a larger "shadow" on the detector such that each pixel represents a smaller area of the sample i.e. higher spatial resolution at the expense of a reduced field of view.

As they are both types of tomography, the general principle of μCT is the same as OPT; the specimen is repeatedly imaged while rotating and these individual projection images are used to reconstruct cross-sectional slices that can be stacked into a 3D volume. For older ($\sim$>60dpf) zebrafish with mineralised and therefore denser skeletal structures, μCT can be used to image the skeleton of fixed specimens for characterising wild-type morphology and mutant phenotypes (Cheng et al., 2011; Hur et al., 2017). For these experiments, a SkyScan 1172 (Bruker microCT) with a 60kV X-ray lamp was used to produce whole-body volumes with 2-6μm voxel sizes.

Contrast-enhanced propagation phase contrast synchrotron radiation micro-computed tomography

For examining less dense skeletal tissue such as unmineralized cartilage, or other soft tissues such as muscles, nervous tissue, and blood vessels, conven-

tional μCT is insufficient to distinguish the tiny density differences between these distinct tissues to produce a usable reconstruction. Instead, a modified technique broadly termed Diffusible Iodine-based Contrast-Enhanced (DICE)-μCT can be used (Metscher, 2009). After fixation, specimens are soaked in a diluted iodine-based solution such as I_2E (iodine in ethanol) or I_2KI (iodine potassium iodide, also known as Lugol's iodine) for hours to weeks, depending on their size, to allow the solution to penetrate all tissues. The dense iodine penetrates different tissues to varying degrees, leading to an increased density of all tissues in addition to differential densities between different tissues, leading to a high-contrast μCT scan of soft tissues (Gignac et al., 2016; Kolmann et al., 2023). In addition to iodine solutions, other chemicals such as phosphotungstic acid (PTA) and phosphomolybdic acid (PMA) can also be used to enhance the contrast of soft tissue, each with slightly different properties and affinities for different tissues (Metscher, 2009; Pauwels et al., 2013; Descamps et al., 2014). A key benefit of using iodine compared to these other chemicals however, is that the density of bone is also increased in addition to the soft tissues, making it easier to distinguish and segment the bones in relation to the surrounding soft tissues. All these different methods of contrast enhancement (CE) can be included under the umbrella term CE-μCT.

CE-μCT is relatively routinely applied by organismal biologists to large specimens including those from natural history collections in order to visualise the morphology of soft tissues such as the brain and nervous system (e.g. George and Holliday, 2013; Camilieri-Asch et al., 2020; Callahan et al., 2021) and musculature (e.g. Cox and Jeffery, 2011; Holliday et al., 2013; Santana, 2018). However, it is less commonly applied to smaller model organisms in experimental research (Babaei et al., 2016; Porro and Richards, 2017), with the exception of the mouse (reviewed by Handschuh and Glösmann, 2022).

In zebrafish, experimental analysis of soft tissues by CE-μCT has only been performed in a handful of quite recent studies on heart defects (Babaei et al., 2016; Dimitriadi et al., 2018; Bensimon-Brito et al., 2022), muscle defects (Watson et al., 2022), or diet-induced disease (Seo et al., 2015), while two earlier papers included zebrafish as samples in establishing contrast-enhanced μCT as a general method (Metscher, 2013; Descamps et al., 2014).

A limitation of conventional μCT-based imaging is that the resolution limit is typically on the order of several microns for specimens as thick as a juvenile or adult zebrafish, which is insufficient for obtaining desirable histological detail. This likely contributes to the poor uptake of CE-μCT in zebrafish research. However, the resolution of CE-μCT can be improved.

Synchrotron radiation μCT (SRμCT) is a type of μCT that uses a synchrotron as an X-ray source instead of a small X-ray lamp in a typical benchtop μCT scanner. In our case, we performed experiments at beamline BM05 of the European Synchrotron Radiation Facility - Extremely Bright Source (ESRF-

EBS) in Grenoble, France. The ESRF-EBS is a large facility whose largest component is an electron storage ring that is 844m in circumference. The beam of electrons is produced by an electron gun and accelerated by a linear accelerator before entering a small (300m circumference) booster synchrotron ring that further accelerates the electrons. Once the electron beam reaches an energy of 6GeV, it is injected into the large storage ring. In order to maintain a permanent electron beam in the storage ring, injections are regularly made from the booster synchrotron. These maintain the beam at a current of 200mA, approximately 1000x greater than a typical X-ray lamp (ESRF, 2023).

Around the storage ring sit 44 beamlines including experimental hutches working with different types of synchrotron radiation, but primarily X-rays. These X-rays are generated by the electron beam in the storage ring using the same principle as the previously described X-ray lamp: electrons are slowed to produce Bremsstrahlung. However, while the X-ray lamps slow electrons by accelerating the beam into a dense metal target and have the positively charged nuclei of this material interact with the negatively charged electrons, the synchrotron uses an electromagnetic field generated by so-called "bending magnets" to curve the path of the electrons and generate X-rays at a tangent to the original beam path. These bending magnets serve a dual function, they are used to generate X-rays for the experiments but simultaneously keep the electron beam flowing around the storage ring (Bonse and Busch, 1996). Other X-ray generating devices such as undulators and wigglers used at some of the ESRF beamlines work on a similar principle but produce more intense X-rays by having the electrons pass through a series of alternating dipole magnets instead of just one, "wiggling" them back and forth to repeatedly generate X-ray photons (Bonse and Busch, 1996).

The X-rays produced by the bending magnet undergo a process of filtering and partial monochromation to produce a parallel beam of in-phase (coherent) X-rays of the desired energy level. After this point, the CT scanning procedure is largely the same as previously described for a standard benchtop μCT scanner, albeit often with improved optics and stage precision. However, there are two important differences to note at this point. The first is that the high current of the synchrotron's electron beam leads to a much greater density of photons, or brightness, in the X-ray beam, and this leads to dramatically reduced imaging times and improved image quality through the greater signal-to-noise ratio. The second is that as the synchrotron's X-ray beam is collimated to be parallel and narrow rather than cone-shaped, the image resolution is improved in addition to typically being magnified by optics in front of the detector sensor.

Clearly, these represent benefits of using SRμCT for X-ray microtomography, but up until this point the described imaging principles remained largely the same - using X-rays to cast shadows on detectors and use this attenuation of the X-ray beam to reconstruct cross-sectional images of the 3D volume. However,

in the 1990s, researchers began to exploit another property of the synchrotron X-rays, the high spatial coherence of the beam (all the light waves have a consistent phase), to develop imaging methodologies based on phase contrast (Snigirev et al., 1995; Bonse and Busch, 1996). These include a simple technique called propagation phase contrast SRμCT (PPC-SRμCT)(Wilkins et al., 1996; Cloetens et al., 1999; Paganin et al., 2002; Tafforeau et al., 2006).

As X-rays pass through tissue boundaries in a sample on their way to the detector, they are not only attenuated but also very slightly diffracted, similar to how light is refracted at the boundary between glass and water in a cup. These diffracted X-rays interfere with the adjacent non- or differentially-diffracted X-rays, with constructive and destructive phase interactions leading to increases and decreases in the intensity of the X-rays that are detected in the image. As the propagation distance between the sample and detector increases there is a greater degree of phase interference detectable as intensity differences (Fresnel fringes), so longer propagation distances are preferable to maximise the phase contrast of the image, up to a limit where the phase interference exceeds the size of the features of interest in the sample and the image becomes blurry. This, in addition to other imaging considerations, means that the propagation distance has to be optimised for different samples and imaging regimes, and for our experiments was in the range of several centimeters for voxel sizes between 0.7μm and 3μm.

The phase interference causes the edges of tissues in the sample to appear in extremely high contrast ("edge enhancement"), even if they are extremely similar in density. These images can be valuable in their own right, but what is more common is to utilise a phase retrieval algorithm to infer the density difference (refractive index) that caused the diffraction in the first place, such that the contrast of the whole tissues are enhanced, not just their boundaries. This transforms a low-contrast image with bright edge fringes into a high-contrast image with suppressed fringes (Paganin et al., 2002; Sanchez et al., 2012; Thompson et al., 2019). A key advantage to using phase contrast-based imaging is that even though attenuation can be low when using high-energy X-rays and/or when imaging soft tissues of very low density, the phase contrast will still be strong (Momose and Fukuda, 1995; Bonse and Busch, 1996) and therefore will produce high contrast images that would be challenging or even impossible to obtain based on attenuation alone (Langer et al., 2008; Thompson et al., 2019).

Using SRμCT, and particularly PPC-SRμCT, soft tissues can be imaged at high resolution due to the high signal-to-noise ratio, spatial resolution, and phase contrast enhancement. However, the relative density between soft tissues is still approximately the same, leading to images with poor relative contrast between different soft tissues. This makes it challenging to recognise and

segment the different tissues (Weide et al., 2010; Dutel et al., 2019; Johnston, 2022).

To overcome this limitation, we combined the principles of DICE-μCT with PPC-SRμCT to produce a protocol for Diffusible Iodine-based Contrast-Enhanced Propagation Phase-Contrast Synchrotron Radiation micro-Computed Tomography (DICE-PPC-SRμCT) that can be applied to zebrafish and other small fish species or tissue samples up to a diameter of several centimetres (Paper **II**). This involves simply incubating the specimens in a solution of 1% iodine in 100% ethanol at room temperature for a number of hours (depending on its size) to allow the iodine to diffuse into the tissues, then removing the excess iodine by washing and storing the specimen in ethanol before PPC-SRμCT imaging.

3D image segmentation

After μCT scanning, the 3D volume of the specimen is reconstructed into a series ("stack") of several thousand image files, each representing a thin virtual slice through the specimen in the plane of the X-ray beam, with the point of rotation in the center. The same principle also applies to OPT reconstructions. Preferred image formats are 16-bit TIFF or BMP as these are lossless and represent the highest image quality without compression, or JPEG 2000 (JP2), which can dramatically compress the image with only minimal artefacts and loss of information, making the data handling and storage more convenient. The reconstruction is performed to result in an isotopic voxel size, where voxels are 3D pixels (cubes instead of squares) formed in the 3D grid created when the images (2D grids of pixels in the X and Y direction) are stacked on top of each other (in the Z direction). The voxel size is isotropic when the spacing between each image in the stack is equal in length to the height and width of each pixel in the images in the stack. For example, a dataset with an isotropic voxel size of 3μm is comprised of images where each pixel has a height and width of 3μm, and the spacing between each image in the stack is also 3μm.

In order to visualise and analyse these datasets, the image stacks are loaded into specialised software designed for handling 3D datasets. I used VGStudio Max (versions 3.2.5-2022.4, Volume Graphics), as although its primary user base is engineers and materials scientists working on CT scans for applications in metal parts fabrication and battery design, it also has found favour among biologists working on scans of animal and plant tissues. The software allows the scan datasets to be explored in "slice view" from all angles but also contains key tools for 3D segmentation. These include global thresholding and region growing tools which isolate voxels based on gray values (brightness) that enable tissues of like density to be instantly isolated together and visualised

in 3D, but also tools for manually drawing masks on the dataset slice-by-slice to slowly but precisely sculpt 3D shapes representing more subtle tissues that have to be recognised by eye amidst a sea of similar gray values. Quantification of properties of the segmented tissues such as volume can be performed by essentially counting the voxels contained within each mask, often using the Porosity/Inclusion Analysis Module (Sanchez et al., 2013).

Research aims

The overall aim of this thesis was to investigate the function and regulation of the transcription factors Nkx3.2 and Mkx and the secreted factor Gdf5 in the development of the vertebrate musculoskeletal system, using the zebrafish (*Danio rerio*) as a model organism.

Paper I: We aimed to generate an *nkx3.2* knockout mutant zebrafish line and describe the impacts of the absence of this transcription factor on jaw joint development and skeletal development throughout the rest of the larval and juvenile body.

Paper II: As we showed in Paper I that the knockout of *nkx3.2* led to gross cartilage and bone defects, we next aimed to determine how a novel contrast-enhanced SRμCT 3D imaging method could be used in characterising defects in soft tissues associated with the skeleton. We intended to simultaneously gain insights into the potentially altered soft tissues of this mutant and also provide a novel imaging protocol that could be applied to other mutants in the future.

Paper III: Together with previous publications, Paper I highlighted the key role of Nkx3.2 in patterning the gnathostome jaw joint. To answer how the expression of this gene is localised to the jaw joint, we aimed to identify and functionally characterise an evolutionarily conserved enhancer of *Nkx3.2* that may have been key in the initial evolution of articulating jaws in the ancestor of gnathostomes.

Paper IV: We aimed to generate a *gdf5* knockout mutant zebrafish line and characterise the resulting mutant phenotypes in the skeleton, particularly in the jaw joint and fin radials during larval and juvenile development.

Paper V: We aimed to identify and functionally characterise an evolutionarily conserved enhancer regulating the expression of the *mkx* gene in the zebrafish musculoskeletal system.

Summary of results

Paper I - *nkx3.2* knockout and phenotypic analysis

Studies in zebrafish and amniotes have shown that Nkx3.2 plays an important role in the early development of the jaw joint. In zebrafish, morpholino-based knockdown experiments resulted in a fusion of the upper and lower jaw cartilages in the absence of the jaw joint. However, as the effects of morpholinos are short-lived, the effects on later development up to adulthood were unknown.

To permanently knock out the *nkx3.2* gene in zebrafish, we used CRISPR/Cas9 genome editing to introduce a 7bp deletion in the first exon that led to a frameshift and premature stop codon in the protein-coding sequence, such that the mutated protein was only 95 amino acids long compared to 245 amino acids in the wild-type. Critically, this mutated protein was missing the DNA-binding homeodomain that is necessary for its function as a transcription factor.

While heterozygous mutants appeared phenotypically normal, homozygous mutants displayed an obvious open-mouth phenotype as a result of the absence of the jaw joint and fusion between Meckel's cartilage and the palatoquadrate, and despite this deformation were able to survive to adulthood. We analysed the fusion in a transgenic *sox10*:eGFP background for the live visualisation of chondrocytes in the lower jaw, where we observed that the fusion occurred as early as 3dpf, and by 14dpf the chondrocytes throughout the fused cartilage elements were homogeneously aligned in stacks. Using histological tissue section stained with Nuclear Red, we found that the clear cartilage fusion was maintained up to 30dpf, and that ossification at 90dpf proceeded normally, leading to fused articular and quadrate bones.

Alcian blue/alizarin red cartilage/bone staining of a series of mutants between 5-30dpf revealed that the open mouth phenotype manifested between 5-9dpf. This was when, in wild-types, Meckel's cartilage began to angle upwards relative to the palatoquadrate, pivoting around the jaw joint, but in the absence of the joint, the lower jaw was held flat and began to protrude from the face. Ossification of the surrounding facial bones appeared to take place normally in mutants. However, looking more posteriorly at the cervical vertebrae and rib-bearing vertebrae in the 30dpf mutants, we noticed a distant lack of the vertebral basiventral cartilages.

We used OPT to 3D image Alcian blue-stained wild-type and mutant larvae at 5dpf, and by aligning the cranial cartilage elements of multiple individuals of each genotype, we were able to highlight voxels that were significantly different between the genotypes, and therefore indicative of morphological differences between them. In addition to highlighting the jaw joint fusion as expected, this comparison provided us with the second hint of mutant phenotypes outside of the jaw skeleton. In the occipital cartilage at the back of the skull, the *nkx3.2* mutants displayed a shortening/reduction of the cartilage that interfaced with the notochord.

To analyse these skeletal phenotypes more comprehensively, we μCT scanned adult wild-type and mutant fish and segmented many individual bones out in 3D. This revealed that as a result of the absence of the basiventral cartilages, the parapophysis bones that normally articulate the rib heads and vertebrae were completely absent, leaving many ribs completely fused to the vertebral centra. We were also able to comprehensively describe malformations to the adult mutant occiput and Weberian apparatus. These included fusions between the exoccipital and basioccipital bones leading to a closure of the cavum sinus impar - the channel for auditory signals from the swim bladder into the inner ear. There were many deformations to the Weberian ossicles, including the loss of the anterior ramus and articulating process of the tripus, and the variable loss/compaction of the anterior-most cervical vertebrae and their ossicles such as lateral process 2.

This study confirmed the key role of Nkx3.2 in the development of the zebrafish jaw joint, extending our understanding of the effect of the loss of this joint into adulthood. The finding and description of axial phenotypes in the occiput and vertebrae were novel in zebrafish, but correspond to some similar defects observed in mutant mouse models but also human disease associated with mutations to *Nkx3.2*, demonstrating a conserved axial role for Nkx3.2 in the sclerotome of bony vertebrates.

Paper II - Contrast-enhanced synchrotron micro-computed tomography of *nkx3.2* mutants

In order to study soft tissues like muscles and ligaments at a high level of detail, traditional histology using physically cut thin sections is a foundational technique. However, in the process, the specimen is damaged or destroyed and is it difficult to interpret the three-dimensional organisation of tissues. μCT scanning of specimens stained with a contrast-enhancing dye can be used to visualise soft tissues in 3D, but typically at a limited resolution. We set out to demonstrate that iodine staining combined with the use of high-resolution propagation phase-contrast synchrotron scanning (DICE-PPC-SRμCT) is ca-

pable of providing near-histological resolution and contrast of soft tissues in small whole organisms such as zebrafish.

In Paper **I**, we demonstrated a range of cartilage and bone phenotypes in *nkx3.2* mutant zebrafish, and were particularly struck by the juvenile and adult deformations of the face and Weberian apparatus. We set out to investigate the effect of these malformations on the associated soft tissues as a proof-of-principle of the power of DICE-PPC-SRμCT for describing soft tissue phenotypes. Zebrafish from 1-3mpf were fixed and stained with iodine overnight, then taken to Beamline 05 of the European Synchrotron Radiation Facility in Grenoble, France where they were scanned using PPC-SRμCT at medium (voxel size: 3μm) and high (voxel size: 0.727μm) resolutions. This raw scan data was processed into image stacks for analysis of 2D virtual thin sections and segmentation of tissues in 3D.

High resolution scans of stained zebrafish resulted in near-histological quality 2D thin sections, allowing for clear visualisation of fine structures including cell layers of the retina, neurons and nerve fibres in the brain and spinal cord, osteocyte lacunae and waves of mineralisation in bones, and chondrocytes in cartilage elements. The use of iodine as a contrast agent instead of other compounds like PTA had the advantage of staining the bone as well as the soft tissues, keeping the high relative contrast between the two. As the dataset was isotropic in 3D, all relevant tissues could be viewed in optimal planes, unlike in traditional histology where physical sections are limited by the plane of the cutting blade.

We segmented in 3D the lower jaw muscles and bones of a 2mpf wild-type and *nkx3.2* mutant zebrafish, identifying disorganised muscle bundles in the adductor mandibulae (AM) and pars hyoideus, the muscles responsible for closing and opening the lower jaw, respectively. The left and right AMs displayed variable defects, for example one appeared to have normal posterior attachment to the quadrate, while the other displayed an unusual inappropriate attachment to the dentary. These muscle defects were interpreted as secondary effects of a misshapen jaw skeleton rather than as a direct effect of the loss of *nkx3.2* function.

In the Weberian apparatus, we segmented the entire auditory chain including the swim bladder, the Weberian ossicles and associated ligaments, and the fluid-filled sinus perilymphaticus and sinus endolymphaticus (which contains the auditory otoliths) that are surrounded by the occipital bones. In mutants, the interossicular and suspensorium ligaments that connect the ossicles in vertebrae 1-4 were poorly formed or completely absent in mutants, while the connection between the swim bladder, the posterior tripus of vertebra 3, and the os suspensorium of vertebra 4 appeared normal. This is consistent with the defects in the ossicles of vertebrae 1-3 described in Paper **I** that serve as the attachment sites and are likely important for the development or maintenance

of these ligaments. Likely as a result of the constriction and closure of the cavum sinus impar that we first noted in Paper **I**, the sinus perilymphaticus appeared to be reduced or absent in the mutants, failing to extend out of the occiput to make contact with the scaphia.

In conclusion, we found that jaw muscles were secondarily deformed as a result of the open-mouth phenotype in *nkx3.2* mutants, and that a series of malformations are present in the auditory chain that must lead to a severe hearing deficiency. Simultaneously, we demonstrated the exceptional quality and volume of data, both qualitative and quantitative, that can be obtained about zebrafish soft tissue micro-anatomy and histology using DICE-PPC-SRμCT.

Paper III - JRS1: a conserved jawed vertebrate *Nkx3.2* enhancer

As mentioned in Papers **I** and **II**, *Nkx3.2* is expressed in the early jaw joint where it is necessary for its development, but little is known about the cis-regulation of this gene and how its expression becomes localised to the interzone. We set out to identify novel proximal cis-regulatory elements based on sequence conservation in a representative sample of vertebrate genomes.

The proximal non-coding sequence around the *Nkx3.2* locus from multiple species was aligned using mVISTA to identify conserved non-coding elements, and we identified a sequence, later designated jaw joint regulatory sequence 1 (JRS1), that was conserved in all major jawed vertebrate clades but absent from the jawless hagfish and lamprey genomes. Interestingly, a detailed analysis of the actinopterygian fish clade revealed an apparent secondary loss of JRS1 in most groups of percomorph fishes encompassing approximately 12,000 species, seemingly beginning with a partial loss in the common ancestor of percomorph and bercyiform fishes.

Within the conserved sequence of JRS1, we used MEME and Tomtom to identify putative transcription factor binding motifs corresponding to a range of known factors in pharyngeal and skeletal development, increasing our confidence that JRS1 was an enhancer of the *Nkx3.2* gene that could be responsible for its focal expression in the gnathostome jaw joint. One of these predicted binding sites, Meis2, was supported by previously published and publicly available *in vivo* ChIP-seq datasets showing strong Meis binding precisely at the JRS1 locus in embryonic mouse branchial arches.

In order to validate the enhancer activity of JRS1, we generated a transgenic enhancer reporter zebrafish line where the fluorescent reporter was under the control of the zebrafish JRS1 sequence. This revealed that JRS1 was activated strongly in the developing jaw joint interzone and perichondrium as early as 40hpf and remained active until at least 14dpf, still localised to the primary

jaw joint. Even in *nkx3.2* knockout fish with fused Meckel's cartilage and palatoquadrate, with no joint tissues apparent, JRS1 was active in the perichondrium surrounding an intermediate region of the fused cartilage where the joint would have formed.

The same enhancer reporter assay was used to assess the activity of human, mouse, frog, bichir, and elephant shark JRS1 sequences in zebrafish, and remarkably, they all displayed the same activity as the zebrafish JRS1 sequence, indicating that the function of JRS1 is likely conserved in all these groups of jawed vertebrates despite them being separated by up to 450 million years of evolution.

To functionally validate the role of JRS1 in the cis-regulation of *nkx3.2*, we used CRISPR/Cas9 genome editing to excise JRS1 from the zebrafish genome. Quantitative analyses of *nkx3.2* gene expression in homozygous mutants revealed a significant reduction in early expression in the jaw joint but no difference in whole-body expression in older 6dpf larvae. This result is consistent with an early expression reduction and later recovery, which would indicate an important role for other as-yet-undiscovered *nkx3.2* enhancers, or it could be that *nkx3.2* expression elsewhere in the body "swamped" a sustained reduction in the jaw joint.

The reduction in *nkx3.2* expression in JRS1 deletion mutants was accompanied by phenotypes in the jaw joint cartilages, more subtle than the outright fusion observed in Paper **I** in the gene knockout mutants. Partial fusions were observed at 5dpf and 9dpf, and geometric morphometric analysis of the joint surface shapes gathered from OPT scanning where consistent with a highly reduced retroarticular process of Meckel's cartilage. However, this dysmorphology appeared to recover back to the wild-type morphology by 14-30dpf, again raising the possibility of *nkx3.2* expression recovery in later developmental stages, or of other joint-patterning factors taking over the process.

In summary, in this study we discovered and characterised the first highly conserved enhancer driving the expression of the *Nkx3.2* gene in the primary jaw joint of gnathostomes, and which was potentially key in the evolution of the first articulating vertebrate jaws.

Paper IV - *gdf5* knockout and phenotypic analysis

Growth and Differentiation Factors (GDFs) play a major role during all stages of skeletogenesis. *Gdf5* is a gene known to be expressed in synovial joint development in amniote limb joints, where it has an early role in promoting mesenchyme condensation and a late role in the mature articular cartilage and synovium. In zebrafish, it is expressed in the primary jaw joint under the

control of *nkx3.2* and also in the pectoral and median fins, although little is known about its role in fin development.

To study the role of Gdf5 in zebrafish skeletal development, we generated a knockout allele of *gdf5* using CRISPR/Cas9 genome editing to target the start of the second exon and introduced a 5bp deletion that led to a premature stop codon and a truncated protein product of 230aa instead of 474aa, deleting the key functional mature domain. Throughout the phenotypic analysis, heterozygote fish appeared normal, but a range of phenotypes were described in homozygous larvae, juveniles, and adults using skeletal staining, OPT, and μCT scanning.

Despite the known expression domain of *gdf5* in the jaw joint, we unexpectedly found no apparent defects to the jaw joint cartilage or bone at any stage of development. Histological thin sections also identified no apparent phenotypes in the dorsal, anal, and caudal fin joints either. It is interesting to speculate whether a paralogous gene with a similar expression pattern, *gdf6a*, could be compensating for the loss of Gdf5 in joint development, at least in the jaw. However, other skeletal elements in the fins displayed dramatic mutant phenotypes.

Zebrafish pectoral fins first develop as an endoskeletal disc of cartilage, and then during late larval development this disc is subdivided into 2 then 4 proximal radials by segmentation zones of dedifferentiating cartilage. Independently, small distal radials condense between these proximal radials and the bony lepidotrichia. In the homozygous *gdf5* mutants, the segmentation zones in the endoskeletal disc appeared to expand dramatically until almost the entire endoskeletal disc dedifferentiated and no longer stained with alcian blue, leaving just the first and most anterior proximal radial. Several of the posterior distal radials also failed to form, and those that remained were often smaller or fused together. This single-proximal radial phenotype persisted into adulthood, although in some mutants an ectopic bone appeared to ossify intramembranously in the space left by the absence of proximal radials 2-4, possibly as an compensatory adaptation to support the fin.

The median fin skeleton develops differently to the pectoral fin, with radials condensing individually instead of segmenting from a larger mass of cartilage. In the dorsal and anal fins, mutant juveniles displayed highly truncated and malformed proximal radials, and similar phenotypes were observed in the caudal fin hypurals. In adults, this corresponded to shortened radial and hypural bones. Notably, in both cases, the more posterior elements appeared to be more severely affected.

These median fin phenotypes are consistent with a conserved role for Gdf5 in cartilage development, as comparable shortened limb and phalanges phenotypes are seen in mouse mutants and human genetic diseases. As the develop-

ment of the zebrafish pectoral fin is quite derived relative to more basal fish fins and made up of distinct elements compared to tetrapod limbs, it is difficult to assign direct functional homologies between these structures. However, studies in mammalian cell cultures demonstrated a role for Gdf5 in inhibiting the expression of cartilage-ECM-degrading MMP enzymes, which could be related to the expanded segmentation zones in the mutant zebrafish endoskeletal discs.

This is the first knockout-based study of the functional role of Gdf5 in the development of the zebrafish skeleton, and we demonstrate some clearly conserved functions in the growth of the cartilaginous median radials. On the other hand, the striking pectoral fin phenotype opens up a range of new questions about actinopterygian endoskeletal disc segmentation, a generally understudied topic.

Paper V - Identification of a novel *Mkx* enhancer

Mohawk Homeobox (Mkx) is a transcription factor known to play a role in the development and maintenance of tendons and ligaments, where it promotes the expression of key extracellular matrix components while repressing chondrogenic and myogenic cell fates. It has primarily been studied in the mouse model, with far less being known about its function in zebrafish. Simultaneously, how the expression of the Mkx gene is specified by cis-regulatory elements to the tendons and ligaments has yet to be explored in any jawed vertebrate species, so we aimed to identify such proximal enhancers.

As in Paper **III**, we used a pipeline consisting of mVISTA, MEME, and Tomtom to identify conserved non-coding sequences proximal to the *Mkx* gene, including one that was conserved in all examined jawed vertebrates that we named *Mkx*(E1). Its sequence was conserved enough to identify with reciprocal mVISTA alignments, but upon closer inspection using MEME and Tomtom, it became clear that there were distinct clade-specific regions of motif conservation that corresponded to different predicted transcription factor-binding sites.

We generated transgenic reporter lines expressing the fluorescent protein mCherry under the control of species-specific *Mkx*(E1) sequences which resulted in detectable reporter activity in four out of the eight tested species. Human, mouse, chicken, and coelacanth *Mkx*(E1) sequences failed to drive reporter activity in F0 zebrafish, while the frog, zebrafish, gar, and elephant shark sequences did and were raised to produce stable lines for detailed descriptions of activity from larvae to juvenile stages of development. The zebrafish and gar *Mkx*(E1) lines displayed reporter activity in a subset of the craniofacial tendons and ligaments, in addition to the ligaments of the Weberian apparatus described in Paper **II**.

Interestingly, the frog and elephant shark *Mkx*(E1) sequences did not drive reporter activity in the same tendons and ligaments, instead being strongly active in the craniofacial muscles and cartilage, respectively. This is likely the result of sequence divergence leading to the aforementioned differing complement of transcription factor-binding sites between species. However, the extent to which these activity patterns in the zebrafish reflect those in the "native environment" of the enhancer sequences in their host species tissues is unknown and could also be the result of developmental system drift.

Future directions

My studies have reinforced the fact that Nkx3.2 has a clear role in the development of the primary jaw joint, but many of the specifics of this role are still open to investigation. When the gene is knocked out or knocked down in early zebrafish development, the jaw joint fails to form, but it would be interesting to use inducible knockout or knockdown methods to determine more precisely when the window of joint induction and differentiation takes place. We identified JRS1 as an important regulator of Nkx3.2 in the jaw joint, but there are evidently other enhancers present that additionally contribute to its expression in the jaw joint as well as other tissues. The relatively proximal nature of JRS1 makes it in a sense low-hanging fruit, so future efforts to search for additional, more distal *Nkx3.2* enhancers will likely need to employ more advanced methods to capture histone modification and chromatin conformation signatures of cis-regulation. That being said, the *Nkx3.2* promoter is also likely to contain a rich landscape of regulatory motifs so is also a promising and accessible candidate for future study.

Homozygous knockout of the *nkx3.2* gene led to complete jaw joint fusion in zebrafish, while homozygous deletion of JRS1 led to milder joint deformations. In both cases, no phenotypes were observed in heterozygous mutants. Previous studies investigating overlapping and apparently redundant enhancer functions have found that in "sensitised" backgrounds where one copy of the gene is absent, the deletion of otherwise redundant enhancers results in stronger phenotypes. Therefore, I would expect that in a heterozygous *nkx3.2* gene mutant background, the deletion of JRS1 would cause a more severe jaw joint fusion phenotype as a result of a decreased gene dosage. Due to the extremely close proximity of the gene and JRS1 in essentially the same locus, such double mutants can't be produced by crossing but could be relatively easily generated as crispants.

From the transgenic reporter assays in zebrafish, we inferred that mammalian JRS1 sequences had conserved activity with other gnathostomes, but the radically different structure of the mammalian middle ear raises the question of to what extent the regulatory landscape of *Nkx3.2* may have evolved in this group. If JRS1 has conserved activity, does that mean it is still redundant with other enhancers, and its deletion would cause a similar mild phenotype in the homologous structures to that observed in zebrafish? It seems well worth exploring the activity of JRS1 in mice using Gal4 reporter assays and deletion mutants.

There is also a clear need for comprehensive investigations into the expression, function, and regulation of *nkx3.2* in jawless fishes. Derived as they may be, lampreys and hagfish are the closest we can get to understanding the development of the ancestral pharyngeal skeleton so we can better understand the series of genetic changes that led to the evolution of the gnathostome jaw.

The unexpectedly dramatic pectoral fin segmentation phenotype in *gdf5* mutant zebrafish makes it an attractive candidate for further study. Normal endoskeletal disc segmentation itself has barely been studied, Dewit et al. (2011) is essentially the only paper investigating the process in some detail, but nothing is known about its development at the genetic level. Studying this segmentation in wild-type fish will help reveal how Gdf5 fits into the process, but equally, the role of Gdf5 can serve as a staging ground for investigations. First, the detailed expression pattern of *gdf5* in the pectoral fin should be described throughout development, and comparative transcriptomic analysis of wild-type and mutant fins will reveal further gene candidates to be explored.

Although we anticipated a jaw joint phenotype in *gdf5* mutant zebrafish, we failed to identify any such defects in the bone or cartilage. As Gdf5-positive cells are known to contribute to the surrounding joint tissues like ligaments and synovial membranes, it would be interesting to search for phenotypes in these tissues in the future. We raised the possibility of genetic compensation by a paralogous gene, *gdf6a*, so analysing double *gdf5/gdf6a* mutants may uncover joint phenotypes similar to those found in the homologous mouse middle ear structures and appendicular skeleton (Settle et al., 2003).

Much remains to be understood about developmental patterning of tendons and ligaments in zebrafish, especially in post-larval stages. This includes a comprehensive description of the expression of *mkx* and subsequent comparison with the activity of our newly discovered enhancer. To understand the divergent activity patterns of *Mkx*(E1), the native gene expression in different species should be characterised, in addition to investigating how the transcription-factor binding motifs present in the sequences of different species contribute to their reporter activity.

We demonstrated the potential of DICE-PPC-SRμCT for carefully analysing skeletal and soft tissue phenotypes in zebrafish, and it could certainly be applied to further analyse *gdf5* or even *mkx* mutants in the future. It has a clear potential for many other studies of a range of different tissues, especially those at the interface of bones and connective tissues. This could include examinations of a range of scoliosis mutant phenotypes to determine how trunk musculature adapts, or in determining how malformed muscles and connective tissues could be driving skeletal phenotypes. Propagation phase-contrast μCT technology is becoming more accessible at laboratory facilities far smaller than synchrotron light sources (Migga et al., 2022), and will provide greater opportunities to apply this imaging methodology in future.

Popular science summary

In the realm of the animal kingdom, vertebrates form a distinct group characterised by their possession of solid skeletons, primarily composed of bone or cartilage. This includes most of the animals we are familiar with: fish, birds, reptiles, and mammals. These skeletons serve several purposes, the most obvious of which are providing structural support and safeguarding internal organs. Complementing these skeletal structures are a range of soft tissues, including muscles and connective tissues like tendons and ligaments. Tendons connect muscles to the skeleton, while ligaments connect skeletal elements like bones together. All these tissues are formed during embryological development, and orchestrating the complex processes underlying this development are hundreds of protein-coding genes. Some proteins like collagen are part of the building blocks of these tissues directly, but many more proteins act as regulators in complex networks of interactions that determine when and where these structural proteins get expressed in order to correctly shape the skeleton and its associated tissues.

Throughout the course of evolution, vertebrates have developed a diverse array of skeletal structures tailored to different functions, like the difference between fish fins and human limbs, or the cartilaginous skeletons of sharks and skates. Varying modes of skeletal development have resulted in morphological differences that allow vertebrates to adapt to their environments and lifestyles. By examining the genetics and developmental patterns in present-day vertebrates within an evolutionary context, we can learn about the mechanisms underlying the morphological evolution of vertebrate skeletons. In cases where other species build their skeleton in similar ways to humans, we can also gain insights into the causes and potential remedies of rare congenital skeletal diseases and more common conditions like osteoarthritis.

Central to these investigations are model organisms like the zebrafish (*Danio rerio*). Zebrafish are a powerful model for studying the development of the skeleton because they are small, develop rapidly from embryos to adults in just two months, are transparent as embryos and young larvae allowing us to see the skeleton through the skin, and have a range of tools available for manipulating their genome. In this thesis, I used zebrafish to study three different genes called NK-3 Homeobox 2 (*nkx3.2*), Growth and Differentiation Factor 5 (*gdf5*), and Mohawk Homeobox (*mkx*), all of which produce proteins regulating different aspects of musculoskeletal development.

In the **first** study, we used CRISPR/Cas9 genome editing technology to mutate ("knockout") the *nkx3.2* in the zebrafish genome and examined how the skeleton developed in its absence using chemical stains and X-ray scanning. We found that it caused the joint in the lower jaw to fuse in early development, leading the fish to have a permanently open mouth. We also found striking defects in the development of the cartilage and bones at the back of the skull and in the specialised neck vertebrae called the Weberian apparatus. Small bones called parapophyses that attach the ribs to the spine normally develop from small ball-shaped cartilages, but these were completely missing in the mutants, leading to the ribs fusing directly onto the spine. Some of these malformations are comparable to defects seen in mouse mutants and a human genetic condition called spondylo-megaepiphyseal-metaphyseal dysplasia, suggesting that this gene is playing a similar role in all three species meaning that zebrafish could be a useful model for further studies trying to better understand the disease.

In the **second** study, we wanted to look in more detail at the effects the deformed skeleton of the *nkx3.2* mutant zebrafish had on the surrounding soft tissues. For example, do the muscles develop normally even when they are attached to misshapen bones? Traditionally, the best way to look in detail at soft tissues is to cut extremely thin two-dimensional sections through the fish and look at these slices of tissue through a microscope. However, this makes it impossible to see the bigger picture of the complex three-dimensional (3D) organisation of tissues, like trying to visualise the internal 3D structure of a skyscraper only from top-down blueprints of a handful of floors. X-ray computed tomography (CT) scanning provides information in 3D by taking hundreds or thousands of X-ray photos from all different angles around 360 degrees of rotation and then using this information to calculate the 3D shape of the object being scanned. We used a high-resolution and high-contrast version of this technique at the European Synchrotron Radiation Facility in Grenoble, France to scan mutant zebrafish in extreme detail, down to the cellular level.

This revealed that the muscles attaching to the deformed lower jaw were indeed deformed in several ways themselves and that several ligaments that normally connect bones in the Weberian apparatus were missing when these bones were deformed or missing themselves. This latter defect, combined with the absence of an important fluid-filled sac that extends out of the skull called the sinus perilymphaticus, led us to the conclusion that the function of the Weberian apparatus, to transmit sound from the fish's swim bladder into the sensory structures of the ear, was damaged beyond repair. These results also serve as an important proof-of-principle for the potential of this synchrotron scanning technique to be used in many future studies to understand the development of other complex soft tissues in 3D.

In the **third** study, we wanted to better understand how the expression of the *nkx3.2* gene was controlled, in particular how it was specified to be expressed in the developing jaw joint. This type of control is managed by short DNA sequences called enhancers that are often found nearby to the DNA sequence of the gene itself. Proteins expressed in the target tissue bind to this enhancer DNA and cause the DNA to bend around until this enhancer/protein complex can physically interact with the start of the gene sequence and cause it to be transcribed into RNA, later being translated into a functional protein. There are a number of ways to identify these enhancer sequences, but we chose one of the simplest: we compared DNA sequences close to the *nkx3.2* gene from a large number of different species, and looked for sequences that were similar - conserved - in all of them. This is because functional sequences are preserved by natural selection during evolution, so tend to be more similar between species than non-functional sequences that accumulate random mutational differences over time.

We identified one such enhancer sequence and named it JRS1. Critically, the enhancer was conserved in all vertebrates with jaws (with the exception of a single group of fish that must have secondarily lost it), and absent from their closest jawless relatives, the lamprey and hagfish. This suggested that this enhancer evolved in the common ancestor of all jawed vertebrates, and could even be part of the reason that articulating jaws (which require a joint) were able to evolve in the first place. Sure enough, when we tested the function of this enhancer in zebrafish, we found that it specifically caused *nkx3.2* to be expressed in the early developing jaw joint, and the same was true for the sequences from other species including humans and sharks. However, when completely deleting JRS1 from the zebrafish genome the expression of *nkx3.2* in the jaw joint wasn't completely abolished, suggesting that there are other enhancer sequences elsewhere in the genome that have yet to be found.

In the **fourth** study, we turned to a different gene, *gdf5*, which is known to be controlled by *nkx3.2* in some tissues, and used the same set of techniques as the first study to look at defects in the development of the skeleton when we knocked out the gene. We were expecting to find some defects to the jaw joint similar to the *nkx3.2* mutants, but in fact, it seemed to develop normally. Instead, we were able to describe some striking deformations to the fin skeleton. Some of the bones of fish fins are equivalent to some of the limb bones of mammals, and the *gdf5* mutant zebrafish showed severe shortening of several of the cartilages and bones in a similar way to what is seen in mouse mutants and human chondrodysplasia diseases associated with the same gene. Once again, it seems like this gene has a conserved function in a wide diversity of species. However, there was a more unique mutant defect in the zebrafish pectoral fin - missing cartilage and bones seemingly as a result of a process of cartilage division going into overdrive. How most fish pectoral fins develop is known to be quite different from how our mammalian limbs develop, but many

of the details have yet to be studied, so the role of *gdf5* will be an interesting piece of this puzzle to be explored more in the future.

Finally, in the **fifth** study, we wanted to learn more about the development of tendons and ligaments by understanding how the *mkx* gene is regulated. This is a gene known as an important factor in the embryological development and adult maintenance of tendons and ligaments, but its expression and regulation in zebrafish and other species is poorly understood. Employing the same set of techniques as in the third study, we identified an enhancer of the *mkx* gene that was conserved in all jawed vertebrate species. When it came to functionally testing this enhancer to see where it drives *mkx* gene expression, we found quite different results to study three. Rather than enhancer sequences from different species all driving expression in the same locations, we found that they tended to show quite different activity patterns, ranging from tendons and ligaments to cartilage and muscles. This is because while the sequence is conserved, it's not *perfectly* conserved, and small species-specific sequence differences in the enhancer are driving the different activity patterns. One thing that remains unclear is whether this would translate to different gene expression patterns in the different species in question, and that will require future studies to answer definitively.

Through these five studies, this thesis serves to improve our understanding of the function and regulation of three important genes in musculoskeletal development from the molecular to the anatomical level and demonstrates powerful new techniques that can be applied by other researchers to answer many more outstanding questions in the field.

Populärvetenskaplig sammanfattning

I djurriket utgör ryggradsdjuren en särskild grupp som kännetecknas av att de har ett solitt skelett, som huvudsakligen består av ben eller brosk. De inkluderar de flesta av de djur vi är bekanta med: fiskar, fåglar, reptiler och däggdjur. Deras skelett tjänar flera syften, varav de mest uppenbara är att ge strukturellt stöd och skydda inre organ. Skelettens strukturer kompletteras av en rad mjukvävnader, inklusive muskler och bindväv som senor och ligament. Senor förbinder musklerna med skelettet, medan ligament förbinder skelettelement, som ben, med varandra. Alla dessa vävnader bildas under den embryologiska utvecklingen, och hundratals proteinkodande gener styr de komplexa processer som ligger till grund för denna utveckling. Vissa proteiner som kollagen ingår direkt i byggstenarna i dessa vävnader, men många fler proteiner fungerar som regulatorer i komplexa nätverk av interaktioner som avgör när och var dessa strukturproteiner uttrycks för att korrekt forma skelettet och dess associerade vävnader.

Under evolutionens gång har ryggradsdjuren utvecklat en mängd olika skelettstrukturer som skräddarsytts för olika funktioner, exempelvis skillnaden mellan fiskfenor och mänskliga lemmar, eller broskskeletten hos hajar och rockor. Olika sätt att utveckla skelettet har resulterat i morfologiska skillnader som gör att ryggradsdjuren kan anpassa sig till sina miljöer och livsstilar. Genom att undersöka genetiken och utvecklingsmönstren hos dagens ryggradsdjur i ett evolutionärt sammanhang, kan vi lära oss mer om de mekanismer som ligger bakom den morfologiska utvecklingen av ryggradsdjurens skelett. I de fall där andra arter bygger upp sitt skelett på liknande sätt som människan kan vi också få insikter om orsakerna till och potentiella lösningar på sällsynta medfödda skelettsjukdomar och vanligare tillstånd som artros.

Modellorganismer som zebrafisken (*Danio rerio*) är centrala för dessa undersökningar. Zebrafiskar är en kraftfull modell för att studera skelettets utveckling eftersom de är små, utvecklas snabbt från embryon till vuxna på bara två månader, är transparenta som embryon och unga larver så att vi kan se skelettet genom huden, samt att det finns en rad verktyg tillgängliga för att manipulera deras genom. I den här avhandlingen använde jag zebrafisk för att studera tre olika gener, NK-3 Homeobox 2 (*nkx3.2*), Growth and Differentiation Factor 5 (*gdf5*) och Mohawk Homeobox (*mkx*), som alla producerar proteiner som reglerar olika aspekter av muskuloskeletal utveckling.

I den **första** studien använde vi CRISPR/Cas9-genomredigeringsteknik för att mutera ("knocka") *nkx3.2* i zebrafiskens genom och undersökte hur skelettet

utvecklades i dess frånvaro med hjälp av kemiska färgämnen och röntgenskanning. Vi fann att mutationen ledde till att leden i underkäken smälte samman under den tidiga utvecklingen, vilket ledde till att fisken fick en permanent öppen mun. Vi fann också slående defekter i utvecklingen av brosk och ben i bakänden av skallen och i de specialiserade halskotor som kallas den weberska apparaten. Små ben som kallas parapofyser och som fäster revbenen vid ryggraden utvecklas normalt från små kulformade brosk, men dessa saknades helt hos mutanterna, vilket ledde till att revbenen smälte samman direkt med ryggraden. Vissa av dessa missbildningar är jämförbara med de defekter som ses hos musmutanter och ett mänskligt genetiskt tillstånd som kallas spondylomegaepifyseal-metafyseal dysplasi, vilket tyder på att denna gen spelar en liknande roll i alla tre arterna, något som innebär att zebrafisk skulle kunna vara en användbar modell för ytterligare studier som syftar till att bättre förstå sjukdomen.

I den **andra** studien ville vi titta närmare på vilka effekter det deformerade skelettet hos den *nkx3.2*-muterade zebrafisken hade på de omgivande mjukvävnaderna. Utvecklas till exempel musklerna normalt även när de är fästa vid missbildade ben? Traditionellt sett är det bästa sättet att titta närmare på mjukvävnader att skära extremt tunna tvådimensionella snitt genom fisken och titta på dessa vävnadsskivor genom ett mikroskop. Detta gör det dock omöjligt att se helheten i vävnadernas komplexa tredimensionella (3D) organisation, vilket är som att försöka visualisera den inre 3D-strukturen i en skyskrapa endast utifrån ritningar av en handfull våningar. Röntgentomografi (CT) ger information i 3D genom att ta hundratals eller tusentals röntgenbilder från alla olika vinklar runt 360 graders rotation och sedan använda denna information för att beräkna 3D-formen på det objekt som skannas. Vi använde en högupplöst och kontrastrik version av denna teknik vid European Synchrotron Radiation Facility i Grenoble, Frankrike, för att skanna mutanta zebrafiskar i extrem detalj, ner till cellnivå.

Det visade sig att de muskler som fästs vid den deformerade underkäken själva var deformerade på flera sätt och att flera ligament som normalt förbinder benen i den weberska apparaten saknades när dessa ben själva var deformerade eller saknades. Den senare defekten, i kombination med avsaknaden av en viktig vätskefylld säck som sträcker sig ut från skallen och kallas sinus perilymphaticus, ledde oss till slutsatsen att den weberska apparatens funktion, att överföra ljud från fiskens simblåsa till örats sensoriska strukturer, var skadad bortom all räddning. Dessa resultat fungerar också som ett viktigt principbevis för att denna synkrotronskanningsteknik kan användas i många framtida studier för att förstå utvecklingen av andra komplexa mjukvävnader i 3D.

I den **tredje** studien ville vi bättre förstå hur uttrycket av *nkx3.2*-genen kontrollerades, i synnerhet hur den specificerades för att uttryckas under käkledens utveckling. Denna typ av kontroll hanteras av korta DNA-sekvenser som

kallas förstärkare och som ofta finns i närheten av DNA-sekvensen för själva genen. Proteiner som uttrycks i målvävnaden binder till detta förstärkar-DNA och får DNA att böjas runt tills detta förstärkar/proteinkomplex fysiskt kan interagera med början av gensekvensen och få den att transkriberas till RNA, som senare översätts till ett funktionellt protein. Det finns ett antal sätt att identifiera dessa förstärkarsekvenser, men vi valde ett av de enklaste: vi jämförde DNA-sekvenser nära *nkx3.2*-genen från ett stort antal olika arter och letade efter sekvenser som var liknande - konserverade - i dem alla. Detta beror på att funktionella sekvenser bevaras genom naturligt urval under evolutionen och därför tenderar att vara mer lika mellan arter än icke-funktionella sekvenser som ackumulerar slumpmässiga mutationsskillnader över tid.

Vi identifierade en sådan förstärkarsekvens och gav den namnet JRS1. Avgörande var att förstärkaren var bevarad hos alla ryggradsdjur med käkar (med undantag för en enda grupp fiskar som måste ha förlorat den sekundärt), men saknades hos deras närmaste käklösa släktingar, nejonögon och pirålar. Detta tyder på att denna förstärkare utvecklades i den gemensamma förfadern till alla ryggradsdjur med käkar, och att den till och med kan vara en del av orsaken till att artikulerande käkar (som kräver en led) kunde utvecklas över huvud taget. När vi testade funktionen hos denna förstärkare i zebrafiskar fann vi att den specifikt orsakade att *nkx3.2* uttrycktes i käkledens tidiga utveckling, och detsamma gällde för sekvenserna från andra arter, inklusive människor och hajar. När JRS1 raderades helt från zebrafiskens genom försvann dock inte uttrycket av *nkx3.2* i käkleden helt, vilket tyder på att det finns andra förstärkarsekvenser någon annanstans i genomet som ännu inte har hittats.

I den **fjärde** studien vände vi oss till en annan gen, *gdf5*, som är känd för att kontrolleras av *nkx3.2* i vissa vävnader, och använde samma uppsättning tekniker som i den första studien för att titta på defekter i skelettets utveckling när vi slog ut genen. Vi förväntade oss att hitta några defekter i käkleden liknande de hos *nkx3.2*-mutanterna, men i själva verket verkade den utvecklas normalt. Istället kunde vi beskriva några slående deformationer i fenskelettet. Vissa av benen i fiskarnas fenor motsvarar vissa av benen i däggdjurens lemmar, och den *gdf5*-muterade zebrafisken uppvisade en kraftig förkortning av flera av brosken och benen på ett liknande sätt som det som ses hos musmutanter och mänskliga kondrodysplasisjukdomar som associeras med samma gen. Återigen verkar det som om denna gen har en bevarad funktion i en stor mängd olika arter. Det fanns dock en mer unik mutantdefekt i bröstfenan hos zebrafiskar - brosk och ben saknades, till synes som ett resultat av en process där broskdelningen gått på högvarv. Det är känt att de flesta fiskars bröstfenor utvecklas på ett helt annat sätt än våra däggdjurslemmar, men många av detaljerna har ännu inte studerats, så *gdf5*:s roll kommer att vara en intressant pusselbit att utforska mer i framtiden.

Slutligen, i den **femte** studien ville vi lära oss mer om utvecklingen av senor och ligament genom att förstå hur *mkx*-genen regleras. Denna gen är känd som en viktig faktor i den embryologiska utvecklingen och underhållet av senor och ligament hos vuxna, men dess uttryck och reglering i zebrafisk och andra arter är dåligt kända. Genom att använda samma uppsättning tekniker som i den tredje studien identifierade vi en förstärkare av *mkx*-genen som var bevarad i alla arter käkförsedda ryggradsdjur. När det gällde att funktionstesta denna förstärkare för att se var den driver *mkx*-genens uttryck fann vi helt andra resultat än i studie tre. I stället för att förstärkarsekvenser från olika arter alla driver uttrycket på samma platser, fann vi att de tenderade att visa ganska olika aktivitetsmönster, allt från senor och ligament till brosk och muskler. Detta beror på att sekvensen visserligen är bevarad, men inte *perfekt* bevarad, och att små artspecifika sekvensskillnader i förstärkaren driver de olika aktivitetsmönstren. En sak som fortfarande är oklar är om detta skulle leda till olika genuttrycksmönster hos de olika arterna i fråga, och det kommer att krävas framtida studier för att ge ett definitivt svar på detta.

Genom dessa fem studier bidrar denna avhandling till att förbättra vår förståelse av funktionen och regleringen av tre viktiga gener i muskuloskeletal utveckling från molekylär till anatomisk nivå, och demonstrerar kraftfulla nya tekniker som kan tillämpas av andra forskare för att besvara många fler kvarstående frågor inom området.

Acknowledgements

To **Tatjana**, my main supervisor since my Master's thesis project. Thank you for seeing something in me and taking me on as your second-ever PhD student, and for giving me the support, opportunities, and freedom to explore a wide range of techniques and topics that led to such a fulfilling research experience over the last 6 years.

To my co-supervisor **Sophie**, thank you for giving me the opportunity to get involved in the world of synchrotron scanning and palaeontology, and for your boundless enthusiasm and positivity. Our trips to the ESRF were an awesome experience.

To my co-supervisor **Per**, thank for you all the support and fascinating discussions over the years, and for overseeing such a wonderful departmental environment. The trips you made possible, particularly those to Prague and ISELV in Qujing and Valencia have been some of the absolute highlights of my PhD.

A huge thanks goes to the co-authors for so many of the important results and insights that went into my thesis papers: **Paul** and **Kathleen** for their irreplaceable expertise and guidance during the synchrotron experiments, **Caroline** for performing the μCT scanning, **Amin** and **Hanqing** for the OPT imaging and analysis, and **Beata** for generating our CRISPR mutants.

Thank you to the other collaborators I've had the pleasure of working with on side projects during my PhD, particularly **Mélanie, Nicolas, Nathan, Kimara, Caitlin, Richard, Jan,** and **Zerina**. I'm excited about our upcoming publications!

Thank you to all the members of the GEZ facility - **Johan, Beata, Tiffany, Joss, Chrysa, João, Therese,** and **Conrad** for their help in the lab and taking such good care of all of our fish, making all this work possible!

Special thanks to **Laura** for being such a brilliant lab mate and co-first author. I learned so much from you especially in those couple of years when we worked closely together on the mutant papers, as well as in my first year when you taught me so many of the basics. You absolutely helped shape me into the scientist I am today.

Thank you to all the friends and colleagues at the department that made the last 6 years at EBC such a fun and productive experience: **Hannah, James, Sifra,**

Philipp, Matthew, Dennis, Melanie, Vincent, Valéria, François, Donglei, Imke, Cecile, Virginia (and Erik), Pan, Mohammed, Jordi, Martin, Anna, Oskar, Daniel, Grzegorz, Henning, Zivile, Elena, Manolis, Adrianne (and Stefan), Ehsan, Bianca (and Seb), and **Carina**. Particular thanks to **Mohammed** for all the help and encouragement to learn to code in R, to **Anna** for the introduction to Illustrator that led to the figures, diagrams, and posters I could be proud of, and to **Daniel**, keeper of hard drives, for helping to solve any computer and data-related problems that came up.

Thanks also to the Bachelor's and Master's students, **Sara, Tara, Branco,** and **Elsa** that contributed to this environment in the department, producing data in the lab, and giving me the opportunity to (hopefully!) pass on some of my knowledge to a new generation of scientists.

Thank you to **Graham** and **Ralf** for being a key part of my introduction to Evo-Devo research during my Master's studies, and for all of Ralf's patience whenever I needed help in the lab.

I'm grateful for all the other staff that taught me during courses, TA'd alongside me during my own teaching, participated in book club discussions, and were just generally part of the IOB and EBC ecosystem.

Thanks to all the new friends and colleagues I met at local and international conferences, for the fun times and interesting discussions, and for broadening my horizons. This especially includes all the directors, TAs, and students of the 2023 Embryology course at Woods Hole for a spectacular and transformative experience that was a perfect capstone to my PhD, and for revitalising me before I tackled the final stretch of thesis writing.

Cheers to the members of the extremely official Uppsala University Wine and Dine Society and the 2016-18 MEME cohort for your friendship when I first arrived in Uppsala.

I could not have undertaken this journey without **Martin Gilbert** inspiring me to study biology in the first place - something I didn't at all expect when I started at Exeter College 12 years ago, thinking I would become a physicist or engineer.

Finally, thank you to my parents, family, and friends for your encouragement to follow my interests and endless support along the way.

References

Adams, D. C., Collyer, M. L., Kaliontzopoulou, A., and Baken, E. K. (2021). *Geomorph: Software for geometric morphometric analyses. R package version 4.0.*

Aghajanian, P. and Mohan, S. (2018). The art of building bone: Emerging role of chondrocyte-to-osteoblast transdifferentiation in endochondral ossification. *Bone Research* 6, 19. DOI: 10.1038/s41413-018-0021-z.

Alberton, P., Popov, C., Prägert, M., Kohler, J., Shukunami, C., Schieker, M., and Docheva, D. (2012). Conversion of Human Bone Marrow-Derived Mesenchymal Stem Cells into Tendon Progenitor Cells by Ectopic Expression of Scleraxis. *Stem Cells and Development* 21(6), 846–858. DOI: 10.1089/scd.2011.0150.

Alexander, C., Piloto, S., Le Pabic, P., and Schilling, T. F. (2014). Wnt Signaling Interacts with Bmp and Edn1 to Regulate Dorsal-Ventral Patterning and Growth of the Craniofacial Skeleton. *PLoS Genetics* 10(7). Ed. by M. C. Mullins, e1004479. DOI: 10.1371/journal.pgen.1004479.

Alexander, C., Zuniga, E., Blitz, I. L., Wada, N., Le Pabic, P., Javidan, Y., Zhang, T., Cho, K. W., Crump, J. G., and Schilling, T. F. (2011). Combinatorial roles for BMPs and Endothelin 1 in patterning the dorsal-ventral axis of the craniofacial skeleton. *Development* 138(23), 5135–5146. DOI: 10.1242/dev.067801.

Allalou, A., Wu, Y., Ghannad-Rezaie, M., Eimon, P. M., and Yanik, M. F. (2017). Automated deep-phenotyping of the vertebrate brain. *eLife* 6, e23379. DOI: 10.7554/eLife.23379.

Amizuka, N., Hasegawa, T., Oda, K., Freitas, P. H. L. de, Hoshi, K., Li, M., and Ozawa, H. (2012). Histology of epiphyseal cartilage calcification and endochondral ossification. *Frontiers in Bioscience* 4(6), 2085–2100. DOI: 10.2741/526.

Anderson, D. M., Arredondo, J., Hahn, K., Valente, G., Martin, J. F., Wilson-Rawls, J., and Rawls, A. (2006). Mohawk is a novel homeobox gene expressed in the developing mouse embryo. *Developmental Dynamics* 235(3), 792–801. DOI: 10.1002/dvdy.20671.

Anderson, D. M., Beres, B. J., Wilson-Rawls, J., and Rawls, A. (2009). The homeobox gene Mohawk represses transcription by recruiting the Sin3A/HDAC co-repressor complex. *Developmental Dynamics* 238(3), 572–580. DOI: 10.1002/dvdy.21873.

Anderson, H. C. and Shapiro, I. M. (2010). The Epiphyseal Growth Plate. In: *Bone and Development, Topics in Bone Biology*. Ed. by F. Bronner, M. C. Farach-Carson, and H. I. Roach. Vol. 6. London: Springer London. Chap. 3, pp. 39–64. DOI: 10.1007/978-1-84882-822-3.

Andersson, R. and Sandelin, A. (2020). Determinants of enhancer and promoter activities of regulatory elements. *Nature Reviews Genetics* 21(2), 71–87. DOI: 10.1038/s41576-019-0173-8.

Angelini, D. (2021). *Tools for reproducible geometric morphometric analysis. R package version 31.03.02*.

Anthwal, N., Joshi, L., and Tucker, A. S. (2013). Evolution of the mammalian middle ear and jaw: Adaptations and novel structures. *Journal of Anatomy* 222(1), 147–160. DOI: 10.1111/j.1469-7580.2012.01526.x.

Anthwal, N. and Tucker, A. S. (2012). Molecular biology of the mammalian dentary: Insights into how complex skeletal elements can be shaped during development and evolution. In: *From Clone to Bone: The Synergy of Morphological and Molecular Tools in Palaeobiology*. Ed. by R. J. Asher and J. Müller. Cambridge University Press, pp. 207–229. DOI: 10.1017/cbo9780511760174.008.

Arnold, M. A., Kim, Y., Czubryt, M. P., Phan, D., McAnally, J., Qi, X., Shelton, J. M., Richardson, J. A., Bassel-Duby, R., and Olson, E. N. (2007). MEF2C Transcription Factor Controls Chondrocyte Hypertrophy and Bone Development. *Developmental Cell* 12(3), 377–389. DOI: 10.1016/j.devcel.2007.02.004.

Arratia, G. (2015). Complexities of Early Teleostei and the Evolution of Particular Morphological Structures through Time. *Copeia* 103(4), 999–1025. DOI: 10.1643/CG-14-184.

Asahara, H., Inui, M., and Lotz, M. K. (2017). Tendons and Ligaments: Connecting Developmental Biology to Musculoskeletal Disease Pathogenesis. *Journal of Bone and Mineral Research* 32(9), 1773–1782. DOI: 10.1002/jbmr.3199.

Azpiazu, N. and Frasch, M. (1993). Tinman and bagpipe: Two homeo box genes that determine cell fates in the dorsal mesoderm of Drosophila. *Genes and Development* 7, 1325–1340. DOI: 10.1101/gad.7.7b.1325.

Babaei, F., Hong, T. L. C., Yeung, K., Cheng, S. H., and Lam, Y. W. (2016). Contrast-Enhanced X-Ray Micro-Computed Tomography as a Versatile Method for Anatomical Studies of Adult Zebrafish. *Zebrafish* 13(4), 310–316. DOI: 10.1089/zeb.2016.1245.

Bailey, T. L., Boden, M., Buske, F. A., Frith, M., Grant, C. E., Clementi, L., Ren, J., Li, W. W., and Noble, W. S. (2009). MEME Suite: Tools for motif discovery and searching. *Nucleic Acids Research* 37, W202–W208. DOI: 10.1093/nar/gkp335.

Bakkers, J. (2011). Zebrafish as a model to study cardiac development and human cardiac disease. *Cardiovascular Research* 91(2), 279–288. DOI: 10.1093/cvr/cvr098.

Barrangou, R. and Doudna, J. A. (2016). Applications of CRISPR technologies in research and beyond. *Nature Biotechnology* 34(9), 933–941. DOI: 10.1038/nbt.3659.

Barrangou, R., Fremaux, C., Deveau, H., Richards, M., Boyaval, P., Moineau, S., Romero, D. A., and Horvath, P. (2007). CRISPR Provides Acquired Resistance Against Viruses in Prokaryotes. *Science* 315(5819), 1709–1712. DOI: 10.1126/science.1138140.

Barske, L., Askary, A., Zuniga, E., Balczerski, B., Bump, P., Nichols, J. T., and Crump, J. G. (2016). Competition between Jagged-Notch and Endothelin1 Signaling Selectively Restricts Cartilage Formation in the Zebrafish Upper Face. *PLoS Genetics* 12(4), e1005967. DOI: 10.1371/journal.pgen.1005967.

Baur, S. T., Mai, J. J., and Dymecki, S. M. (2000). Combinatorial signaling through BMP receptor IB and GDF5: Shaping of the distal mouse limb and the genetics of distal limb diversity. *Development* 127(3), 605–619. DOI: 10.1242/dev.127.3.605.

Bearden, J. (1967). X-ray Wavelengths. *Reviews of Modern Physics* 39(1), 78–124. DOI: 10.1088/0031-9120/5/2/001.

Bénazet, J. D., Pignatti, E., Nugent, A., Unal, E., Laurent, F., and Zeller, R. (2012). Smad4 is required to induce digit ray primordia and to initiate the aggregation and differentiation of chondrogenic progenitors in mouse limb buds. *Development* 139(22), 4250–4260. DOI: 10.1242/dev.084822.

Benjamini, Y. and Hochberg, Y. (1995). Controlling the False Discovery Rate: A Practical and Powerful Approach to Multiple Testing. *Journal of the Royal Statistical Society: Series B (Methodological)* 57(1), 289–300. DOI: 10.1111/j.2517-6161.1995.tb02031.x.

Bensimon-Brito, A., Boezio, G. L. M., Cardeira-da-Silva, J., Wietelmann, A., Ramkumar, S., Lundegaard, P. R., Helker, C. S. M., Ramadass, R., Piesker, J., Nauerth, A., Mueller, C., and Stainier, D. Y. R. (2022). Integration of multiple imaging platforms to uncover cardiovascular defects in adult zebrafish. *Cardiovascular Research* 118(12), 2665–2687. DOI: 10.1093/cvr/cvab310.

Benton, M. J. (2005). Vertebrate Palaeontology. 3rd Ed. Oxford: Blackwell Science Ltd.

Berendsen, A. D. and Olsen, B. R. (2015). Bone development. *Bone* 80, 14–18. DOI: 10.1016/j.bone.2015.04.035.

Bernard, P., Gabarit, P., Bahassi, E. M., and Couturier, M. (1994). Positive-selection vectors using the F plasmid ccdB killer gene. *Gene* 148(1), 71–74. DOI: 10.1016/0378-1119(94)90235-6.

Berthet, E., Chen, C., Butcher, K., Schneider, R. A., Alliston, T., and Amirtharajah, M. (2013). Smad3 binds Scleraxis and Mohawk and regulates tendon matrix organization. *Journal of Orthopaedic Research* 31(9), 1475–1483. DOI: 10.1002/jor.22382.

Bi, W., Deng, J. M., Zhang, Z., Behringer, R. R., and De Crombrugghe, B. (1999). Sox9 is required for cartilage formation. *Nature Genetics* 22(1), 85–89. DOI: 10.1038/8792.

Bi, X., Wang, K., Yang, L., Pan, H., Jiang, H., Wei, Q., Fang, M., Yu, H., Zhu, C., Cai, Y., He, Y., Gan, X., Zeng, H., Yu, D., Zhu, Y., et al. (2021). Tracing the genetic footprints of vertebrate landing in non-teleost ray-finned fishes. *Cell* 184(5), 1377–1391. DOI: 10.1016/j.cell.2021.01.046.

Blitz, E., Sharir, A., Akiyama, H., and Zelzer, E. (2013). Tendon-bone attachment unit is formed modularly by a distinct pool of Scx-and Sox9-positive progenitors. *Development* 140(13), 2680–2690. DOI: 10.1242/dev.093906.

Bluteau, G., Julien, M., Magne, D., Mallein-Gerin, F., Weiss, P., Daculsi, G., and Guicheux, J. (2007). VEGF and VEGF receptors are differentially expressed in chondrocytes. *Bone* 40(3), 568–576. DOI: 10.1016/j.bone.2006.09.024.

Bobzin, L., Roberts, R. R., Chen, H.-J., Crump, J. G., and Merrill, A. E. (2021). Development and maintenance of tendons and ligaments. *Development* 148(8), dev186916. DOI: 10.1242/dev.186916.

Bonse, U. and Busch, F. (1996). X-ray computed microtomography (μCT) using synchrotron radiation (SR). *Progress in Biophysics and Molecular Biology* 65(1), 133–169. DOI: 10.1016/S0079-6107(96)00011-9.

Bookstein, F. L. (1991). Morphometric Tools for Landmark Data: Geometry and Biology. Cambridge: Cambridge University Press. DOI: 10.1017/CBO9780511573064.

Braasch, I., Gehrke, A. R., Smith, J. J., Kawasaki, K., Manousaki, T., Pasquier, J., Amores, A., Desvignes, T., Batzel, P., Catchen, J., Berlin, A. M., Campbell, M. S., Barrell, D., Martin, K. J., Mulley, J. F., et al. (2016). The spotted gar genome illuminates vertebrate evolution and facilitates human-teleost comparisons. *Nature Genetics* 48(4), 427–437. DOI: 10.1038/ng.3526.

Brazeau, M. D. (2009). The braincase and jaws of a Devonian 'acanthodian' and modern gnathostome origins. *Nature* 457(7227), 305–308. DOI: 10.1038/nature07436.

Brazeau, M. D. and Friedman, M. (2015). The origin and early phylogenetic history of jawed vertebrates. *Nature* 520(7548), 490–497. DOI: 10.1038/nature14438.

Brazeau, M. D. and Winter, V. de (2015). The hyoid arch and braincase anatomy of Acanthodes support chondrichthyan affinity of 'acanthodians'. *Proceedings of the Royal Society B: Biological Sciences* 282(1821), 20152210. DOI: 10.1098/rspb.2015.2210.

Brennan, K. J., Weilert, M., Krueger, S., Pampari, A., Liu, H.-y., Yang, A. W., Morrison, J. A., Hughes, T. R., Rushlow, C. A., Kundaje, A., and Zeitlinger, J. (2023). Chromatin accessibility in the Drosophila embryo is

determined by transcription factor pioneering and enhancer activation. *Developmental Cell* 58, 1–19. DOI: 10.1016/j.devcel.2023.07.007.

Brent, A. E., Braun, T., and Tabin, C. J. (2005). Genetic analysis of interactions between the somitic muscle, cartilage and tendon cell lineages during mouse development. *Development* 132(3), 515–528. DOI: 10.1242/dev.01605.

Brent, A. E., Schweitzer, R., and Tabin, C. J. (2003). A somitic compartment of tendon progenitors. *Cell* 113(2), 235–248. DOI: 10.1016/S0092-8674(03)00268-X.

Brent, A. E. and Tabin, C. J. (2004). FGF acts directly on the somitic tendon progenitors through the Ets transcription factors Pea3 and Erm to regulate scleraxis expression. *Development* 131(16), 3885–3896. DOI: 10.1242/dev.01275.

Bruneau, S., Mourrain, P., and Rosa, F. M. (1997). Expression of contact, a new zebrafish DVR member, marks mesenchymal cell lineages in the developing pectoral fins and head and is regulated by retinoic acid. *Mechanisms of Development* 65(1-2), 163–173. DOI: 10.1016/S0925-4773(97)00072-5.

Brunt, L. H., Begg, K., Kague, E., Cross, S., and Hammond, C. L. (2017). Wnt signalling controls the response to mechanical loading during Zebrafish joint development. *Development* 144(15), 2798–2809. DOI: 10.1242/dev.153528.

Brunt, L. H., Norton, J. L., Bright, J. A., Rayfield, E. J., and Hammond, C. L. (2015). Finite element modelling predicts changes in joint shape and cell behaviour due to loss of muscle strain in jaw development. *Journal of Biomechanics* 48(12), 3112–3122. DOI: 10.1016/j.jbiomech.2015.07.017.

Buxton, P., Edwards, C., Archer, C. W., and Francis-West, P. (2001). Growth/Differentiation Factor-5 (GDF-5) and Skeletal Development. *The Journal of Bone & Joint Surgery* 83(1), 23–30.

Callahan, S., Crowe-Riddell, J. M., Nagesan, R. S., Gray, J. A., and Davis Rabosky, A. R. (2021). A guide for optimal iodine staining and high-throughput diceCT scanning in snakes. *Ecology and Evolution* 11(17), 11587–11603. DOI: 10.1002/ece3.7467.

Camilieri-Asch, V., Shaw, J. A., Mehnert, A., Yopak, K. E., Partridge, J. C., and Collin, S. P. (2020). diceCT: A Valuable Technique to Study the Nervous System of Fish. *eneuro* 7(4). DOI: 10.1523/ENEURO.0076-20.2020.

Caron, M. M., Emans, P. J., Surtel, D. A., Van Der Kraan, P. M., Van Rhijn, L. W., and Welting, T. J. (2015). BAPX-1/NKX-3.2 acts as a chondrocyte hypertrophy molecular switch in osteoarthritis. *Arthritis and Rheumatology* 67(11), 2944–2956. DOI: 10.1002/art.39293.

Cerny, R., Cattell, M., Sauka-Spengler, T., Bronner-Fraser, M., Yu, F., and Medeiros, D. M. (2010). Evidence for the prepattern/cooption model of

vertebrate jaw evolution. *Proceedings of the National Academy of Sciences* 107(40), 17262–17267. DOI: 10.1073/pnas.1009304107.

Charpentier, E., Richter, H., Van Der Oost, J., and White, M. F. (2015). Biogenesis pathways of RNA guides in archaeal and bacterial CRISPR-Cas adaptive immunity. *FEMS Microbiology Reviews* 39(3), 428–441. DOI: 10.1093/femsre/fuv023.

Chen, H., Capellini, T. D., Schoor, M., Mortlock, D. P., Reddi, A. H., and Kingsley, D. M. (2016a). Heads, Shoulders, Elbows, Knees, and Toes: Modular Gdf5 Enhancers Control Different Joints in the Vertebrate Skeleton. *PLoS Genetics* 12(11), 1–27. DOI: 10.1371/journal.pgen.1006454.

Chen, J. W. and Galloway, J. L. (2014). The development of zebrafish tendon and ligament progenitors. *Development* 141(10), 2035–2045. DOI: 10.1242/dev.104067.

Chen, N., Wu, R. W., Lam, Y., Chan, W. C., and Chan, D. (2023). Hypertrophic chondrocytes at the junction of musculoskeletal structures. *Bone Reports* 19, 101698. DOI: 10.1016/j.bonr.2023.101698.

Chen, Q., Shou, P., Zheng, C., Jiang, M., Cao, G., Yang, Q., Cao, J., Xie, N., Velletri, T., Zhang, X., Xu, C., Zhang, L., Yang, H., Hou, J., Wang, Y., et al. (2016b). Fate decision of mesenchymal stem cells: Adipocytes or osteoblasts? *Cell Death and Differentiation* 23(7), 1128–1139. DOI: 10.1038/cdd.2015.168.

Chen, Z., Snetkova, V., Bower, G., Jacinto, S., Clock, B., Barozzi, I., Mannion, B. J., Alcaina-Caro, A., Lopez-Rios, J., Dickel, D. E., Visel, A., Pennacchio, L. A., and Kvon, E. Z. (2022). Widespread Increase in Enhancer-Promoter Interactions during Developmental Enhancer Activation in Mammals. *bioRxiv*. DOI: 10.1101/2022.11.18.516017.

Cheng, K. C., Xin, X., Clark, D. P., and La Riviere, P. (2011). Whole-animal imaging, gene function, and the Zebrafish Phenome Project. *Current Opinion in Genetics and Development* 21(5), 620–629. DOI: 10.1016/j.gde.2011.08.006.

Choi, S. W., Jeong, D. U., Kim, J. A., Lee, B., Joeng, K. S., Long, F., and Kim, D. W. (2012). Indian Hedgehog signalling triggers Nkx3.2 protein degradation during chondrocyte maturation. *Biochemical Journal* 443(3), 789–798. DOI: 10.1042/BJ20112062.

Chuang, H. N., Cheng, H. Y., Hsiao, K. M., Lin, C. W., Lin, M. L., and Pan, H. (2010). The zebrafish homeobox gene irxl1 is required for brain and pharyngeal arch morphogenesis. *Developmental dynamics* 239(2), 639–650. DOI: 10.1002/dvdy.22187.

Chuang, H. N., Hsiao, K. M., Chang, H. Y., Wu, C. C., and Pan, H. (2014). The homeobox transcription factor Irxl1 negatively regulates MyoD expression and myoblast differentiation. *FEBS Journal* 281(13), 2990–3003. DOI: 10.1111/febs.12837.

Chung, U.-I. (2004). Essential Role of Hypertrophic Chondrocytes in Endochondral Bone Development. *Endocrine Journal* 51(1), 19–24. DOI: 10.1507/endocrj.51.19.

Clack, J. A. (2012). Gaining Ground: The Origin and Evolution of Tetrapods. 2nd Ed. Bloomington, Indiana: Indiana University Press.

Cloetens, P., Ludwig, W., Baruchel, J., Van Dyck, D., Van Landuyt, J., Guigay, J. P., and Schlenker, M. (1999). Holotomography: Quantitative phase tomography with micrometer resolution using hard synchrotron radiation x rays. *Applied Physics Letters* 75(19), 2912–2914. DOI: 10.1063/1.125225.

Coleman, C. M. and Tuan, R. S. (2003). Growth/differentiation factor 5 enhances chondrocyte maturation. *Developmental Dynamics* 228(2), 208–216. DOI: 10.1002/dvdy.10369.

Cong, L., Ran, F. A., Cox, D., Lin, S., Barretto, R., Hsu, P. D., Wu, X., Jiang, W., Marraffini, L., and Zhang, F. (2013). Multiplex Genome Engineering Using CRISPR/Cas Systems. *Science* 339(6121), 819–823. DOI: 10.1126/science.1231143.

Cox, P. G. and Jeffery, N. (2011). Reviewing the Morphology of the Jaw-Closing Musculature in Squirrels, Rats, and Guinea Pigs with Contrast-Enhanced MicroCT. *The Anatomical Record* 294(6), 915–928. DOI: 10.1002/ar.21381.

Crotwell, P. L., Clark, T. G., and Mabee, P. M. (2001). Gdf5 is expressed in the developing skeleton of median fins of late-stage zebrafish, Danio rerio. *Development Genes and Evolution* 211(11), 555–558. DOI: 10.1007/s00427-001-0186-z.

Cunningham, T. J., Lancman, J. J., Berenguer, M., Dong, P. D. S., and Duester, G. (2018). Genomic Knockout of Two Presumed Forelimb Tbx5 Enhancers Reveals They Are Nonessential for Limb Development. *Cell Reports* 23(11), 3146–3151. DOI: 10.1016/j.celrep.2018.05.052.

Dale, R. M. and Topczewski, J. (2011). Identification of an evolutionarily conserved regulatory element of the zebrafish col2a1a gene. *Developmental Biology* 357(2), 518–531. DOI: 10.1016/j.ydbio.2011.06.020.

Davesne, D., Schmitt, A. D., Fernandez, V., Benson, R. B., and Sanchez, S. (2020). Three-dimensional characterisation of osteocyte volumes at multiple scales, and its relationship with bone biology and genome evolution in ray-finned fishes. *Journal of Evolutionary Biology* 33(6), 808–830. DOI: 10.1111/jeb.13612.

Davidson, A. (2003). Efficient gene delivery and gene expression in zebrafish using the Sleeping Beauty transposon. *Developmental Biology* 263, 191–202. DOI: 10.1016/s0012-1606(03)00439-1.

Davis, S. P., Finarelli, J. A., and Coates, M. I. (2012). Acanthodes and shark-like conditions in the last common ancestor of modern gnathostomes. *Nature* 486(7402), 247–250. DOI: 10.1038/nature11080.

Day, T. F., Guo, X., Garrett-Beal, L., and Yang, Y. (2005). Wnt/β-catenin signaling in mesenchymal progenitors controls osteoblast and chondrocyte differentiation during vertebrate skeletogenesis. *Developmental Cell* 8(5), 739–750. DOI: 10.1016/j.devcel.2005.03.016.

Dean, M. N. and Summers, A. P. (2006). Mineralized cartialge in the skeleton of chondrichthyan fishes. *Zoology* 109, 164–168. DOI: 10.1016/j.zool.2006.03.002.

Dean, M. N., Mull, C. G., Gorb, S. N., and Summers, A. P. (2009). Ontogeny of the tessellated skeleton: Insight from the skeletal growth of the round stingray Urobatis halleri. *Journal of Anatomy* 215(3), 227–239. DOI: 10.1111/j.1469-7580.2009.01116.x.

Debiais-Thibaud, M. (2019). The Evolution of Endoskeletal Mineralisation in Chondrichthyan Fish. In: *Evolution and Development of Fishes*. Ed. by Z. Johanson, C. Underwood, and M. Richter. Cambridge: Cambridge University Press. Chap. 6, pp. 110–125. DOI: 10.1017/9781316832172.007.

Decker, R. S., Koyama, E., and Pacifici, M. (2015). Articular Cartilage: Structural and Developmental Intricacies and Questions. *Current Osteoporosis Reports* 13(6), 407–414. DOI: 10.1007/s11914-015-0290-z.

Deltcheva, E., Chylinski, K., Sharma, C. M., Gonzales, K., Chao, Y., Pirzada, Z. A., Eckert, M. R., Vogel, J., and Charpentier, E. (2011). CRISPR RNA maturation by trans-encoded small RNA and host factor RNase III. *Nature* 471(7340), 602–607. DOI: 10.1038/nature09886.

Descamps, E., Sochacka, A., De Kegel, B., Van Loo, D., Van Hoorebeke, L., and Adriaens, D. (2014). Soft tissue discrimination with contrast agents using micro-CT scanning. *Belgian Journal of Zoology* 144(1). DOI: 10.26496/bjz.2014.63.

Dewit, J., Witten, P. E., and Huysseune, A. (2011). The mechanism of cartilage subdivision in the reorganization of the zebrafish pectoral fin endoskeleton. *Journal of Experimental Zoology Part B: Molecular and Developmental Evolution* 316(8), 584–597. DOI: 10.1002/jez.b.21433.

Dimitriadi, A., Beis, D., Arvanitidis, C., Adriaens, D., and Koumoundouros, G. (2018). Developmental temperature has persistent, sexually dimorphic effects on zebrafish cardiac anatomy. *Scientific Reports* 8(1), 8125. DOI: 10.1038/s41598-018-25991-8.

Docheva, D., Hunziker, E. B., Fässler, R., and Brandau, O. (2005). Tenomodulin Is Necessary for Tenocyte Proliferation and Tendon Maturation. *Molecular and Cellular Biology* 25(2), 699–705. DOI: 10.1128/mcb.25.2.699-705.2005.

Donoghue, P. (2017). Evolution: Divining the Nature of the Ancestral Vertebrate. *Current Biology* 27(7), R277–R279. DOI: 10.1016/j.cub.2017.02.029.

Douissard, P.-A., Cecilia, A., Rochet, X., Chapel, X., Martin, T., Kamp, T. V. D., Helfen, L., Baumbach, T., Luquot, L., Xiao, X., Meinhardt, J., and Rack, A. (2012). A versatile indirect detector design for hard X-ray microimaging. *Journal of Instrumentation* 7, P09016. DOI: 10.1088/1748-0221/7/09/P09016.

Du Plessis, A., Broeckhoven, C., Guelpa, A., and Le Roux, S. G. (2017). Laboratory x-ray micro-computed tomography: a user guideline for biological samples. *GigaScience* 6(6), gix027. DOI: 10.1093/gigascience/gix027.

Ducy, P., Zhang, R., Geoffroy, V., Ridall, A. L., and Karsenty, G. (1997). Osf2/Cbfa1: A Transcriptional Activator of Osteoblast Differentiation. *Cell* 89(5), 747–754. DOI: 10.1016/S0092-8674(00)80257-3.

Dutel, H., Galland, M., Tafforeau, P., Long, J. A., Fagan, M. J., Janvier, P., Herrel, A., Santin, M. D., Clément, G., and Herbin, M. (2019). Neurocranial development of the coelacanth and the evolution of the sarcopterygian head. *Nature* 569(7757), 556–559. DOI: 10.1038/s41586-019-1117-3.

Dwek, J. R. (2010). The periosteum: What is it, where is it, and what mimics it in its absence? *Skeletal Radiology* 39(4), 319–323. DOI: 10.1007/s00256-009-0849-9.

Edom-Vovard, F., Schuler, B., Bonnin, M. A., Teillet, M. A., and Duprez, D. (2002). Fgf4 positively regulates scleraxis and tenascin expression in chick limb tendons. *Developmental Biology* 247(2), 351–366. DOI: 10.1006/dbio.2002.0707.

Engeszer, R. E., Patterson, L. B., Rao, A. A., and Parichy, D. M. (2007). Zebrafish in The Wild: A Review of Natural History And New Notes from The Field. *Zebrafish* 4(1), 21–40. DOI: 10.1089/zeb.2006.9997.

Espira, L., Lamoureux, L., Jones, S. C., Gerard, R. D., Dixon, I. M., and Czubryt, M. P. (2009). The basic helix-loop-helix transcription factor scleraxis regulates fibroblast collagen synthesis. *Journal of Molecular and Cellular Cardiology* 47(2), 188–195. DOI: 10.1016/j.yjmcc.2009.03.024.

ESRF (2023). *EBS Parameters*. URL: https://www.esrf.fr/home/UsersAndScience/Accelerators/ebs---extremely-brilliant-source/ebs-parameters.html (visited on 08/01/2023).

Evangelou, E., Chapman, K., Meulenbelt, I., Karassa, F. B., Loughlin, J., Carr, A., Doherty, M., Doherty, S., Gómez-Reino, J. J., Gonzalez, A., Halldorsson, B. V., Hauksson, V. B., Hofman, A., Hart, D. J., Ikegawa, S., et al. (2009). Large-scale analysis of association between *GDF5* and *FRZB* variants and osteoarthritis of the hip, knee, and hand. *Arthritis & Rheumatism* 60(6), 1710–1721. DOI: 10.1002/art.24524.

Fabik, J., Psutkova, V., and Machon, O. (2021). The mandibular and hyoid arches-from molecular patterning to shaping bone and cartilage.

International Journal of Molecular Sciences 22(14), 7529. DOI: 10.3390/ijms22147529.

Farley, E. K., Olson, K. M., Zhang, W., Brandt, A. J., Rokhsar, D. S., and Levine, M. S. (2015). Suboptimization of developmental enhancers. *Science* 350(6258), 325–328. DOI: 10.1126/science.aac6948.

Foley, J. E., Maeder, M. L., Pearlberg, J., Joung, J. K., Peterson, R. T., and Yeh, J. R. J. (2009). Targeted mutagenesis in zebrafish using customized zinc-finger nucleases. *Nature Protocols* 4(12), 1855–1868. DOI: 10.1038/nprot.2009.209.

Francillon-Vieillot, H., Buffrénil, V. de, Castanet, J., Géraudie, J., Meunier, F., Sire, J., Zylberberg, L., and Ricqlès, A. J. de (1990). Microstructure and Mineralization of Vertebrate Skeletal Tissues. In: *Skeletal Biomineralization: Patterns, Processes and Evolutionary Trends. Volume I*. Ed. by J. Carte. January. New York: Van Nostrand Reinhold, pp. 471–530. DOI: 10.1029/SC005p0175.

Franz-Odendaal, T. A., Hall, B. K., and Witten, P. E. (2006). Buried alive: How osteoblasts become osteocytes. *Developmental Dynamics* 235(1), 176–190. DOI: 10.1002/dvdy.20603.

Frazer, K. A., Pachter, L., Poliakov, A., Rubin, E. M., and Dubchak, I. (2004). VISTA: Computational tools for comparative genomics. *Nucleic Acids Research* 32, W273–W279. DOI: 10.1093/nar/gkh458.

Friedman, M. and Brazeau, M. D. (2010). A reappraisal of the origin and basal radiation of the Osteichthyes. *Journal of Vertebrate Paleontology* 30(1), 36–56. DOI: 10.1080/02724630903409071.

Fujimura, K., Terai, Y., Ishiguro, N., Miya, M., Nishida, M., and Okada, N. (2008). Heterotypy in the N-terminal region of growth/differentiation factor 5 (GDF5) mature protein during teleost evolution. *Molecular Biology and Evolution* 25(5), 797–800. DOI: 10.1093/molbev/msn041.

Furlong, E. E. and Levine, M. (2018). Developmental enhancers and chromosome topology. *Science* 361(6409), 1341–1345. DOI: 10.1126/science.aau0320.

Gehrke, A. R., Schneider, I., Calle-Mustienes, E. de la, Tena, J. J., Gomez-Marin, C., Chandran, M., Nakamura, T., Braasch, I., Postlethwait, J. H., Gómez-Skarmeta, J. L., and Shubin, N. H. (2015). Deep conservation of wrist and digit enhancers in fish. *Proceedings of the National Academy of Sciences* 112(3), 803–808. DOI: 10.1073/pnas.1420208112.

Gemberling, M., Bailey, T. J., Hyde, D. R., and Poss, K. D. (2013). The zebrafish as a model for complex tissue regeneration. *Trends in Genetics* 29(11), 611–620. DOI: 10.1016/j.tig.2013.07.003.

George, I. D. and Holliday, C. M. (2013). Trigeminal Nerve Morphology in *Alligator mississippiensis* and Its Significance for Crocodyliform Facial Sensation and Evolution: Crocodyliform Facial Sensation and Evolution. *The Anatomical Record* 296(4), 670–680. DOI: 10.1002/ar.22666.

Germain, D. and Ladevèze, S. (2021). The New Scalpel: Basic Aspects of CT-Scan Imaging. In: *Vertebrate Skeletal Histology and Paleohistology*. Ed. by V. de Buffrénil, A. J. de Ricqlès, L. Zylberberg, and K. Padian. 1st Ed. Boca Raton: CRC Press, pp. 55–58. DOI: 10.1201/9781351189590.

Ghezelayagh, A., Harrington, R. C., Burress, E. D., Campbell, M. A., Buckner, J. C., Chakrabarty, P., Glass, J. R., McCraney, W. T., Unmack, P. J., Thacker, C. E., Alfaro, M. E., Friedman, S. T., Ludt, W. B., Cowman, P. F., Friedman, M., et al. (2022). Prolonged morphological expansion of spiny-rayed fishes following the end-Cretaceous. *Nature Ecology & Evolution* 6, 1211–1220. DOI: 10.1038/s41559-022-01801-3.

Gibson, G. (1998). Active Role of Chondrocyte Apoptosis in Endochondral Ossification. *Microscopy Research and Technique* 43(2), 191–204. DOI: 10.1002/(SICI)1097-0029(19981015)43:2<191::AID-JEMT10>3.0.CO;2-T.

Gignac, P. M., Kley, N. J., Clarke, J. A., Colbert, M. W., Morhardt, A. C., Cerio, D., Cost, I. N., Cox, P. G., Daza, J. D., Early, C. M., Echols, M. S., Henkelman, R. M., Herdina, A. N., Holliday, C. M., Li, Z., et al. (2016). Diffusible iodine-based contrast-enhanced computed tomography (diceCT): an emerging tool for rapid, high-resolution, 3-D imaging of metazoan soft tissues. *Journal of Anatomy* 228(6), 889–909. DOI: 10.1111/joa.12449.

Giles, S., Friedman, M., and Brazeau, M. D. (2015). Osteichthyan-like cranial conditions in an Early Devonian stem gnathostome. *Nature* 520(7545), 82–85. DOI: 10.1038/nature14065.

Gipson, G. R., Goebel, E. J., Hart, K. N., Kappes, E. C., Kattamuri, C., McCoy, J. C., and Thompson, T. B. (2020). Structural perspective of BMP ligands and signaling. *Bone* 140, 115549. DOI: 10.1016/j.bone.2020.115549.

Gipson, G. R., Nolan, K., Kattamuri, C., Kenny, A. P., Agricola, Z., Edwards, N. A., Zinski, J., Czepnik, M., Mullins, M. C., Zorn, A. M., and Thompson, T. B. (2023). Formation and characterization of BMP2/GDF5 and BMP4/GDF5 heterodimers. *BMC Biology* 21(1), 16. DOI: 10.1186/s12915-023-01522-4.

Glasauer, S. M. and Neuhauss, S. C. (2014). Whole-genome duplication in teleost fishes and its evolutionary consequences. *Molecular Genetics and Genomics* 289(6). ISBN: 1617-4615, 1045–1060. DOI: 10.1007/s00438-014-0889-2.

Glyn-Jones, S., Palmer, A. J., Agricola, R., Price, A. J., Vincent, T. L., Weinans, H., and Carr, A. J. (2015). Osteoarthritis. *The Lancet* 386(9991), 376–387. DOI: 10.1016/S0140-6736(14)60802-3.

Godivier, J., Lawrence, E. A., Wang, M., Hammond, C. L., and Nowlan, N. C. (2023). Cyclical compression loading is the dominant

mechanoregulator of synovial joint morphogenesis. *bioRxiv*. DOI: 10.1101/2023.02.09.527957.

Grall, E., Feregrino, C., Fischer, S., Courten, A. D., and Tschopp, P. (2023). Self-organized BMP signaling dynamics underlie the development and evolution of tetrapod digit patterns. *bioRxiv*. DOI: 10.1101/2023.03.28.534660.

Grenier, J., Teillet, M. A., Grifone, R., Kelly, R. G., and Duprez, D. (2009). Relationship between neural crest cells and cranial mesoderm during head muscle development. *PLoS ONE* 4(2), e4381. DOI: 10.1371/journal.pone.0004381.

Grossman, S. R., Engreitz, J., Ray, J. P., Nguyen, T. H., Hacohen, N., and Lander, E. S. (2018). Positional specificity of different transcription factor classes within enhancers. *Proceedings of the National Academy of Sciences* 115(30), E7222–E7230. DOI: 10.1073/pnas.1804663115.

Gruneberg, H. and Lee, A. J. (1973). The anatomy and development of brachypodism in the mouse. *Journal of Embryology and Experimental Morphology* 30(1), 119–141. DOI: 10.1242/dev.30.1.119.

Guo, Y., Monahan, K., Wu, H., Gertz, J., Varley, K. E., Li, W., Myers, R. M., Maniatis, T., and Wu, Q. (2012). CTCF/cohesin-mediated DNA looping is required for protocadherin α promoter choice. *Proceedings of the National Academy of Sciences* 109(51), 21081–21086. DOI: 10.1073/pnas.1219280110.

Gupta, S., Stamatoyannopoulos, J. A., Bailey, T. L., and Noble, W. (2007). Quantifying similarity between motifs. *Genome Biology* 8(2), R24. DOI: 10.1186/gb-2007-8-2-r24.

Haffter, P., Granato, M., Brand, M., Mullins, M. C., Hammerschmidt, M., Kane, D. A., Odenthal, J., Van Eeden, F. J., Jiang, Y. J., Heisenberg, C. P., Kelsh, R. N., Furutani-Seiki, M., Vogelsang, E., Beuchle, D., Schach, U., et al. (1996). The identification of genes with unique and essential functions in the development of the zebrafish, Danio rerio. *Development* 123(1), 1–36. DOI: 10.1242/dev.123.1.1.

Hall, B. K. (2000). The neural crest as a fourth germ layer and vertebrates as quadroblastic not triploblastic. *Evolution and Development* 2(1), 3–5. DOI: 10.1046/j.1525-142X.2000.00032.x.

– (2005). Bones and Cartilage: Developmental and Evolutionary Skeletal Biology. London: Elsevier/Academic Press. DOI: 10.1016/B978-0-12-319060-4.X5000-3.

Hall, B. K. and Miyake, T. (2000). All for one and one for all: Condensations and the initiation of skeletal development. *BioEssays* 22(2), 138–147. DOI: 10.1002/(SICI)1521-1878(200002)22:2<138::AID-BIES5>3.0.CO;2-4.

Hamilton, F. (1822). An account of the fishes found in the river Ganges and its branches. Edinburgh: Archibald Constable and Company. DOI: 10.5962/bhl.title.6897.

Han, Y. and Lefebvre, V. (2008). L-Sox5 and Sox6 Drive Expression of the Aggrecan Gene in Cartilage by Securing Binding of Sox9 to a Far-Upstream Enhancer. *Molecular and Cellular Biology* 28(16), 4999–5013. DOI: 10.1128/mcb.00695-08.

Handschuh, S. and Glösmann, M. (2022). Mouse embryo phenotyping using X-ray microCT. *Frontiers in Cell and Developmental Biology* 10, 949184. DOI: 10.3389/fcell.2022.949184.

Hartley, J. L., Temple, G. F., and Brasch, M. A. (2000). DNA Cloning Using In Vitro Site-Specific Recombination. *Genome Research* 10(11), 1788–1795. DOI: 10.1101/gr.143000.

Hedges, S. B. (2012). Amniote phylogeny and the position of turtles. *BMC Biology* 10, 10–11. DOI: 10.1186/1741-7007-10-64.

Heler, R., Samai, P., Modell, J. W., Weiner, C., Goldberg, G. W., Bikard, D., and Marraffini, L. A. (2015). Cas9 specifies functional viral targets during CRISPR-Cas adaptation. *Nature* 519(7542), 199–202. DOI: 10.1038/nature14245.

Hellemans, J., Simon, M., Dheedene, A., Alanay, Y., Mihci, E., Rifai, L., Sefiani, A., Bever, Y. van, Meradji, M., Superti-Furga, A., and Mortier, G. (2009). Homozygous Inactivating Mutations in the NKX3-2 Gene Result in Spondylo-Megaepiphyseal-Metaphyseal Dysplasia. *American Journal of Human Genetics* 85(6), 916–922. DOI: 10.1016/j.ajhg.2009.11.005.

Hill, A. J., Teraoka, H., Heideman, W., and Peterson, R. E. (2005). Zebrafish as a model vertebrate for investigating chemical toxicity. *Toxicological Sciences* 86(1), 6–19. DOI: 10.1093/toxsci/kfi110.

Hirasawa, T. and Kuratani, S. (2015). Evolution of the vertebrate skeleton: morphology, embryology, and development. *Zoological Letters* 1, 2. DOI: 10.1186/s40851-014-0007-7.

Ho, T. T., Zhou, N., Huang, J., Koirala, P., Xu, M., Fung, R., Wu, F., and Mo, Y. Y. (2015). Targeting non-coding RNAs with the CRISPR/Cas9 system in human cell lines. *Nucleic Acids Research* 43(3), e17. DOI: 10.1093/nar/gku1198.

Hobert, O. (2010). Gene regulation: Enhancers stepping out of the shadow. *Current Biology* 20(17), R697–R699. DOI: 10.1016/j.cub.2010.07.035.

Holliday, C. M., Tsai, H. P., Skiljan, R. J., George, I. D., and Pathan, S. (2013). A 3D Interactive Model and Atlas of the Jaw Musculature of Alligator mississippiensis. *PLoS ONE* 8(6), e62806. DOI: 10.1371/journal.pone.0062806.

Holmbeck, K., Bianco, P., Pidoux, I., Inoue, S., Billinghurst, R. C., Wu, W., Chrysovergis, K., Yamada, S., Birkedal-Hansen, H., and Poole, A. R. (2005). The metalloproteinase MT1-MMP is required for normal development and maintenance of osteocyte processes in bone. *Journal of Cell Science* 118(1), 147–156. DOI: 10.1242/jcs.01581.

Howe, K., Clark, M. D., Torroja, C. F., Torrance, J., Berthelot, C., Muffato, M., Collins, J. E., Humphray, S., McLaren, K., Matthews, L., McLaren, S., Sealy, I., Caccamo, M., Churcher, C., Scott, C., et al. (2013). The zebrafish reference genome sequence and its relationship to the human genome. *Nature* 496(7446), 498–503. DOI: 10.1038/nature12111.

Huang, A. H., Riordan, T. J., Pryce, B., Weibel, J. L., Watson, S. S., Long, F., Lefebvre, V., Harfe, B. D., Stadler, H. S., Akiyama, H., Tufa, S. F., Keene, D. R., and Schweitzer, R. (2015). Musculoskeletal integration at the wrist underlies the modular development of limb tendons. *Development* 142(14), 2431–2441. DOI: 10.1242/dev.122374.

Huang, A. H., Watson, S. S., Wang, L., Baker, B., Akiyama, H., Brigande, J. V., and Schweitzer, R. (2019). Requirement for Scleraxis in the recruitment of mesenchymal progenitors during embryonic tendon elongation. *Development* 146(20), dev.182782. DOI: 10.1242/dev.182782.

Hughes, L. C., Ortí, G., Huang, Y., Sun, Y., Baldwin, C. C., Thompson, A. W., Arcila, D., Betancur, R., Li, C., Becker, L., Bellora, N., Zhao, X., Li, X., Wang, M., Fang, C., et al. (2018). Comprehensive phylogeny of ray-finned fishes (Actinopterygii) based on transcriptomic and genomic data. *Proceedings of the National Academy of Sciences* 115(24), 6249–6254. DOI: 10.1073/pnas.1719358115.

Hur, M., Gistelinck, C. A., Huber, P., Lee, J., Thompson, M. H., Monstad-Rios, A. T., Watson, C. J., McMenamin, S. K., Willaert, A., Parichy, D. M., Coucke, P., and Kwon, R. Y. (2017). MicroCT-Based Phenomics in the Zebrafish Skeleton Reveals Virtues of Deep Phenotyping in a Distributed Organ System. *eLife* 6, e26014. DOI: 10.7554/eLife.26014.

Hwang, W. Y., Fu, Y., Reyon, D., Maeder, M. L., Shengdar, Q., Sander, J. D., Peterson, R. T., Yeh, J. J., and Keith, J. (2013). Efficient In Vivo Genome Editing Using RNA-Guided Nucleases. *Nature Biotechnology* 31(3), 227–229. DOI: 10.1038/nbt.2501.

Hwang, W. Y., Peterson, R. T., and Yeh, J. R. J. (2014). Methods for targeted mutagenesis in zebrafish using TALENs. *Methods* 69(1), 76–84. DOI: 10.1016/j.ymeth.2014.04.009.

Inada, M., Wang, Y., Byrne, M. H., Rahman, M. U., Miyaura, C., López-Otín, C., and Krane, S. M. (2004). Critical roles for collagenase-3 (Mmp13) in development of growth plate cartilage and in endochondral ossification. *Proceedings of the National Academy of Sciences* 101(49), 17192–17197. DOI: 10.1073/pnas.0407788101.

Indjeian, V. B., Kingman, G. A., Jones, F. C., Guenther, C. A., Grimwood, J., Schmutz, J., Myers, R. M., and Kingsley, D. M. (2016). Evolving New Skeletal Traits by cis-Regulatory Changes in Bone Morphogenetic Proteins. *Cell* 164(1-2), 45–56. DOI: 10.1016/j.cell.2015.12.007.

Ito, Y., Toriuchi, N., Yoshitaka, T., Ueno-Kudoh, H., Sato, T., Yokoyama, S., Nishida, K., Akimoto, T., Takahashi, M., Miyaki, S., and Asahara, H. (2010). The Mohawk homeobox gene is a critical regulator of tendon differentiation. *Proceedings of the National Academy of Sciences* 107(23), 10538–10542. DOI: 10.1073/pnas.1000525107.

St-Jacques, B., Hammerschmidt, M., and McMahon, A. P. (1999). Indian hedgehog signaling regulates proliferation and differentiation of chondrocytes and is essential for bone formation. *Genes and Development* 13(16), 2072–2086. DOI: 10.1101/gad.13.16.2072.

Janvier, P. (2008). Early Jawless Vertebrates and Cyclostome Origins. *Zoological Science* 25(10), 1045–1056. DOI: 10.2108/zsj.25.1045.

Jelinsky, S. A., Archambault, J., Li, L., and Seeherman, H. (2010). Tendon-selective genes identified from rat and human musculoskeletal tissues. *Journal of Orthopaedic Research* 28(3), 289–297. DOI: 10.1002/jor.20999.

Jepsen, K. J., Wu, F., Peragallo, J. H., Paul, J., Roberts, L., Ezura, Y., Oldberg, A., Birk, D. E., and Chakravarti, S. (2002). A syndrome of joint laxity and impaired tendon integrity in lumican- and fibromodulin-deficient mice. *Journal of Biological Chemistry* 277(38), 35532–35540. DOI: 10.1074/jbc.M205398200.

Jinek, M., Chylinski, K., Fonfara, I., Hauer, M., Doudna, J. A., and Charpentier, E. (2012). A Programmable Dual-RNA-Guided DNA Endonuclease in Adaptive Bacterial Immunity. *Science* 337(6096), 816–822. DOI: 10.1126/science.1225829.

Johnston, P. (2022). The missing anatomy of the living coelacanth, *Latimeria chalumnae* (Smith, 1939). *Vertebrate Zoology* 72, 513–531. DOI: 10.3897/vz.72.e84274.

Joung, J. K. and Sander, J. D. (2013). TALENs: A widely applicable technology for targeted genome editing. *Nature Reviews Molecular Cell Biology* 14(1), 49–55. DOI: 10.1038/nrm3486.

Ju, B., Chong, S. W., He, J., Wang, X., Xu, Y., Wan, H., Tong, Y., Yan, T., Korzh, V., and Gong, Z. (2003). Recapitulation of fast skeletal muscle development in zebrafish by transgenic expression of GFP under the mylz2 promoter. *Developmental Dynamics* 227(1), 14–26. DOI: 10.1002/dvdy.10273.

Kagey, M. H., Newman, J. J., Bilodeau, S., Zhan, Y., Orlando, D. A., Van Berkum, N. L., Ebmeier, C. C., Goossens, J., Rahl, P. B., Levine, S. S., Taatjes, D. J., Dekker, J., and Young, R. A. (2010). Mediator and cohesin connect gene expression and chromatin architecture. *Nature* 467(7314), 430–435. DOI: 10.1038/nature09380.

Kague, E., Hughes, S. M., Lawrence, E. A., Cross, S., Martin-Silverstone, E., Hammond, C. L., and Hinits, Y. (2019). Scleraxis genes are required for normal musculoskeletal development and for rib growth and

mineralization in zebrafish. *FASEB Journal* 33(8), 9116–9130. DOI: 10.1096/fj.201802654RR.

Kammandel, B., Chowdhury, K., Stoykova, A., Aparicio, S., Brenner, S., and Gruss, P. (1999). Distinct cis-essential modules direct the time-space pattern of the Pax6 gene activity. *Developmental Biology* 205(1), 79–97. DOI: 10.1006/dbio.1998.9128.

Kang, J. S., Alliston, T., Delston, R., and Derynck, R. (2005). Repression of Runx2 function by TGF-β through recruitment of class II histone deacetylases by Smad3. *EMBO Journal* 24(14), 2543–2555. DOI: 10.1038/sj.emboj.7600729.

Kania, K., Colella, F., Riemen, A. H. K., Wang, H., Howard, K. A., Aigner, T., Dell'Accio, F., Capellini, T. D., Roelofs, A. J., and De Bari, C. (2020). Regulation of Gdf5 expression in joint remodelling, repair and osteoarthritis. *Scientific Reports* 10, 157. DOI: 10.1038/s41598-019-57011-8.

Kardon, G. (1998). Muscle and tendon morphogenesis in the avian hind limb. *Development* 125(20), 4019–4032. DOI: 10.1242/dev.125.20.4019.

Katayama, R., Wakitani, S., Tsumaki, N., Morita, Y., Matsushita, I., Gejo, R., and Kimura, T. (2004). Repair of articular cartilage defects in rabbits using CDMP1 gene-transfected autologous mesenchymal cells derived from bone marrow. *Rheumatology* 43(8), 980–985. DOI: 10.1093/rheumatology/keh240.

Kaucka, M., Zikmund, T., Tesarova, M., Gyllborg, D., Hellander, A., Jaros, J., Kaiser, J., Petersen, J., Szarowska, B., Newton, P. T., Dyachuk, V., Li, L., Qian, H., Johansson, A.-S., Mishina, Y., et al. (2017). Oriented clonal cell dynamics enables accurate growth and shaping of vertebrate cartilage. *eLife* 6, e25902. DOI: 10.7554/eLife.25902.

Kawakami, K. (2007). Tol2: A versatile gene transfer vector in vertebrates. *Genome Biology* 8, S7. DOI: 10.1186/gb-2007-8-s1-s7.

Kayama, T., Mori, M., Ito, Y., Matsushima, T., Nakamichi, R., Suzuki, H., Ichinose, S., Saito, M., Marumo, K., and Asahara, H. (2016). Gtf2ird1-Dependent Mohawk Expression Regulates Mechanosensing Properties of the Tendon. *Molecular and Cellular Biology* 36(8), 1297–1309. DOI: 10.1128/MCB.00950-15.Address.

Kerschnitzki, M., Zander, T., Zaslansky, P., Fratzl, P., Shahar, R., and Wagermaier, W. (2014). Rapid alterations of avian medullary bone material during the daily egg-laying cycle. *Bone* 69, 109–117. DOI: 10.1016/j.bone.2014.08.019.

Kielty, C. M., Kwan, A. P., Holmes, D. F., Schor, S. L., and Grant, M. E. (1985). Type X collagen, a product of hypertrophic chondrocytes. *Biochemical Journal* 227(2), 545–554. DOI: 10.1042/bj2270545.

Killian, M. L. and Thomopoulos, S. (2016). Scleraxis is required for the development of a functional tendon enthesis. *FASEB Journal* 30(1), 301–311. DOI: 10.1096/fj.14-258236.

Kim, D.-W. and Lassar, A. B. (2003). Smad-Dependent Recruitment of a Histone Deacetylase/Sin3A Complex Modulates the Bone Morphogenetic Protein-Dependent Transcriptional Repressor Activity of Nkx3.2. *Molecular and Cellular Biology* 23(23), 8704–8717. DOI: 10.1128/mcb.23.23.8704-8717.2003.

Kim, H.-S., Neugebauer, J., McKnite, A., Tilak, A., and Christian, J. L. (2019). BMP7 functions predominantly as a heterodimer with BMP2 or BMP4 during mammalian embryogenesis. *eLife* 8, e48872. DOI: 10.7554/eLife.48872.

Kimmel, C. B., Ballard, W. W., Kimmel, S. R., Ullmann, B., and Schilling, T. F. (1995). Stages of embryonic development of the zebrafish. *Developmental Dynamics* 203(3), 253–310. DOI: 10.1002/aja.1002030302.

Kimmel, C. B., Miller, C. T., and Moens, C. B. (2001). Specification and Morphogenesis of the Zebrafish Larval Head Skeleton. *Developmental Biology* 233(2), 239–257. DOI: 10.1006/dbio.2001.0201.

King, B., Qiao, T., Lee, M. S., Zhu, M., and Long, J. A. (2017). Bayesian Morphological Clock Methods Resurrect Placoderm Monophyly and Reveal Rapid Early Evolution in Jawed Vertebrates. *Systematic Biology* 66(4), 499–516. DOI: 10.1093/sysbio/syw107.

Kjær, M. (2004). Role of Extracellular Matrix in Adaptation of Tendon and Skeletal Muscle to Mechanical Loading. *Physiological Reviews* 84(2), 649–698. DOI: 10.1152/physrev.00031.2003.

Klammert, U., Mueller, T. D., Hellmann, T. V., Wuerzler, K. K., Kotzsch, A., Schliermann, A., Schmitz, W., Kuebler, A. C., Sebald, W., and Nickel, J. (2015). GDF-5 can act as a context-dependent BMP-2 antagonist. *BMC Biology* 13, 77. DOI: 10.1186/s12915-015-0183-8.

Klein, S., Staring, M., Murphy, K., Viergever, M. A., and Pluim, J. P. (2010). Elastix: A toolbox for intensity-based medical image registration. *IEEE Transactions on Medical Imaging* 29(1), 196–205. DOI: 10.1109/TMI.2009.2035616.

Kolmann, M. A., Nagesan, R. S., Andrews, J. V., Borstein, S. R., Figueroa, R. T., Singer, R. A., Friedman, M., and López–Fernández, H. (2023). DiceCT for fishes: recommendations for pairing iodine contrast agents with μCT to visualize soft tissues in fishes. *Journal of Fish Biology* 102(4), 893–903. DOI: 10.1111/jfb.15320.

Komori, T., Yagi, H., Nomura, S., Yamaguchi, A., Sasaki, K., Deguchi, K., Shimizu, Y., Bronson, R. T., Inada, M., Sato, M., Okamoto, R., Kitamura, Y., Yoshiki, S., and Kishimoto, T. (1997). Targeted Disruption of Cbfa1 Results in a Complete Lack of Bone Formation owing to Maturational Arrest of Osteoblasts. *Cell* 89(5), 755–764. DOI: 10.1016/S0092-8674(00)80258-5.

Koshikawa, S., Giorgianni, M. W., Vaccaro, K., Kassner, V. A., Yoder, J. H., Werner, T., and Carroll, S. B. (2015). Gain of cis-regulatory activities

underlies novel domains of wingless gene expression in Drosophila. *Proceedings of the National Academy of Sciences* 112(24), 7524–7529. DOI: 10.1073/pnas.1509022112.

Kuraku, S., Takio, Y., Sugahara, F., Takechi, M., and Kuratani, S. (2010). Evolution of oropharyngeal patterning mechanisms involving Dlx and endothelins in vertebrates. *Developmental Biology* 341(1), 315–323. DOI: 10.1016/j.ydbio.2010.02.013.

Kvon, E. Z. (2015). Using transgenic reporter assays to functionally characterize enhancers in animals. *Genomics* 106(3), 185–192. DOI: 10.1016/J.YGENO.2015.06.007.

Kvon, E. Z., Waymack, R., Gad, M., and Wunderlich, Z. (2021). Enhancer redundancy in development and disease. *Nature Reviews Genetics* 22(5), 324–336. DOI: 10.1038/s41576-020-00311-x.

Kwan, K. M., Fujimoto, E., Grabher, C., Mangum, B. D., Hardy, M. E., Campbell, D. S., Parant, J. M., Yost, H. J., Kanki, J. P., and Chien, C. B. (2007). The Tol2kit: A multisite gateway-based construction Kit for Tol2 transposon transgenesis constructs. *Developmental Dynamics* 236(11), 3088–3099. DOI: 10.1002/dvdy.21343.

Laale, H. W. (1977). The biology and use of zebrafish, Brachydanio rerio in fisheries research. A literature review. *Journal of Fish Biology* 10(2), 121–173. DOI: 10.1111/j.1095-8649.1977.tb04049.x.

Labun, K., Montague, T. G., Gagnon, J. A., Thyme, S. B., and Valen, E. (2016). CHOPCHOP v2: a web tool for the next generation of CRISPR genome engineering. *Nucleic acids research* 44(W1), W272–W276. DOI: 10.1093/nar/gkw398.

Langer, M., Cloetens, P., Guigay, J.-P., and Peyrin, F. (2008). Quantitative comparison of direct phase retrieval algorithms in in-line phase tomography: Quantitative comparison of direct phase retrieval algorithms. *Medical Physics* 35(10), 4556–4566. DOI: 10.1118/1.2975224.

Laurin, M., Quilhac, A., and Buffrénil, V. de (2021). The Vertebrate Skeleton: A Brief Introduction. In: *Vertebrate Skeletal Histology and Paleohistology*. Ed. by V. de Buffrénil, A. J. de Ricqlès, L. Zylberberg, and K. Padian. 1st Ed. Boca Raton: CRC Press. Chap. 3, pp. 39–58. DOI: 10.1201/9781351189590.

Le Pabic, P., Dranow, D. B., Hoyle, D. J., and Schilling, T. F. (2022). Zebrafish endochondral growth zones as they relate to human bone size, shape and disease. *Frontiers in Endocrinology* 13, 1060187. DOI: 10.3389/fendo.2022.1060187.

Lee, C., Wang, K., Qin, T., and Sartor, M. A. (2020). Testing Proximity of Genomic Regions to Transcription Start Sites and Enhancers Complements Gene Set Enrichment Testing. *Frontiers in Genetics* 11, 199. DOI: 10.3389/fgene.2020.00199.

Léjard, V., Brideau, G., Blais, F., Salingcarnboriboon, R., Wagner, G., Roehrl, M. H., Noda, M., Duprez, D., Houillier, P., and Rossert, J. (2007).

Scleraxis and NFATc regulate the expression of the pro-α1(I) collagen gene in tendon fibroblasts. *Journal of Biological Chemistry* 282(24), 17665–17675. DOI: 10.1074/jbc.M610113200.

Lengner, C. J., Hassan, M. Q., Serra, R. W., Lepper, C., Van Wijnen, A. J., Stein, J. L., Lian, J. B., and Stein, G. S. (2005). Nkx3.2-mediated repression of Runx2 promotes chondrogenic differentiation. *Journal of Biological Chemistry* 280(16), 15872–15879. DOI: 10.1074/jbc.M411144200.

Lettice, L. A., Purdie, L. A., Carlson, G. J., Kilanowski, F., Dorin, J., and Hill, R. E. (Aug. 1999). The mouse bagpipe gene controls development of axial skeleton, skull, and spleen. *Proceedings of the National Academy of Sciences* 96(17), 9695–9700. DOI: 10.1073/pnas.96.17.9695.

Lettice, L. A., Heaney, S. J., Purdie, L. A., Li, L., Beer, P. de, Oostra, B. A., Goode, D., Elgar, G., Hill, R. E., and Graaff, E. de (2003). A long-range Shh enhancer regulates expression in the developing limb and fin and is associated with preaxial polydactyly. *Human Molecular Genetics* 12(14), 1725–1735. DOI: 10.1093/hmg/ddg180.

Li, L., Newton, P. T., Bouderlique, T., Sejnohova, M., Zikmund, T., Kozhemyakina, E., Xie, M., Krivanek, J., Kaiser, J., Qian, H., Dyachuk, V., Lassar, A. B., Warman, M. L., Barenius, B., Adameyko, I., et al. (2017). Superficial cells are self-renewing chondrocyte progenitors, which form the articular cartilage in juvenile mice. *The FASEB Journal* 31(3), 1067–1084. DOI: 10.1096/fj.201600918R.

Lim, J., Tu, X., Choi, K., Akiyama, H., Mishina, Y., and Long, F. (2015). BMP-Smad4 signaling is required for precartilaginous mesenchymal condensation independent of Sox9 in the mouse. *Developmental Biology* 400(1), 132–138. DOI: 10.1016/j.ydbio.2015.01.022.

Liu, D., Black, B. L., and Derynck, R. (2001). TGF-β inhibits muscle differentiation through functional repression of myogenic transcription factors by Smad3. *Genes and Development* 15(22), 2950–2966. DOI: 10.1101/gad.925901.

Liu, H., Xu, J., and Jiang, R. (2019). Mkx-Deficient Mice Exhibit Hedgehog Signaling-Dependent Ectopic Ossification in the Achilles Tendons. *Journal of Bone and Mineral Research* 34(3), 557–569. DOI: 10.1002/jbmr.3630.

Liu, H., Zhang, C., Zhu, S., Lu, P., Zhu, T., Gong, X., Zhang, Z., Hu, J., Yin, Z., Chin Heng, B., Chen, X., and Wei Ouyang, H. (2015). Mohawk promotes the tenogenesis of mesenchymal stem cells through activation of the TGFβ signaling pathway. *Stem Cells* 33(2), 443–455. DOI: 10.1002/stem.1866.

Liu, S. and Leach, S. D. (2011). Zebrafish models for cancer. *Annual Review of Pathology: Mechanisms of Disease* 6, 71–93. DOI: 10.1146/annurev-pathol-011110-130330.

Liu, W., Watson, S. S., Lan, Y., Keene, D. R., Ovitt, C. E., Liu, H., Schweitzer, R., and Jiang, R. (2010). The Atypical Homeodomain Transcription Factor Mohawk Controls Tendon Morphogenesis. *Molecular and Cellular Biology* 30(20), 4797–4807. DOI: 10.1128/mcb.00207-10.

Long, J. T., Leinroth, A., Liao, Y., Ren, Y., Mirando, A. J., Nguyen, T., Guo, W., Sharma, D., Rouse, D., Wu, C., Cheah, K. S. E., Karner, C. M., and Hilton, M. J. (2022). Hypertrophic chondrocytes serve as a reservoir for marrow-associated skeletal stem and progenitor cells, osteoblasts, and adipocytes during skeletal development. *eLife* 11, e76932. DOI: 10.7554/eLife.76932.

Long, J. A., Burrow, C. J., Ginter, M., Maisey, J. G., Trinajstic, K. M., Coates, M. I., Young, G. C., and Senden, T. J. (2015a). First shark from the late devonian (Frasnian) gogo formation, Western Australia sheds new light on the development of tessellated calcified cartilage. *PLoS ONE* 10(5), e0126066. DOI: 10.1371/journal.pone.0126066.

Long, J. A., Mark-Kurik, E., Johanson, Z., Lee, M. S., Young, G. C., Zhu, M., Ahlberg, P. E., Newman, M., Jones, R., Blaauwen, J. den, Choo, B., and Trinajstic, K. (2015b). Copulation in antiarch placoderms and the origin of gnathostome internal fertilization. *Nature* 517, 196–199. DOI: 10.1038/nature13825.

Lukas, P. and Olsson, L. (2018a). Bapx1 is required for jaw joint development in amphibians. *Evolution & Development* 20(6), 192–206. DOI: 10.1111/ede.12267.

– (2018b). Bapx1 upregulation is associated with ectopic mandibular cartilage development in amphibians. *Zoological Letters* 4, 16. DOI: 10.1186/s40851-018-0101-3.

Luo, Z.-X. (2011). Developmental Patterns in Mesozoic Evolution of Mammal Ears. *Annual Review of Ecology, Evolution, and Systematics* 42, 355–380. DOI: 10.1146/annurev-ecolsys-032511-142302.

Lyons, K. M. and Rosen, V. (2019). BMPs, TGFβ, and border security at the interzone. In: *Current Topics in Developmental Biology*. Vol. 133. Elsevier, pp. 153–170. DOI: 10.1016/bs.ctdb.2019.02.001.

Maeda, T., Sakabe, T., Sunaga, A., Sakai, K., Rivera, A. L., Keene, D. R., Sasaki, T., Stavnezer, E., Iannotti, J., Schweitzer, R., Ilic, D., Baskaran, H., and Sakai, T. (2011). Conversion of mechanical force into TGF-β-mediated biochemical signals. *Current Biology* 21(11), 933–941. DOI: 10.1016/j.cub.2011.04.007.

Maisey, J. G., Miller, R., Pradel, A., Denton, J. S., Bronson, A., and Janvier, P. (2017). Pectoral morphology in Doliodus: Bridging the 'acanthodian'-chondrichthyan divide. *American Museum Novitates* 3875, 1–15. DOI: 10.1206/3875.1.

Marjanović, D. (2021). The Making of Calibration Sausage Exemplified by Recalibrating the Transcriptomic Timetree of Jawed Vertebrates. *Frontiers in Genetics* 12, 521693. DOI: 10.3389/fgene.2021.521693.

Marraffini, L. A. (2015). CRISPR-Cas immunity in prokaryotes. *Nature* 526(7571), 55–61. DOI: 10.1038/nature15386.

Martin, T. and Koch, A. (2006). Recent developments in X-ray imaging with micrometer spatial resolution. *Journal of Synchrotron Radiation* 13(2), 180–194. DOI: 10.1107/S0909049506000550.

Martinez-Garcia, M., Garcia-Canto, E., Fenollar-Cortes, M., Aytes, A. P., and Trujillo-Tiebas, M. J. (2016). Characterization of an acromesomelic dysplasia, Grebe type case: novel mutation affecting the recognition motif at the processing site of GDF5. *Journal of Bone and Mineral Metabolism* 34(5), 599–603. DOI: 10.1007/s00774-015-0693-z.

Mayr-Wohlfart, U., Waltenberger, J., Hausser, H., Kessler, S., Günther, K. P., Dehio, C., Puhl, W., and Brenner, R. E. (2002). Vascular endothelial growth factor stimulates chemotactic migration of primary human osteoblasts. *Bone* 30(3), 472–477. DOI: 10.1016/S8756-3282(01)00690-1.

Mendias, C. L., Gumucio, J. P., Bakhurin, K. I., Lynch, E. B., and Brooks, S. V. (2012). Physiological loading of tendons induces scleraxis expression in epitenon fibroblasts. *Journal of Orthopaedic Research* 30(4), 606–612. DOI: 10.1002/jor.21550.

Merino, R., Macias, D., Gañan, Y., Economides, A. N., Wang, X., Wu, Q., Stahl, N., Sampath, K. T., Varona, P., and Hurle, J. M. (1999). Expression and Function of Gdf-5 during Digit Skeletogenesis in the Embryonic Chick Leg Bud. *Developmental Biology* (206), 33–45. DOI: 10.1006/dbio.1998.9129.

Metscher, B. D. (2013). Biological applications of X-ray microtomography: imaging micro- anatomy, molecular expression and organismal diversity. *Microscopy and Analysis* 27(2), 4.

– (2009). Micro CT for comparative morphology: Simple staining methods allow high-contrast 3D imaging of diverse non-mineralized animal tissues. *BMC Physiology* 9, 11. DOI: 10.1186/1472-6793-9-11.

Meyers, J. R. (2018). Zebrafish: Development of a Vertebrate Model Organism. *Current Protocols in Essential Laboratory Techniques* e19. DOI: 10.1002/cpet.19.

Migga, A., Schulz, G., Rodgers, G., Osterwalder, M., Tanner, C., Blank, H., Jerjen, I., Salmon, P., Twengström, W., Scheel, M., Weitkamp, T., Schlepütz, C. M., Bolten, J. S., Huwyler, J., Hotz, G., et al. (2022). Comparative hard x-ray tomography for virtual histology of zebrafish larva, human tooth cementum, and porcine nerve. *Journal of Medical Imaging* 9(3). DOI: 10.1117/1.JMI.9.3.031507.

Miller, C. T., Yelon, D., Stainier, D. Y. R., and Kimmel, C. B. (2003). Two endothelin 1 effectors, hand2 and bapx1, pattern ventral pharyngeal cartilage and the jaw joint. *Development* 130(7), 1353–1365. DOI: 10.1242/dev.00339.

Miller, S. W. and Posakony, J. W. (2020). Disparate expression specificities coded by a shared Hox-C enhancer. *eLife* 9, e39876. DOI: 10.7554/eLife.39876.

Mills, C., Muruganujan, A., Ebert, D., Marconett, C. N., Lewinger, J. P., Thomas, P. D., and Mi, H. (2020). PEREGRINE: A genome-wide prediction of enhancer to gene relationships supported by experimental evidence. *PLoS ONE* 15(12), e0243791. DOI: 10.1371/journal.pone.0243791.

Miyamoto, Y., Mabuchi, A., Shi, D., Kubo, T., Takatori, Y., Saito, S., Fujioka, M., Sudo, A., Uchida, A., Yamamoto, S., Ozaki, K., Takigawa, M., Tanaka, T., Nakamura, Y., Jiang, Q., et al. (2007). A functional polymorphism in the 5' UTR of GDF5 is associated with susceptibility to osteoarthritis. *Nature Genetics* 39(4), 529–533. DOI: 10.1038/2005.

Miyashita, T., Coates, M. I., Farrar, R., Larson, P., Manning, P. L., Wogelius, R. A., Edwards, N. P., Anné, J., Bergmann, U., Richard Palmer, A., and Currie, P. J. (2019). Hagfish from the Cretaceous Tethys Sea and a reconciliation of the morphological-molecular conflict in early vertebrate phylogeny. *Proceedings of the National Academy of Sciences* 116(6), 2146–2151. DOI: 10.1073/pnas.1814794116.

Momose, A. and Fukuda, J. (1995). Phase-contrast radiographs of nonstained rat cerebellar specimen. *Medical Physics* 22(4), 375–379. DOI: 10.1118/1.597472.

Murchison, N. D., Price, B. A., Conner, D. A., Keene, D. R., Olson, E. N., Tabin, C. J., and Schweitzer, R. (2007). Regulation of tendon differentiation by scleraxis distinguishes force-transmitting tendons from muscle-anchoring tendons. *Development* 134(14), 2697–2708. DOI: 10.1242/dev.001933.

Murtaugh, L. C., Zeng, L., Chyung, J. H., and Lassar, A. B. (2001). The Chick Transcriptional Repressor Nkx3.2 Acts Downstream of Shh to Promote BMP-Dependent Axial Chondrogenesis. *Developmental Cell* 1(3), 411–422. DOI: 10.1016/S1534-5807(01)00039-9.

Nair, S., Li, W., Cornell, R., and Schilling, T. F. (2007). Requirements for Endothelin type-A receptors and Endothelin-1 signaling in the facial ectoderm for the patterning of skeletogenic neural crest cells in zebrafish. *Development* 134(2), 335–345. DOI: 10.1242/dev.02704.

Nakahara, H., Hasegawa, A., Otabe, K., Ayabe, F., Matsukawa, T., Onizuka, N., Ito, Y., Ozaki, T., Lotz, M. K., and Asahara, H. (2013). Transcription factor Mohawk and the pathogenesis of human anterior cruciate ligament degradation. *Arthritis and Rheumatism* 65(8), 2081–2089. DOI: 10.1002/art.38020.

Nakashima, K., Zhou, X., Kunkel, G., Zhang, Z., Deng, J. M., Behringer, R. R., and De Crombrugghe, B. (2002). The Novel Zinc Finger-Containing Transcription Factor Osterix Is Required for Osteoblast

Differentiation and Bone Formation. *Cell* 108(2), 17–29. DOI: 10.1016/S0092-8674(01)00622-5.

Nassari, S., Duprez, D., and Fournier-Thibault, C. (2017). Non-myogenic Contribution to Muscle Development and Homeostasis: The Role of Connective Tissues. *Frontiers in Cell and Developmental Biology* 5, 22. DOI: 10.3389/fcell.2017.00022.

Nelson, J. S., Grande, T. C., and Wilson, M. V. H. (2016). Fishes of the World. 5th Ed. Hoboken, New Jersey: John Wiley & Sons, Ltd. DOI: 10.1002/9781119174844.

Nichols, J. T., Pan, L., Moens, C. B., and Kimmel, C. B. (2013). Barx1 Represses Joints and Promotes Cartilage in the Craniofacial Skeleton. *Development* 140(13), 2765–2775. DOI: 10.1242/dev.090639.

Nishitoh, H., Ichijo, H., Kimura, M., Matsumoto, T., Makishima, F., Yamaguchi, A., Yamashita, H., Enomoto, S., and Miyazono, K. (1996). Identification of type I and type II serine/threonine kinase receptors for growth/differentiation factor-5. *Journal of Biological Chemistry* 271(35), 21345–21352. DOI: 10.1074/jbc.271.35.21345.

Nourissat, G., Berenbaum, F., and Duprez, D. (2015). Tendon injury: From biology to tendon repair. *Nature Reviews Rheumatology* 11(4), 223–233. DOI: 10.1038/nrrheum.2015.26.

Nuñez, J. K., Bai, L., Harrington, L. B., Hinder, T. L., and Doudna, J. A. (2016). CRISPR Immunological Memory Requires a Host Factor for Specificity. *Molecular Cell* 62(6), 824–833. DOI: 10.1016/j.molcel.2016.04.027.

Oh, H. K., Park, M., Choi, S. W., Jeong, D. U., Kim, B. J., Kim, J. A., Choi, H. J., Lee, J., Cho, Y., Kim, J. H., Seong, J. K., Choi, B. H., Min, B. H., and Kim, D. W. (2021). Suppression of Osteoarthritis progression by post-natal Induction of Nkx3.2. *Biochemical and Biophysical Research Communications* 571, 188–194. DOI: 10.1016/j.bbrc.2021.07.074.

Osterwalder, M., Barozzi, I., Tissiéres, V., Fukuda-Yuzawa, Y., Mannion, B. J., Afzal, S. Y., Lee, E. A., Zhu, Y., Plajzer-Frick, I., Pickle, C. S., Kato, M., Garvin, T. H., Pham, Q. T., Harrington, A. N., Akiyama, J. A., et al. (2018). Enhancer redundancy provides phenotypic robustness in mammalian development. *Nature* 554(7691), 239–243. DOI: 10.1038/nature25461.

Otabe, K., Nakahara, H., Hasegawa, A., Matsukawa, T., Ayabe, F., Onizuka, N., Inui, M., Takada, S., Ito, Y., Sekiya, I., Muneta, T., Lotz, M., and Asahara, H. (2015). Transcription factor mohawk controls tenogenic differentiation of bone marrow mesenchymal stem cells in vitro and in vivo. *Journal of Orthopaedic Research* 33(1), 1–8. DOI: 10.1002/jor.22750.

Paganin, D., Mayo, S. C., Gureyev, T. E., Miller, P. R., and Wilkins, S. W. (2002). Simultaneous phase and amplitude extraction from a single

defocused image of a homogeneous object. *Journal of Microscopy* 206(1), 33–40. DOI: 10.1046/j.1365-2818.2002.01010.x.

Palenstijn, W. J., Batenburg, K. J., and Sijbers, J. (2013). The ASTRA Tomography Toolbox. In: *Proceedings of the 13th International Conference on Computational and Mathematical Methods in Science and Engineering*. Vol. 4, pp. 1139–1145.

Parrish, W., Byers, B., Su, D., Geesin, J., Herzberg, U., Wadsworth, S., Bendele, A., and Story, B. (2017). Intra-articular therapy with recombinant human GDF5 arrests disease progression and stimulates cartilage repair in the rat medial meniscus transection (MMT) model of osteoarthritis. *Osteoarthritis and Cartilage* 25(4), 554–560. DOI: 10.1016/j.joca.2016.11.002.

Pauwels, E., Van Loo, D., Cornillie, P., Brabant, L., and Van Hoorebeke, L. (2013). An exploratory study of contrast agents for soft tissue visualization by means of high resolution X-ray computed tomography imaging. *Journal of Microscopy* 250(1), 21–31. DOI: 10.1111/jmi.12013.

Peacock, M. (2010). Calcium Metabolism in Health and Disease. *Clinical Journal of the American Society of Nephrology* 5(Supplement 1), 23–30. DOI: 10.2215/CJN.05910809.

Percival, C. J. and Richtsmeier, J. T. (2013). Angiogenesis and Intramembranous Osteogenesis. *Developmental Dynamics* 242(8), 909–922. DOI: 10.1002/dvdy.23992.

Perry, M. W., Boettiger, A. N., Bothma, J. P., and Levine, M. (2010). Shadow enhancers foster robustness of drosophila gastrulation. *Current Biology* 20(17), 1562–1567. DOI: 10.1016/j.cub.2010.07.043.

Peter, I. S. and Davidson, E. H. (2015). Genomic Control Process: Development and Evolution. San Diego: Academic Press.

Pfaffl, M. W. (2001). A new mathematical model for relative quantification in real-time RT-PCR. *Nucleic Acids Research* 29(9), E45. DOI: 10.1093/nar/29.9.e45.

Porro, L. B. and Richards, C. T. (2017). Digital dissection of the model organism *Xenopus laevis* using contrast-enhanced computed tomography. *Journal of Anatomy* 231(2), 169–191. DOI: 10.1111/joa.12625.

Portnoy, M. E., McDermott, K. J., Antonellis, A., Margulies, E. H., Prasad, A. B., NISC Comparative Sequencing Program, Kingsley, D. M., Green, E. D., and Mortlock, D. P. (2005). Detection of potential GDF6 regulatory elements by multispecies sequence comparisons and identification of a skeletal joint enhancer. *Genomics* 86(3), 295–305. DOI: 10.1016/J.YGENO.2005.05.003.

Prescott, S. L., Srinivasan, R., Marchetto, M. C., Grishina, I., Narvaiza, I., Selleri, L., Gage, F. H., Swigut, T., and Wysocka, J. (2015). Enhancer Divergence and cis-Regulatory Evolution in the Human and Chimp Neural Crest. *Cell* 163(1), 68–84. DOI: 10.1016/j.cell.2015.08.036.

Provot, S., Kempf, H., Murtaugh, L. C., Chung, U.-i., Kim, D. W., Chyung, J., Kronenberg, H. M., and Lassar, A. B. (2006). Nkx3.2/Bapx1 acts as a negative regulator of chondrocyte maturation. *Development* 133(4), 651–62. DOI: 10.1242/dev.02258.

Pryce, B. A., Watson, S. S., Murchison, N. D., Staverosky, J. A., Dünker, N., and Schweitzer, R. (2009). Recruitment and maintenance of tendon progenitors by TGFβ signaling are essential for tendon formation. *Development* 136(8), 1351–1361. DOI: 10.1242/dev.027342.

Qiao, T., King, B., Long, J. A., Ahlberg, P. E., and Zhu, M. (2016). Early gnathostome phylogeny revisited: Multiple method consensus. *PLoS ONE* 11(9), e0163157. DOI: 10.1371/journal.pone.0163157.

R Development Core Team, R. (2021). *R: A Language and Environment for Statistical Computing*. Vienna, Austria.

Rainbow, R. S., Kwon, H., and Zeng, L. (2014). The role of Nkx3.2 in chondrogenesis. *Frontiers in Biology* 9(5), 376–381. DOI: 10.1007/s11515-014-1321-3.

Reddy, P. M., Stamatoyannopoulos, G., Papayannopoulou, T., and Shen, C. K. (1994). Genomic footprinting and sequencing of human β-globin locus. Tissue specificity and cell line artifact. *Journal of Biological Chemistry* 269(11), 8287–8295. DOI: 10.1016/s0021-9258(17)37191-0.

Reynard, L. N., Bui, C., Syddall, C. M., and Loughlin, J. (2014). CpG methylation regulates allelic expression of GDF5 by modulating binding of SP1 and SP3 repressor proteins to the osteoarthritis susceptibility SNP rs143383. *Human Genetics* 133(8), 1059–1073. DOI: 10.1007/s00439-014-1447-z.

Rhee, D. K., Marcelino, J., Baker, M., Gong, Y., Smits, P., Lefebvre, V., Jay, G. D., Stewart, M., Wang, H., Warman, M. L., and Carpten, J. D. (2005). The secreted glycoprotein lubricin protects cartilage surfaces and inhibits synovial cell overgrowth. *Journal of Clinical Investigation* 115(3), 622–631. DOI: 10.1172/JCI200522263.

Rodrigo, I., Bovolenta, P., Mankoo, B. S., and Imai, K. (2004). Meox Homeodomain Proteins Are Required for Bapx1 Expression in the Sclerotome and Activate Its Transcription by Direct Binding to Its Promoter. *Molecular and Cellular Biology* 24(7), 2757–2766. DOI: 10.1128/mcb.24.7.2757-2766.2004.

Rodrigo, I., Hill, R. E., Balling, R., Münsterberg, A., and Imai, K. (2003). Pax1 and Pax9 activate Bapx1 to induce chondrogenic differentation in the sclerotome. *Development* 130(3), 473–482. DOI: 10.1242/dev.00240.

Rowan, S., Siggers, T., Lachke, S. A., Yue, Y., Bulyk, M. L., and Maas, R. L. (2010). Precise temporal control of the eye regulatory gene Pax6 via enhancer-binding site affinity. *Genes and Development* 24(10), 980–985. DOI: 10.1101/gad.1890410.

Salazar, V. S., Gamer, L. W., and Rosen, V. (2016). BMP signalling in skeletal development, disease and repair. *Nature Reviews Endocrinology* 12(4), 203–221. DOI: 10.1038/nrendo.2016.12.

Sanchez, S., Ahlberg, P. E., Trinajstic, K. M., Mirone, A., and Tafforeau, P. (2012). Three-dimensional synchrotron virtual paleohistology: A new insight into the world of fossil bone microstructures. *Microscopy and Microanalysis* 18(5), 1095–1105. DOI: 10.1017/S1431927612001079.

Sanchez, S., Dupret, V., Tafforeau, P., Trinajstic, K. M., Ryll, B., Gouttenoire, P. J., Wretman, L., Zylberberg, L., Peyrin, F., and Ahlberg, P. E. (2013). 3D Microstructural Architecture of Muscle Attachments in Extant and Fossil Vertebrates Revealed by Synchrotron Microtomography. *PLoS ONE* 8(2), e56992. DOI: 10.1371/journal.pone.0056992.

Santana, S. E. (2018). Comparative Anatomy of Bat Jaw Musculature via Diffusible Iodine-Based Contrast-Enhanced Computed Tomography. *The Anatomical Record* 301(2), 267–278. DOI: 10.1002/ar.23721.

Satoh, A., Suzuki, M., Amano, T., Tamura, K., and Ide, H. (2005). Joint development in Xenopus laevis and induction of segmentations in regenerating froglet limb (spike). *Developmental Dynamics* 233(4), 1444–1453. DOI: 10.1002/dvdy.20484.

Schindelin, J., Arganda-Carreras, I., Frise, E., Kaynig, V., Longair, M., Pietzsch, T., Preibisch, S., Rueden, C., Saalfeld, S., Schmid, B., Tinevez, J.-Y., White, D. J., Hartenstein, V., Eliceiri, K., Tomancak, P., et al. (2012). Fiji: an open-source platform for biological-image analysis. *Nature Methods* 9(7), 676–682. DOI: 10.1038/nmeth.2019.

Schmidt, R., Strähle, U., and Scholpp, S. (2013). Neurogenesis in zebrafish - from embryo to adult. *Neural Development* 8, 3. DOI: 10.1186/1749-8104-8-3.

Schweitzer, R., Zelzer, E., and Volk, T. (2010). Connecting muscles to tendons: tendons and musculoskeletal development in flies and vertebrates. *Development* 137(19), 3347–3347. DOI: 10.1242/dev.057885.

Schweitzer, R., Chyung, J. H., Murtaugh, L. C., Brent, A. E., Rosen, V., Olson, E. N., Lassar, A., and Tabin, C. J. (2001). Analysis of the tendon cell fate using Scleraxis, a specific marker for tendons and ligaments. *Development* 128(19), 3855–3866. DOI: 10.1242/dev.001933.

Schwend, T. and Ahlgren, S. C. (2009). Zebrafish con/disp1 reveals multiple spatiotemporal requirements for Hedgehog-signaling in craniofacial development. *BMC Developmental Biology* 9, 59. DOI: 10.1186/1471-213X-9-59.

Seo, E., Lim, J.-H., Seo, S. J., and Lee, S. J. (2015). Whole-Body Imaging of a Hypercholesterolemic Female Zebrafish by Using Synchrotron X-Ray Micro-CT. *Zebrafish* 12(1), 11–20. DOI: 10.1089/zeb.2014.1039.

Settle, S. H., Rountree, R. B., Sinha, A., Thacker, A., Higgins, K., and Kingsley, D. M. (2003). Multiple joint and skeletal patterning defects

caused by single and double mutations in the mouse Gdf6 and Gdf5 genes. *Developmental Biology* 254(1), 116–130. DOI: 10.1016/S0012-1606(02)00022-2.

Shamonin, D. P., Bron, E. E., Lelieveldt, B. P., Smits, M., Klein, S., and Staring, M. (2014). Fast parallel image registration on CPU and GPU for diagnostic classification of Alzheimer's disease. *Frontiers in Neuroinformatics* 7, 50. DOI: 10.3389/fninf.2013.00050.

Sharpe, J. (2003). Optical projection tomography as a new tool for studying embryo anatomy. *Journal of Anatomy* 202(2), 175–181. DOI: 10.1046/j.1469-7580.2003.00155.x.

Sharpe, J., Ahlgren, U., Perry, P., Hill, B., Ross, A., Hecksher-Sørensen, J., Baldock, R., and Davidson, D. (2002). Optical projection tomography as a tool for 3D microscopy and gene expression studies. *Science* 296(5567), 541–545. DOI: 10.1126/science.1068206.

Shukunami, C., Takimoto, A., Nishizaki, Y., Yoshimoto, Y., Tanaka, S., Miura, S., Watanabe, H., Sakuma, T., Yamamoto, T., Kondoh, G., and Hiraki, Y. (2018). Scleraxis is a transcriptional activator that regulates the expression of Tenomodulin, a marker of mature tenocytes and ligamentocytes. *Scientific Reports* 8, 3155. DOI: 10.1038/s41598-018-21194-3.

Shukunami, C., Takimoto, A., Oro, M., and Hiraki, Y. (2006). Scleraxis positively regulates the expression of tenomodulin, a differentiation marker of tenocytes. *Developmental Biology* 298(1), 234–247. DOI: 10.1016/j.ydbio.2006.06.036.

Shwartz, Y., Viukov, S., Krief, S., and Zelzer, E. (2016). Joint Development Involves a Continuous Influx of Gdf5-Positive Cells. *Cell Reports* 15(12), 2577–2587. DOI: 10.1016/j.celrep.2016.05.055.

Simsek-Kiper, P. O., Kosukcu, C., Akgun-Dogan, O., Gocmen, R., Utine, G. E., Soyer, T., Korkmaz-Toygar, A., Nishimura, G., Alikasifoglu, M., and Boduroglu, K. (2019). A novel NKX3-2 mutation associated with perinatal lethal phenotype of spondylo-megaepiphyseal-metaphyseal dysplasia in a neonate. *European Journal of Medical Genetics* 62(1), 21–26. DOI: 10.1016/j.ejmg.2018.04.013.

Smeeton, J., Askary, A., and Crump, J. G. (2016). Building and maintaining joints by exquisite local control of cell fate. *Wiley Interdisciplinary Reviews: Developmental Biology* 6(1), e245. DOI: 10.1002/wdev.245.

Snigirev, A., Snigireva, I., Kohn, V., Kuznetsov, S., and Schelokov, I. (1995). On the possibilities of x-ray phase contrast microimaging by coherent high-energy synchrotron radiation. *Review of Scientific Instruments* 66(12), 5486–5492. DOI: 10.1063/1.1146073.

Sophia Fox, A. J., Bedi, A., and Rodeo, S. A. (2009). The basic science of articular cartilage: Structure, composition, and function. *Sports Health* 1(6), 461–468. DOI: 10.1177/1941738109350438.

Square, T., Jandzik, D., Cattell, M., Coe, A., Doherty, J., and Medeiros, D. M. (2015). A gene expression map of the larval Xenopus laevis head reveals developmental changes underlying the evolution of new skeletal elements. *Developmental Biology* 397(2), 293–304. DOI: 10.1016/j.ydbio.2014.10.016.

Sroga, G. E., Karim, L., Colon, W., and Vashishth, D. (2011). Biochemical characterization of major bone-matrix proteins using nanoscale-size bone samples and proteomics methodology. *Molecular and Cellular Proteomics* 10(9), 1–12. DOI: 10.1074/mcp.M110.006718.

Stickens, D., Behonick, D. J., Ortega, N., Heyer, B., Hartenstein, B., Yu, Y., Fosang, A. J., Schorpp-Kistner, M., Angel, P., and Werb, Z. (2004). Altered endochondral bone development in matrix metalloproteinase 13-deficient mice. *Development* 131(23), 5883–5895. DOI: 10.1242/dev.01461.

Storm, E. E., Huynh, T. V., Copeland, N. G., Jenkins, N. A., Kingsley, D. M., and Lee, S.-J. (1994). Limb alterations in brachypodism mice due to mutations in a new member of the TGFβ-superfamily. *Nature* 368, 639–643. DOI: 10.1038/368639a0.

Storm, E. E. and Kingsley, D. M. (1996). Joint patterning defects caused by single and double mutations in members of the bone morphogenetic protein (BMP) family. *Development* 122(12), 3969–3979. DOI: 10.1242/dev.122.12.3969.

– (1999). GDF5 coordinates bone and joint formation during digit development. *Developmental Biology* 209(1), 11–27. DOI: 10.1006/dbio.1999.9241.

Streisinger, G., Walker, C., Dower, N., Knauber, D., and Singer, F. (1981). Production of clones of homozygous diploid zebra fish (Brachydanio rerio). *Nature* 291, 293–296. DOI: 10.1038/291293a0.

Stricker, S. and Mundlos, S. (2011). Mechanisms of digit formation: Human malformation syndromes tell the story. *Developmental Dynamics* 240(5), 990–1004. DOI: 10.1002/dvdy.22565.

Subramanian, A., Kanzaki, L. F., and Schilling, T. F. (2023). Mechanical force regulates Sox9 expression at the developing enthesis. *Development* 150(16), dev201141. DOI: 10.1242/dev.201141.

Subramanian, A., Kanzaki, L. F., Galloway, J. L., and Schilling, T. F. (2018). Mechanical force regulates tendon extracellular matrix organization and tenocyte morphogenesis through TGFbeta signaling. *eLife* 7, e38069. DOI: 10.7554/eLife.38069.

Subramanian, A. and Schilling, T. F. (2015). Tendon development and musculoskeletal assembly: emerging roles for the extracellular matrix. *Development* 142(24), 4191–4204. DOI: 10.1242/dev.114777.

– (2014). Thrombospondin-4 controls matrix assembly during development and repair of myotendinous junctions. *eLife* 3, e02372. DOI: 10.7554/eLife.02372.

Sullivan, C. and Kim, C. H. (2008). Zebrafish as a model for infectious disease and immune function. *Fish and Shellfish Immunology* 25(4), 341–350. DOI: 10.1016/j.fsi.2008.05.005.

Sun, K., Guo, J., Yao, X., Guo, Z., and Guo, F. (2021). Growth differentiation factor 5 in cartilage and osteoarthritis: A possible therapeutic candidate. *Cell Proliferation* 54(3), e12998. DOI: 10.1111/cpr.12998.

Suzuki, H., Ito, Y., Shinohara, M., Yamashita, S., Ichinose, S., Kishida, A., Oyaizu, T., Kayama, T., Nakamichi, R., Koda, N., Yagishita, K., Lotz, M. K., Okawa, A., and Asahara, H. (2016). Gene targeting of the transcription factor Mohawk in rats causes heterotopic ossification of Achilles tendon via failed tenogenesis. *Proceedings of the National Academy of Sciences* 113(28), 7840–7845. DOI: 10.1073/pnas.1522054113.

Tafforeau, P., Boistel, R., Boller, E., Bravin, A., Brunet, M., Chaimanee, Y., Cloetens, P., Feist, M., Hoszowska, J., Jaeger, J. J., Kay, R. F., Lazzari, V., Marivaux, L., Nel, A., Nemoz, C., et al. (2006). Applications of X-ray synchrotron microtomography for non-destructive 3D studies of paleontological specimens. *Applied Physics A: Materials Science and Processing* 83(2), 195–202. DOI: 10.1007/s00339-006-3507-2.

Takeuchi, J. K. and Bruneau, B. G. (2007). Irxl1, a divergent Iroquois homeobox family transcription factor gene. *Gene Expression Patterns* 7(1-2), 51–56. DOI: 10.1016/j.modgep.2006.05.007.

Tanaka, E., Detamore, M. S., Tanimoto, K., and Kawai, N. (2008). Lubrication of the Temporomandibular Joint. *Annals of Biomedical Engineering* 36(1), 14–29. DOI: 10.1007/s10439-007-9401-z.

Tang, Y. and Fu, Y. (2018). Class 2 CRISPR/Cas: an expanding biotechnology toolbox for and beyond genome editing. *Cell & Bioscience* 8, 59. DOI: 10.1186/s13578-018-0255-x.

Thomas, J. T., Lin, K., Nandedkar, M., Camargo, M., Cervenka, J., and Luyten, F. P. (1996). A human chondrodysplasia due to a mutation in a TGF-β superfamily member. *Nature Genetics* 12(3), 315–317. DOI: 10.1038/ng0396-315.

Thompson, D. A., Nesterets, Y. I., Pavlov, K. M., and Gureyev, T. E. (2019). Fast three-dimensional phase retrieval in propagation-based X-ray tomography. *Journal of Synchrotron Radiation* 26(3), 825–838. DOI: 10.1107/S1600577519002133.

Tonelli, F., Bek, J. W., Besio, R., and Clercq, A. D. (2020). Zebrafish: A Resourceful Vertebrate Model to Investigate Skeletal Disorders. *Frontiers in Endocrinology* 11, 489. DOI: 10.3389/fendo.2020.00489.

Tribioli, C. and Lufkin, T. (1999). The murine Bapx1 homeobox gene plays a critical role in embryonic development of the axial skeleton and spleen. *Development* 126(24), 5699–5711. DOI: 10.1242/dev.126.24.5699.

Tsai, Y.-C., Cooke, N. E., and Liebhaber, S. A. (2016). Long-range looping of a locus control region drives tissue-specific chromatin packing within a

multigene cluster. *Nucleic Acids Research* 44(10), 4651–4664. DOI: 10.1093/nar/gkw090.

Tschentscher, T. and Suortti, P. (1998). Experiments with very high energy synchrotron radiation. *Journal of Synchrotron Radiation* 5(3), 286–292. DOI: 10.1107/S0909049597014775.

Tsumaki, N., Tanaka, K., Arikawa-Hirasawa, E., Nakase, T., Kimura, T., Terrig Thomas, J., Ochi, T., Luyten, F. P., and Yamada, Y. (1999). Role of CDMP-1 in skeletal morphogenesis: Promotion of mesenchymal cell recruitment and chondrocyte differentiation. *Journal of Cell Biology* 144(1), 161–173. DOI: 10.1083/jcb.144.1.161.

Tucker, A. S., Watson, R. P., Lettice, L. A., Yamada, G., and Hill, R. E. (2004). Bapx1 regulates patterning in the middle ear: altered regulatory role in the transition from the proximal jaw during vertebrate evolution. *Development* 131(6), 1235–1245. DOI: 10.1242/dev.01017.

Tucker, A. S. (2017). Major evolutionary transitions and innovations: the tympanic middle ear. *Philosophical Transactions of the Royal Society B: Biological Sciences* 372(1713), 20150483. DOI: 10.1098/rstb.2015.0483.

Ullah, I., Subbarao, R. B., and Rho, G. J. (2015). Human mesenchymal stem cells - Current trends and future prospective. *Bioscience Reports* 35, e00191. DOI: 10.1042/BSR20150025.

Varshney, G. K., Carrington, B., Pei, W., Bishop, K., Chen, Z., Fan, C., Xu, L., Jones, M., LaFave, M. C., Ledin, J., Sood, R., and Burgess, S. M. (2016). A high-throughput functional genomics workflow based on CRISPR/Cas9-mediated targeted mutagenesis in zebrafish. *Nature Protocols* 11(12), 2357–2375. DOI: 10.1038/nprot.2016.141.

Varshney, G. K., Pei, W., Lafave, M. C., Idol, J., Xu, L., Gallardo, V., Carrington, B., Bishop, K., Jones, M., Li, M., Harper, U., Huang, S. C., Prakash, A., Chen, W., Sood, R., et al. (2015). High-throughput gene targeting and phenotyping in zebrafish using CRISPR/Cas9. *Genome Research* 25(7), 1030–1042. DOI: 10.1101/gr.186379.114.

Vásárhelyi, L., Kónya, Z., Kukovecz, Á., and Vajtai, R. (2020). Microcomputed tomography-based characterization of advanced materials: a review. *Materials Today Advances* 8, 100084. DOI: 10.1016/j.mtadv.2020.100084.

Vaškaninová, V., Chen, D., Tafforeau, P., Johanson, Z., Ekrt, B., Blom, H., and Ahlberg, P. E. (2020). Marginal dentition and multiple dermal jawbones as the ancestral condition of jawed vertebrates. *Science* 369(6500), 211–216. DOI: 10.1126/science.aaz9431.

Visel, A., Prabhakar, S., Akiyama, J. A., Shoukry, M., Lewis, K. D., Holt, A., Plajzer-Frick, I., Afzal, V., Rubin, E. M., and Pennacchio, L. A. (2008). Ultraconservation identifies a small subset of extremely constrained developmental enhancers. *Nature Genetics* 40(2), 158–160. DOI: 10.1038/ng.2007.55.

Walhout, A. J., Temple, G. F., Brasch, M. A., Hartley, J. L., Lorson, M. A., Van Den Heuvel, S., and Vidal, M. (2000). GATEWAY recombinational cloning: Application to the cloning of large numbers of open reading frames or ORFeomes. In: *Methods in Enzymology*. Vol. 328. Elsevier, pp. 575–592. DOI: 10.1016/S0076-6879(00)28419-X.

Walker, M. B. and Kimmel, C. B. (2007). A two-color acid-free cartilage and bone stain for zebrafish larvae. *Biotechnic and Histochemistry* 82(1), 23–28. DOI: 10.1080/10520290701333558.

Wang, X. and Goldstein, D. B. (2020). Enhancer Domains Predict Gene Pathogenicity and Inform Gene Discovery in Complex Disease. *American Journal of Human Genetics* 106(2), 215–233. DOI: 10.1016/j.ajhg.2020.01.012.

Watson, C. J., Tang, W. J., Rojas, M. F., Fiedler, I. A. K., Morfin Montes De Oca, E., Cronrath, A. R., Callies, L. K., Swearer, A. A., Ahmed, A. R., Sethuraman, V., Addish, S., Farr, G. H., Gómez, A. E., Rai, J., Monstad-Rios, A. T., et al. (2022). wnt16 regulates spine and muscle morphogenesis through parallel signals from notochord and dermomyotome. *PLOS Genetics* 18(11), e1010496. DOI: 10.1371/journal.pgen.1010496.

Weide, D., Thayer, M. K., Newton, A. F., and Betz, O. (2010). Comparative morphology of the head of selected sporophagous and non-sporophagous Aleocharinae (Coleoptera: Staphylinidae): Musculature and hypopharynx-prementum complex. *Journal of Morphology* 271, 910–931. DOI: 10.1002/jmor.10841.

Westerfield, M. (2000). The Zebrafish Book: A Guide for the Laboratory Use of Zebrafish (Danio rerio). 4th Ed. Eugene: University of Oregon Press.

Wickham, H. (2016). ggplot2: Elegant Graphics for Data Analysis. Springer-Verlag New York.

Wilkins, S. W., Gureyev, T. E., Gao, D., Pogany, A., and Stevenson, A. W. (1996). Phase-constrast imaing using polychromatic hard X-rays. *Nature* 384, 335–338. DOI: 10.1038/384335a0.

Wilkinson, M., Drabavicius, G., Silanskas, A., Gasiunas, G., Siksnys, V., and Wigley, D. B. (2019). Structure of the DNA-Bound Spacer Capture Complex of a Type II CRISPR-Cas System. *Molecular Cell* 75(1), 90–101. DOI: 10.1016/j.molcel.2019.04.020.

Wilson, D. E. and Reeder, D. M. (2005). Mammal Species of the World. A taxonomic and geographic reference. 3rd Ed. Baltimore: Johns Hopkins University Press.

Wilson, J. and Tucker, A. S. (2004). Fgf and Bmp signals repress the expression of Bapx1 in the mandibular mesenchyme and control the position of the developing jaw joint. *Developmental Biology* 266(1), 138–150. DOI: 10.1016/j.ydbio.2003.10.012.

Withers, P. J., Bouman, C., Carmignato, S., Cnudde, V., Grimaldi, D., Hagen, C. K., Maire, E., Manley, M., Du Plessis, A., and Stock, S. R.

(2021). X-ray computed tomography. *Nature Reviews Methods Primers* 1(18), 1–21. DOI: 10.1038/s43586-021-00015-4.

Wollesen, L., Riva, F., Douissard, P.-A., Pauwels, K., Martin, T., and Dujardin, C. (2022). Scintillating thin film design for ultimate high resolution X-ray imaging. *Journal of Materials Chemistry C* 10(24), 9257–9265. DOI: 10.1039/D2TC01274J.

Wright, A. V. and Doudna, J. A. (2016). Protecting genome integrity during CRISPR immune adaptation. *Nature Structural & Molecular Biology* 23(10), 876–883. DOI: 10.1038/nsmb.3289.

Xu, P., Yu, H. V., Tseng, K.-C., Flath, M., Fabian, P., Segil, N., and Crump, J. G. (2021). Foxc1 establishes enhancer accessibility for craniofacial cartilage differentiation. *eLife* 10, e63595. DOI: 10.7554/eLife.63595.

Yamashita, S., Andoh, M., Ueno-Kudoh, H., Sato, T., Miyaki, S., and Asahara, H. (2009). Sox9 directly promotes Bapx1 gene expression to repress Runx2 in chondrocytes. *Experimental Cell Research* 315(13), 2231–2240. DOI: 10.1016/j.yexcr.2009.03.008.

Yang, G., Zhu, L., Hou, N., Lan, Y., Wu, X.-M., Zhou, B., Teng, Y., and Yang, X. (2014a). Osteogenic fate of hypertrophic chondrocytes. *Cell Research* 24(10), 1266–1269. DOI: 10.1038/cr.2014.111.

Yang, L., Tsang, K. Y., Tang, H. C., Chan, D., and Cheah, K. S. E. (2014b). Hypertrophic chondrocytes can become osteoblasts and osteocytes in endochondral bone formation. *Proceedings of the National Academy of Sciences* 111(33), 12097–12102. DOI: 10.1073/pnas.1302703111.

Yang, S., Oksenberg, N., Takayama, S., Heo, S. J., Poliakov, A., Ahituv, N., Dubchak, I., and Boffelli, D. (2015). Functionally conserved enhancers with divergent sequences in distant vertebrates. *BMC Genomics* 16, 882. DOI: 10.1186/s12864-015-2070-7.

Yoshida, C. A., Yamamoto, H., Fujita, T., Furuichi, T., Ito, K., Inoue, K. I., Yamana, K., Zanma, A., Takada, K., Ito, Y., and Komori, T. (2004). Runx2 and Runx3 are essential for chondrocyte maturation, and Runx2 regulates limb growth through induction of Indian hedgehog. *Genes and Development* 18(8), 952–963. DOI: 10.1101/gad.1174704.

Zeng, L., Kempf, H., Murtaugh, L. C., Sato, M. E., and Lassar, A. B. (2002). Shh establishes an Nkx3.2/Sox9 autoregulatory loop that is maintained by BMP signals to induce somitic chondrogenesis. *Genes and Development* 16(15), 1990–2005. DOI: 10.1101/gad.1008002.

Zhang, H., Waldmann, L., Manuel, R., Boije, H., Haitina, T., and Allalou, A. (2020). zOPT: an open source optical projection tomography system and methods for rapid 3D zebrafish imaging. *Biomedical Optics Express* 11(8), 4290–4305. DOI: 10.1364/boe.393519.

Zhou, R., Zhou, X., Li, X., Cai, Y., and Liu, F. (2016). Study of the Microfocus X-Ray Tube Based on a Point-Like Target Used for

Micro-Computed Tomography. *PLOS ONE* 11(6), e0156224. DOI: 10.1371/journal.pone.0156224.

Zhou, X., Von Der Mark, K., Henry, S., Norton, W., Adams, H., and De Crombrugghe, B. (2014). Chondrocytes Transdifferentiate into Osteoblasts in Endochondral Bone during Development, Postnatal Growth and Fracture Healing in Mice. *PLoS Genetics* 10(12), e1004820. DOI: 10.1371/journal.pgen.1004820.

Zhu, M., Ahlberg, P. E., Pan, Z., Zhu, Y., Qiao, T., Zhao, W., Jia, L., and Lu, J. (2016). A Silurian maxillate placoderm illuminates jaw evolution. *Science* 354(6310), 334–336. DOI: 10.1126/science.aah3764.

Zhu, M., Yu, X., Ahlberg, P. E., Choo, B., Lu, J., Qiao, T., Qu, Q., Zhao, W., Jia, L., Blom, H., and Zhu, Y. (2013). A Silurian placoderm with osteichthyan-like marginal jaw bones. *Nature* 502(7470), 188–193. DOI: 10.1038/nature12617.

Zuniga, E., Rippen, M., Alexander, C., Schilling, T. F., and Crump, J. G. (2011). Gremlin 2 regulates distinct roles of BMP and Endothelin 1 signaling in dorsoventral patterning of the facial skeleton. *Development* 138(23), 5147–5156. DOI: 10.1242/dev.067785.

Zuniga, E., Stellabotte, F., and Gage Crump, J. (2010). Jagged-Notch signaling ensures dorsal skeletal identity in the vertebrate face. *Development* 137(11), 1843–1852. DOI: 10.1242/dev.049056.

Acta Universitatis Upsaliensis

Digital Comprehensive Summaries of Uppsala Dissertations from the Faculty of Science and Technology 2298

Editor: The Dean of the Faculty of Science and Technology

A doctoral dissertation from the Faculty of Science and Technology, Uppsala University, is usually a summary of a number of papers. A few copies of the complete dissertation are kept at major Swedish research libraries, while the summary alone is distributed internationally through the series Digital Comprehensive Summaries of Uppsala Dissertations from the Faculty of Science and Technology. (Prior to January, 2005, the series was published under the title "Comprehensive Summaries of Uppsala Dissertations from the Faculty of Science and Technology".)

Distribution: publications.uu.se
urn:nbn:se:uu:diva-509354

ACTA UNIVERSITATIS
UPSALIENSIS
2023